SLAC-50
UC-28, Particle Accelerators
and High-Voltage Machines
UC-34, Physics
TID-4500 (44th Ed.)

CONSOLIDATION OF RESULTS OF PRELIMINARY BEAM TESTS WITH SECTORS 1 AND 2

September 1965

Technical Report
Prepared Under
Contract AT(04-3)-400
for the USAEC
San Francisco Operations Office

Printed in USA. Price $3.00. Available from CFSTI, National Bureau of Standards, U.S. Department of Commerce, Springfield, Virginia.

TABLE OF CONTENTS

LIST OF FIGURES

LIST OF FIGURES - (continued)

LIST OF FIGURES - (continued)

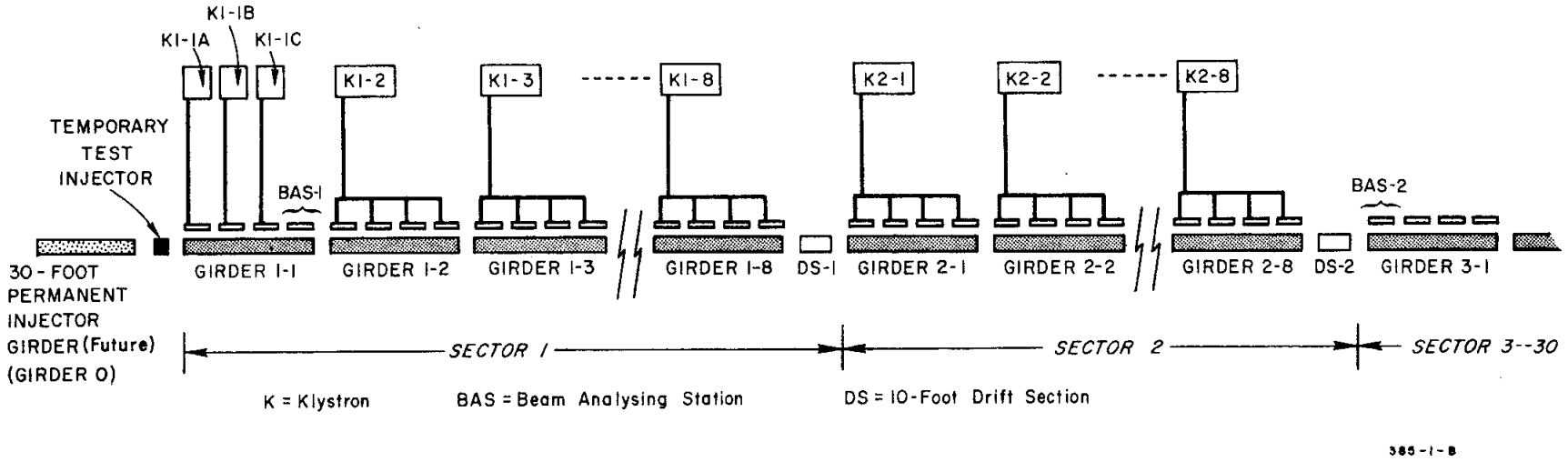

FIG. 0-1 SECTORS 1 AND 2 SCHEMATIC DIAGRAM

CONSOLIDATION OF RESULTS OF PRELIMINARY BEAM TESTS WITH SECTORS 1 AND 2

FOREWORD

This report summarizes the main results obtained from the beam tests carried out between January and July, 1965, in the first two 333-foot sectors of the Stanford 20-BeV accelerator now nearing completion. The tests and measurements were made by a large group of experimenters working in close collaboration with the Sector Test Team. For each run, an operator from the Sector Test Team was in charge of setting up the machine and a chief experimenter was responsible for the tests and measurements. The names of the chief experimenters appear under the titles of the various sections of the report.

The following figure diagrams the first two sectors. Each of the thirty sectors of the machine will include eight 40-foot girders on each of which are mounted four ten-foot sections of disk-loaded accelerator waveguide. At all regular girders but girder 1-1 (the first 40-foot girder of the first sector), power-splitting permits one 24-MW klystron to feed in parallel four ten-foot accelerator sections on that girder.

I. INTRODUCTION: GENERAL TEST CONDITIONS

G. A. Loew

The beam tests in Sectors 1 and 2 described in this report were carried out between January and July 1965. The specific conditions under which each test was done are described in the respective following sections. However, a few preliminary general statements should be made concerning the status of the machine:

1. Although by the end of 1964 most of the major systems were in place, gradual improvements, particularly in the instrumentation, were made throughout the testing period.
2. The alignment of Sectors 1 and 2 was done several times. Overall alignment was done using the stretched wire technique and spirit levels.
3. The injector used for these tests was not the final injector to be installed. In fact, the final 30-foot injector girder was not in the housing during the testing period. The temporary injector which was used for these tests consisted of an oxide gun, SLAC Model 1-1, the gun modulator originally used in the now-dismantled 20-foot test prototype Mark IV accelerator, a prebuncher, a valve, two lenses, a toroid and special steering. No buncher nor any other special instrumentation was available and the beam was directly injected into Girder 1-1. A summary of gun and gun-modulator characteristics is given in Table I-I. Considerable improvements in beam optics and transmission are expected with the final injector.
4. All energy measurements were made by means of two momentum spectrometers, Beam Analyzing Station No. 1 (BAS-1) at the 40-foot point and Beam Analyzing Station No. 2 (BAS-2) at the end of Sector 2. Pictures of these beam analyzing stations are shown in Figs. I-1 and I-2 and a summary of their characteristics is given in Table I-II.
5. Except for local injector and BAS-1 controls at the 40-foot point, most of the tests were carried out by using a temporary

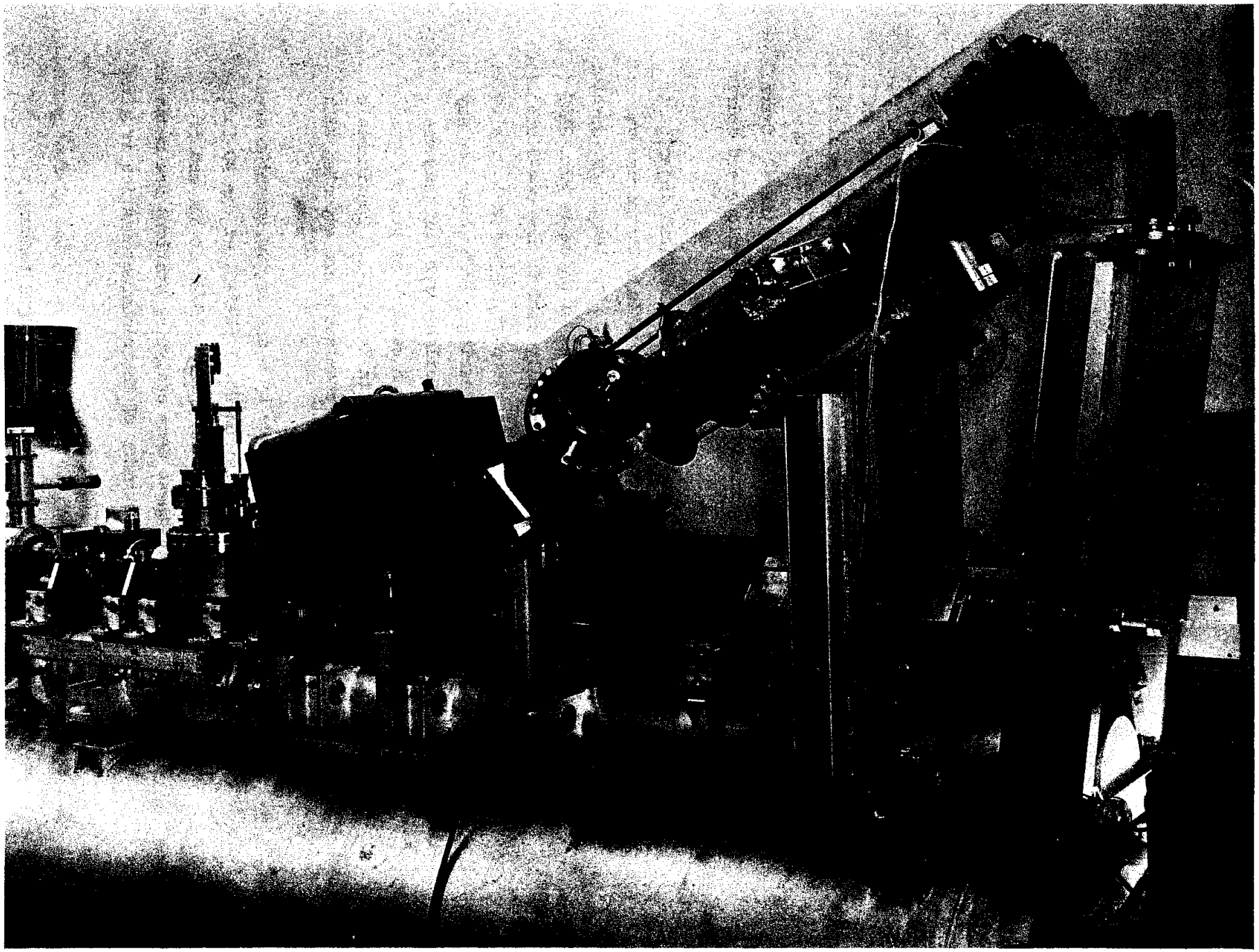

FIG. I-1 Beam analyzing station (BAS-1) at 40-foot point.

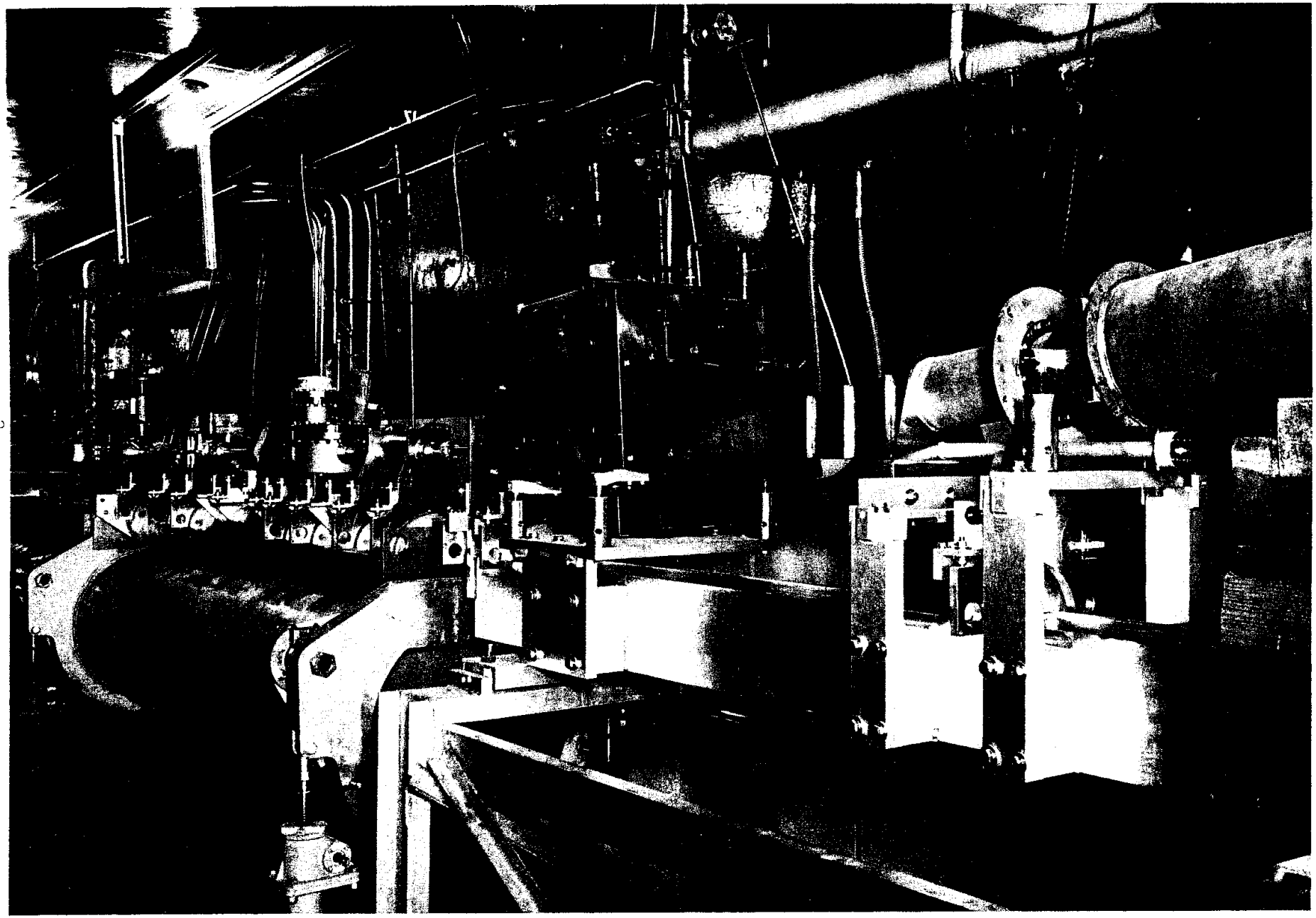

FIG. I-2 Beam analyzing station (BAS-2) at 666-foot point.

340-2-A

central control in Sector 2 alcove. A list of temporary instrumentation and controls is given in Table I-III.

TABLE I-I

(J. Berk)

Gun Characteristics

Model SLAC 1-1 (original design used on Mark II, III, and IV)	
Nickel cathode sprayed with barium-strontium oxide	
Thoriated tungsten filament	
Filament power	30 - 55 watts
Maximum current at 3-kV grid-to-cathode voltage	200 mA
Total gun perveance	≈ 0.01 microperveance
Beam diameter at prebuncher	< 1 cm
Differential pumping	8 liters/sec at gun
	50 liters/sec downbeam

Gun Modulator Characteristics

Cathode-anode pulse amplitude	3 - 80 kV
10% - 90% rise time	1 μsec
90% - 10% fall time	2 μsec
Maximum cathode flat top	3 μsec
Pulse droop at 100 mA	5%
Grid pulse amplitude	250 volts - 3 kV
Grid pulse length	1.3 μsec
10%-90% grid pulse rise and fall times	0.2 μsec
Pulse top flatness	5 - 10%

TABLE I-II

SUMMARY OF CHARACTERISTICS FOR BAS SPECTROMETERS

(M. Lee)

	BAS-1	BAS-2
Maximum energy	205 MeV	1450 MeV
Maximum field	8 kG	15 kG
Maximum current	120 amps	320 amps
Energy calibration	25.02 MeV/kG	9.67 MeV/kG
Energy acceptance	25 %	25 %
Bending radius	32.9 inches	126.9 inches
Bending angle	30°	7.7°
Pole face rotation		
Entrance face	-1.5°	-12.4°
Exit face	-1.5°	-12.4°
Focal point location		
Coordinates*: X =	60.5 inches	231.9 inches
Z =	30.3 inches	30.2 inches
Distance from exit pole face	51.6 inches	216.0 inches
Vacuum pipe		
Size: at magnet exit	1-3/4 inches	≈ 2 inches
at focal plane	8-5/8 inches	8-5/8 inches

*Position is measured relative to the point of intersection of the magnet entrance pole face and the beam axis.

TABLE I - III

W. Struven

SECTOR 2 TEMPORARY INSTRUMENTATION AND CONTROLS FOR SECTORS 1 AND 2 AND BEAM TESTS

In order to run a beam more efficiently in Sectors 1 and 2, certain temporary instrumentation and controls were installed in Sector 2 I/C Alcove. These included the instrumentation and controls for:

1. BAS-2 spectrometer including x, y plotter, foil scope and bending magnet power supply.
2. Drift sections 1 and 2 profile monitor including monitor TV, crystal insertion controls and status lights, light dimmer controls and a camera selection switch.
3. Panofsky Long Ion Chamber (PLIC) including readout oscilloscope and gallery electronics.
4. Log Q, x and y signals from the 30-foot point, DS1 and DS2, including baseband electronics with recorder output and a four-channel oscilloscope.
5. Quadrupoles at the 30-foot and DS1 point including power supply on/off control, increase/decrease current control, current meters and status lights for each supply.
6. Steering at the 30-foot point, Fiat 1-4, Fiat 1-6 and DS1, including controls, status lights and meters for each supply.
7. Degaussing at DS1 and DS2 including status and meters for each supply.
8. Klystron status lights for Sector 1 including Mod Available, Mod Not Available, Mod On, RF OK, Accelerate and Standby Trigger Mode.
9. Sectors 1 and 2 Klystron Accelerate and Standby Controls.
10. Sectors 0, 1 and 2 Trigger controls including Sequence, Rate and Pattern Selector Switches.
11. Temporary controls and status lights for the Personnel Protection System in Sectors 0 through 5.
12. Linear beam Q including preamplifiers at Beam Monitoring Racks 1 and 2 and a readout (termination) chassis in Sector 2 I/C Alcove.
13. Variable Voltage Substation Circuit Breaker Controls (V1A and V1B) as well as the Reference and de-Q'ing systems for all modulators in Sectors 1 and 2.

II. KLYSTRON PERFORMANCE

W. R. Fowkes, J. V. Lebacqz, J. Jasberg

A. GENERAL PERFORMANCE

In general, the performance of the klystrons in Sectors 1 and 2 has been good. Three tubes have failed in the gallery since operation began there a year ago. Nine tubes were moved due to faulty ancillary equipment and of these, one failed during a subsequent test.

The eighteen klystrons in the first two sectors were operated stably as a group, up to a reference voltage of 114 volts. In the earlier stages of sector operation, the operating levels were limited by the waveguide vacuum conditions, uncertainty in voltage and power measurements, and finally, the variation from station to station in measured beam voltages for a given reference voltage. Of much concern is the last item, which has not been completely resolved.

B. POWER OUTPUT

It is felt that the measurement of klystron power output is reasonably good. Upon removal of klystrons, some of the couplers have been recalibrated using a different calibration technique. The results have agreed with the original calibrations to better than 0.2 dB. The power meters are occasionally cross-checked against one another.

Typical klystron power outputs and beam voltages are shown in Table II-I and the average of all peak power outputs from klystrons 1-2 through 2-8 are plotted as a function of reference voltage in Fig. II-1. The klystron power output appears to be relatively independent of pulse repetition rate.

C. BEAM VOLTAGE

Unfortunately, the klystron beam voltage does not appear to be a consistent function of reference voltage. The fact that the power output appears to be essentially independent of pulse repetition rate suggests that there may be an error in the voltage measurement from one repetition rate to another. A series of tests are being planned which hopefully will resolve this uncertainty.

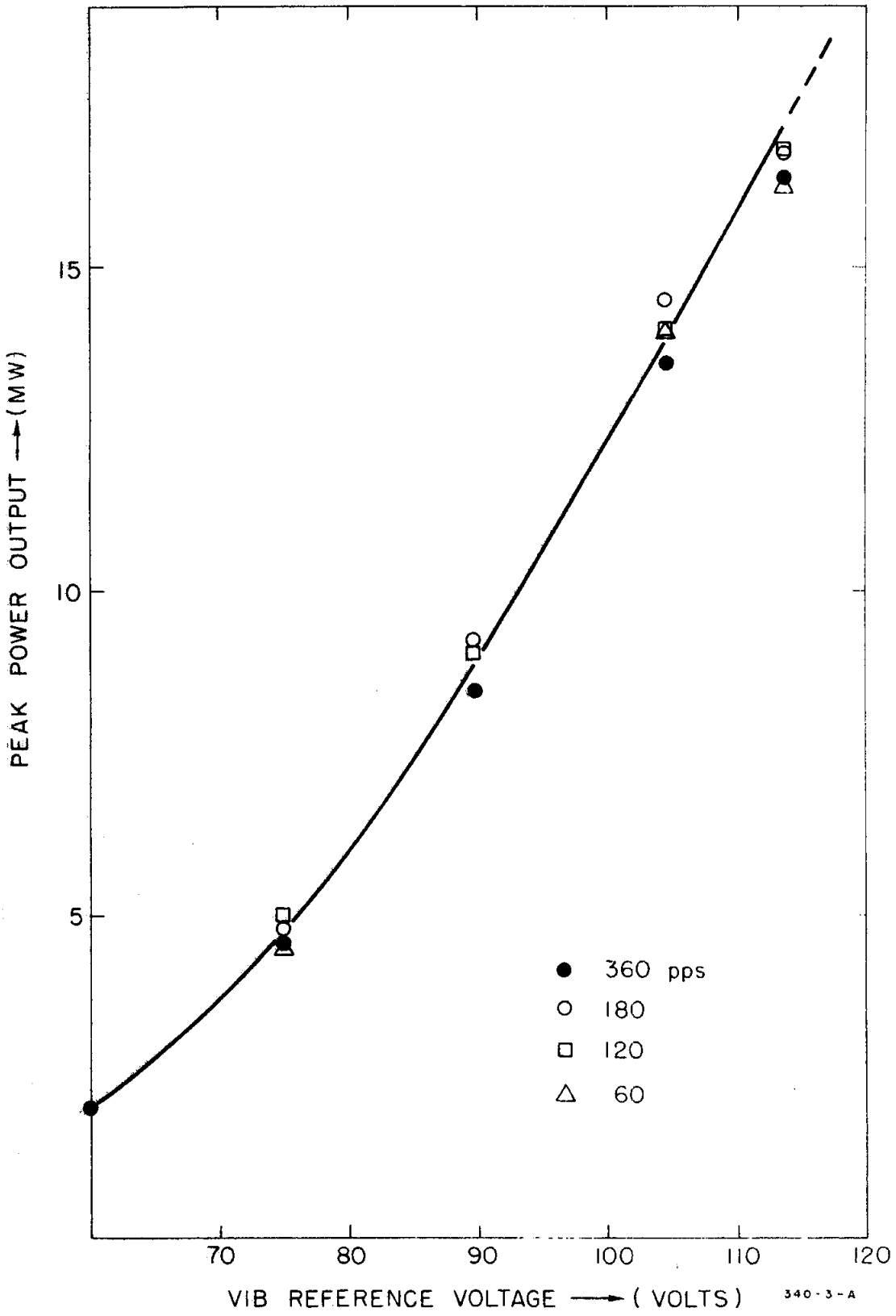

FIG. II-1 Averaged klystron peak power output vs. V1B reference voltage, klystrons 1-2 to 2-8.

The data obtained prior to and during the endurance run of June 14-18 suggests that a more systematic approach for setting up the de-Q'ing is necessary. During the past year, the de-Q'ing has been set at various levels at each station and at present the tracking between the reference voltage, the variable voltage substation voltage and the klystron beam voltage is not consistent. Data on klystron power output and beam voltage was taken at four different pulse repetition rates. There are variations as high as 10% in beam voltage from station to station at a given reference voltage and repetition rate, as well as variations as high as 5% when the pulse repetition rate is changed from 60 to 360. It can be seen from Fig. II-2 that the slope of the curve of beam voltage versus reference voltage at 360 pps differs noticeably from the slope at the lower three pulse repetition rates. Furthermore, the beam voltage was relatively insensitive to changes in pulse repetition rate for 60, 120 and 180 pps. Sector 2 exhibits the same behavior.

D. REFLECTED ENERGY PROTECTION

The reflected energy portion of the modulator-klystron protection unit was initially adjusted to disable the modulator when power reflections of the order of 0.5 MW occurred. There were several stations which repeatedly responded to these faults without noticeable improvement and it was decided to relax the trip level to 2 MW reflected power. It is felt that there is still adequate protection for the klystron output window at this higher level. Also, the outages due to lower level and harmless reflections are curtailed, and the output waveguide processing time is reduced considerably.

E. PHASE STABILITY

The possibility of klystron output phase instability due to the presence of the waveguide valve was investigated. Of concern was the possible interaction between harmonic reflections from the valve and the output phase at the operating frequency. The phase display setup allowed easily discernible phase instabilities as small as 0.1 electrical degrees to be detected, if present. The measurements were made on all eighteen klystrons at an average beam voltage of 230 kV. Photographs

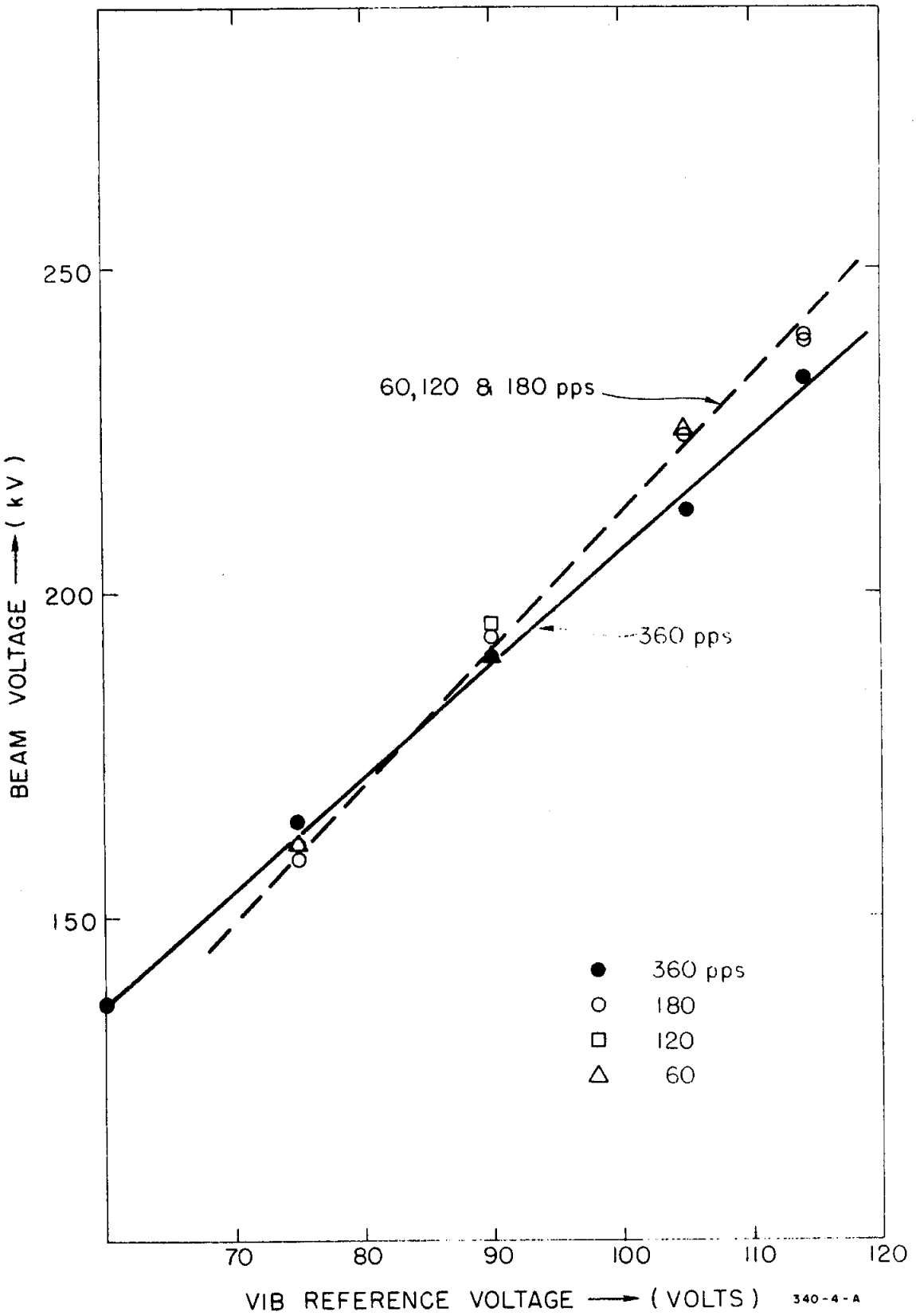

FIG. II-2 Averaged klystron beam voltage vs. V1B reference voltage, klystrons 1-2 to 1-8.

were taken of the beam voltage pulse top, the detected rf output pulse, and the phase display for each klystron. Close inspection of the pictures revealed no phase variations in excess of 0.2 electrical degrees which were not directly related to the deviation from flatness of the beam voltage pulse top or the beam amplitude jitter. At the time the measurements were made (approximately March 26), the phase variation across the rf pulses due to the non-flatness of the beam voltage pulses averaged about two electrical degrees.

TABLE II.-I.

TYPICAL KLYSTRON POWER OUTPUT AND BEAM VOLTAGE

Pulse Repetition Rate: 360 pps

Station	90 Volts Ref.		105 Volts Ref.		114 Volts Ref.	
	V_o (kV)	P_o (MW)	V_o (kV)	P_o (MW)	V_o (kV)	P_o (MW)
1-2	194	8.8	215	15.8	235	19.1
1-3	196	8.5	215	13.5	235	15.9
1-4	194	6.3	212	10.8	232	14.5
1-5	199	7.9	217	13.6	237	17.1
1-6	195	8.6	212	14.4	233	17.8
1-7	190	9.1	208	14.5	225	17.7
1-8	194	8.6	213	12.9	232	15.6
2-1	185	7.6	198	12.4	217	15.4
2-2	200	9.7	215	16.0	234	19.4
2-3	195	8.6	210	13.9	225	17.7
2-4	193	8.6	208	12.0	227	15.0
2-5	196	9.8	210	13.9	230	16.3
2-6	190	8.8	208	13.3	226	16.0
2-7	191	8.7	205	13.3	225	15.0
2-8	186	7.4	200	12.5	220	15.4
Average	193	8.45	209	13.5	231	16.3
1-1A	225	13.5				
1-1B	223	16.8	VIA Reference Voltage = 116 volts			
1-1C	225	15.9				

III. VOLTAGE AND PHASE STABILITY OF KLYSTRONS

R. McConnell

Measurements were made at each klystron in Sector 1 of the following characteristics:

(a) Klystron beam voltage

(b) Phase at the klystron output

(c) Phase at the accelerator section output

(d) Klystron rf output envelope

(e) Accelerator section rf output envelope

For klystron 1-1A, 1-1B and 1-1C, items (c) and (e) were measured at the output of the 10-foot sections fed by those klystrons.

For klystrons 1-2 through 1-8, items (c) and (e) were measured at the output of the third section in each girder.

The block diagram of Fig. III-1 shows the points in the system where the phase measurements were made.

For rf envelope measurements, the reference arm of the bridge was disabled and the active arm was used simply as an rf detector.

In Fig. III-1, point A provides a cw reference signal to one arm of a phase bridge. When point B is connected to the other arm of the bridge, the bridge measures phase across the sub-booster and klystron. When point C is connected, the bridge measures phase across the sub-booster, klystron, and accelerator section. By disconnecting point A, rf amplitude detection at points B or C can be accomplished.

As shown in the photographs in Figs. III-2 and 3, amplitude and phase variations in the sub-booster are negligible compared to the amplitude and phase variations of the klystrons. Therefore, even though the sub-booster is in the phase and amplitude path, the variations of phase and amplitude may be attributed entirely to the klystron and accelerator sections.

In Figs. III-2 through 13, the following calibrations apply:

Phase: 1.75° per cm

Beam Voltage: 1/2% per cm.

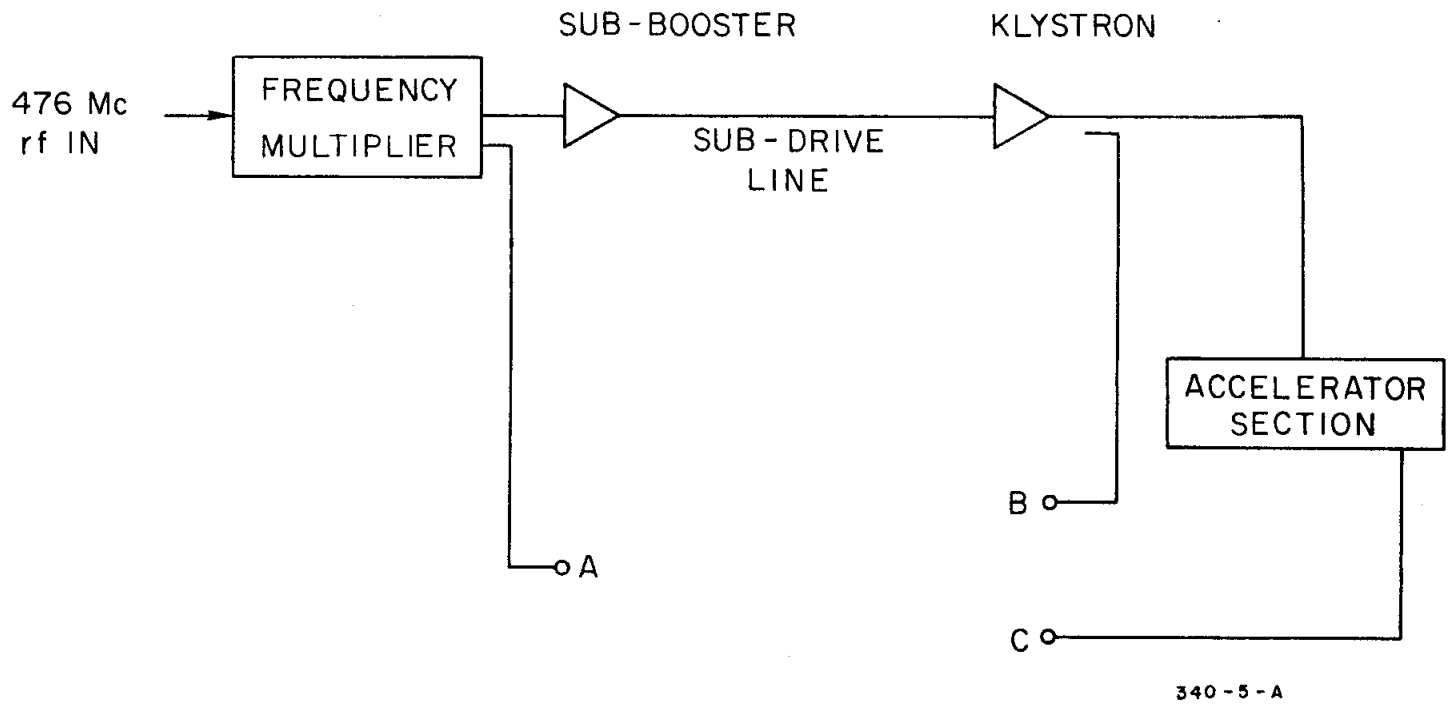

FIG. III-1 Circuit layout for amplitude and phase measurements across klystron and accelerator section.

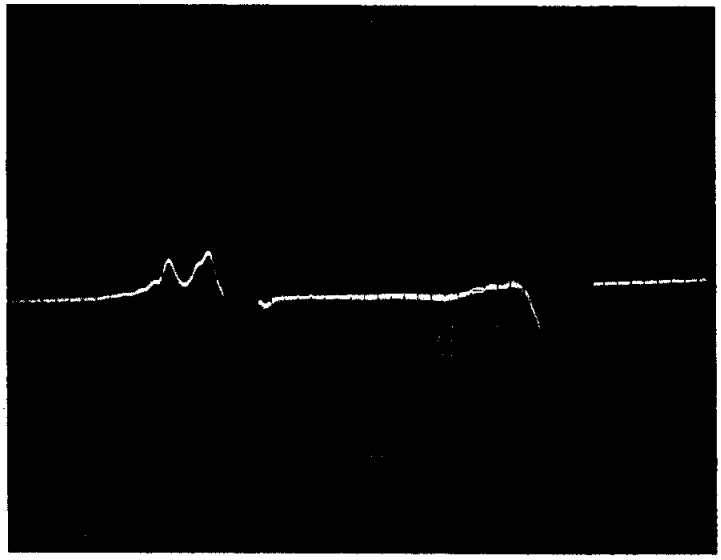

FIG. III-2 Phase at output of sub-booster klystron.

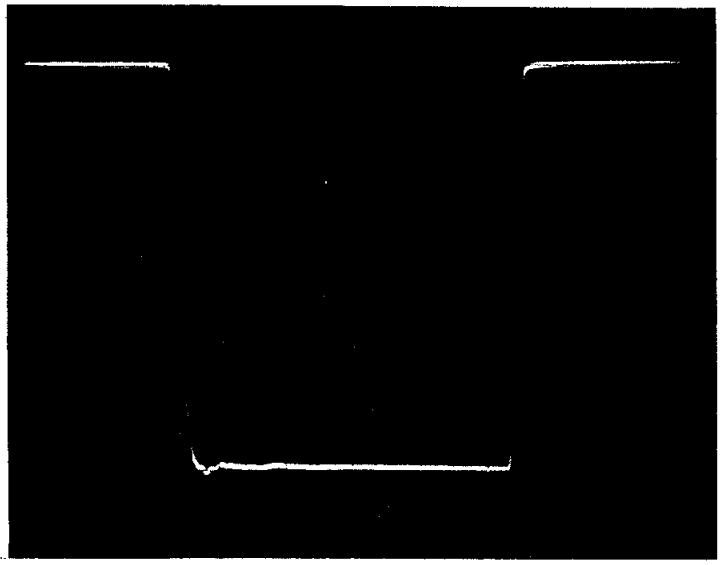

FIG. III-3 RF envelope at output of sub-booster klystron.

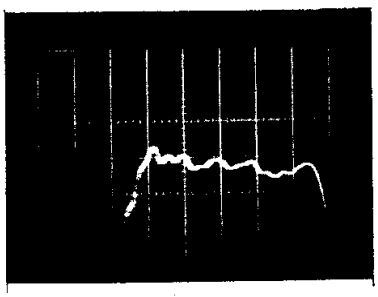

(a)

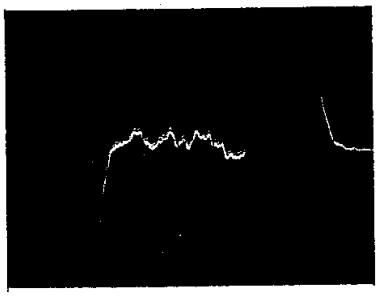

(b)

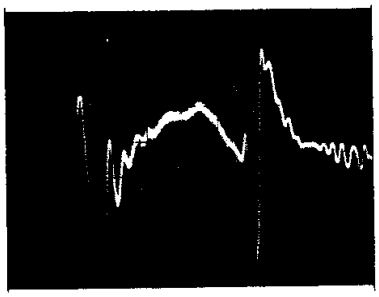

(c)

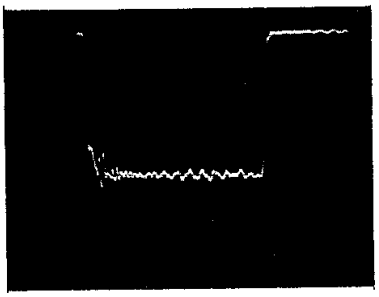

(d)

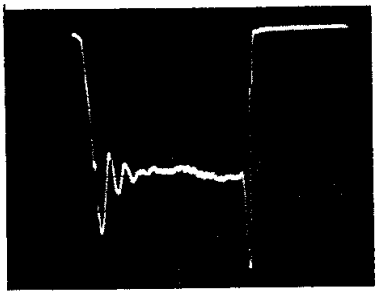

(e)

FIG. III-4 KLYSTRON 1-1A

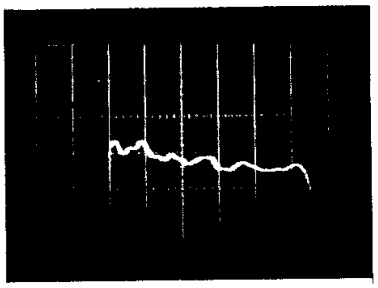

(a)

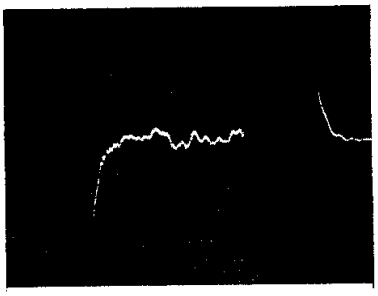

(b)

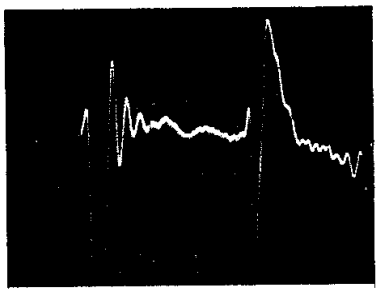

(c)

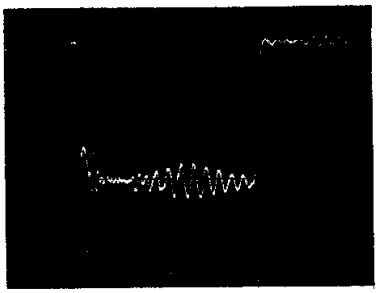

(d)

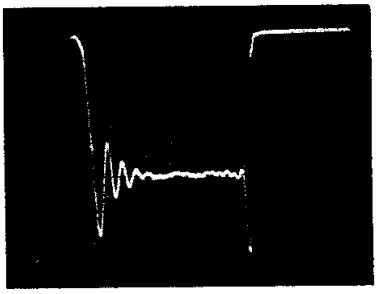

(e)

FIG. III-5 KLYSTRON 1-1B

(a) Klystron beam voltage.
(b) Phase at output of klystron.
(c) Phase at output of accelerator section.
(d) RF envelope at output of klystron.
(e) RF envelope at output of accelerator section.

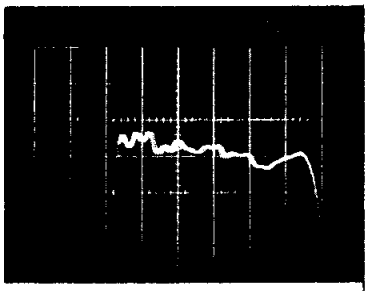

(a)

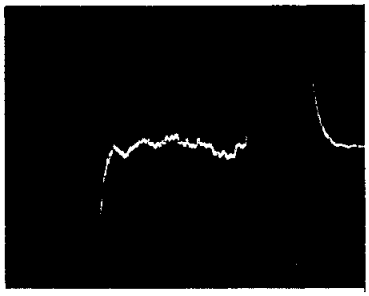

(b)

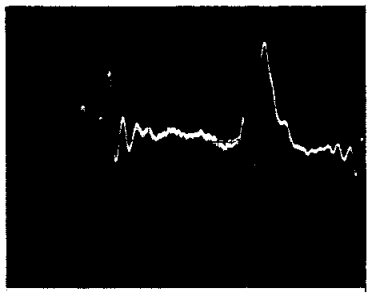

(c)

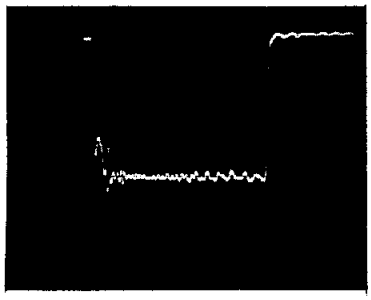

(d)

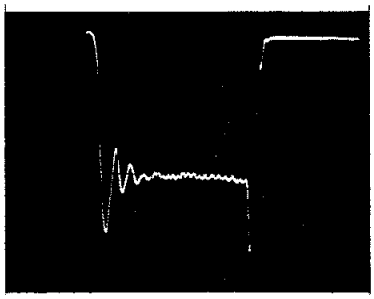

(e)

FIG. III-6 KLYSTRON 1-1C

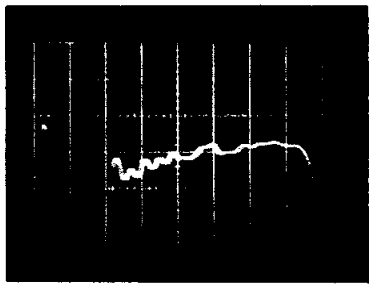

(a)

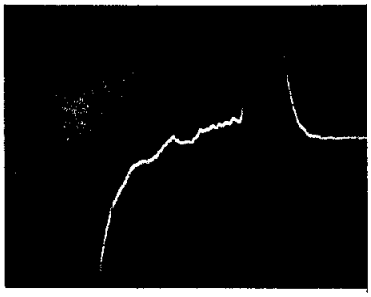

(b)

(c)

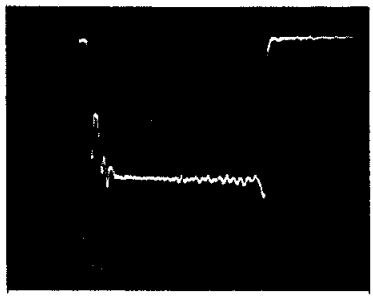

(d)

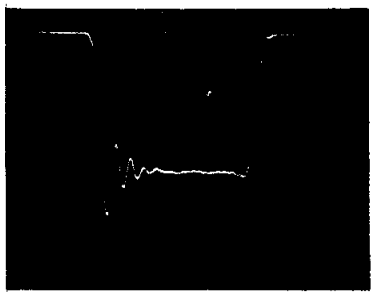

(e)

FIG. III-7 KLYSTRON 1-2

(a) Klystron beam voltage.
(b) Phase at output of klystron.
(c) Phase at output of accelerator section.
(d) RF envelope at output of klystron.
(e) RF envelope at output of accelerator section.

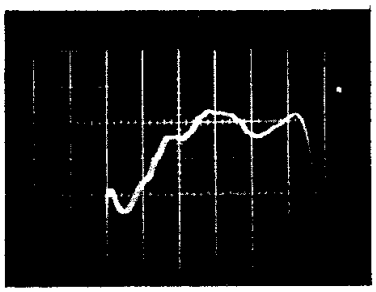

(a)

(b)

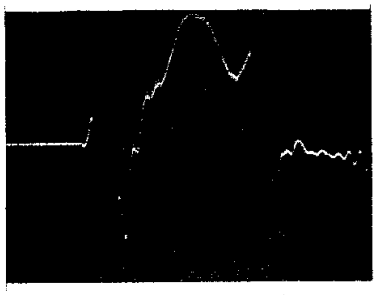

(c)

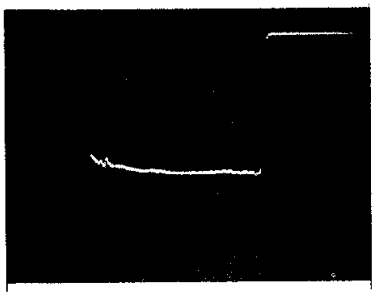

(d)

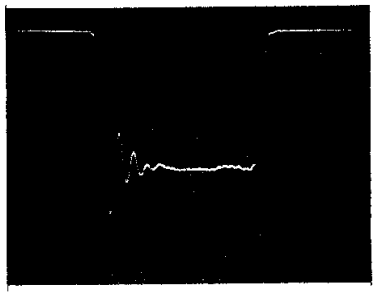

(e)

FIG. III-8 KLYSTRON 1-3

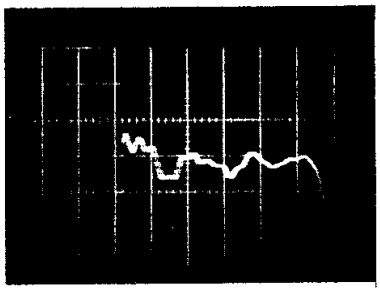

(a)

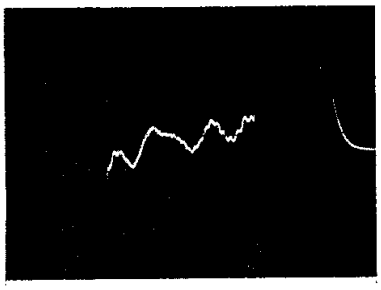

(b)

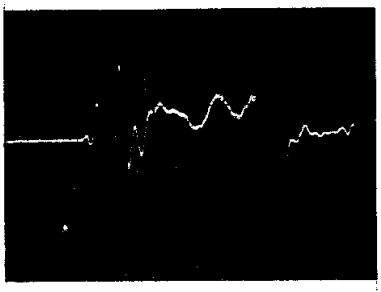

(c)

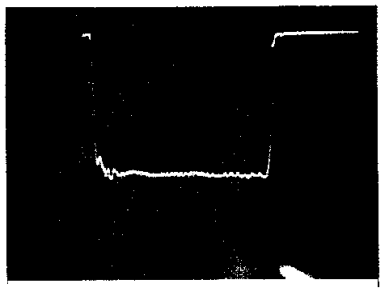

(d)

(e)

FIG. III-9 KLYSTRON 1-4

(a) Klystron beam voltage.
(b) Phase at output of klystron.
(c) Phase at output of accelerator section.
(d) RF envelope at output of klystron.
(e) RF envelope at output of accelerator section.

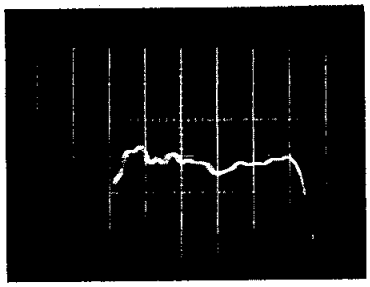

(a)

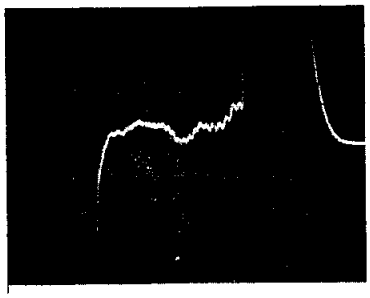

(b)

(c)

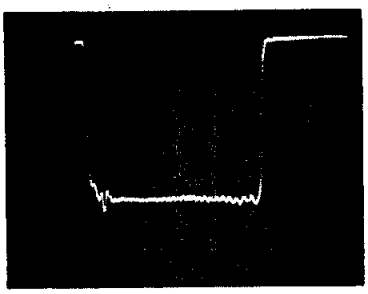

(d)

(e)

FIG. III-10 KLYSTRON 1-5

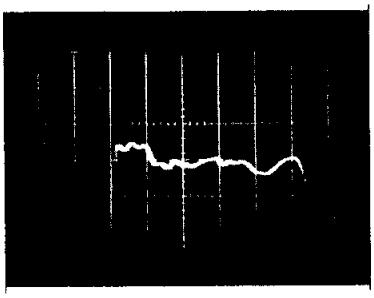

(a)

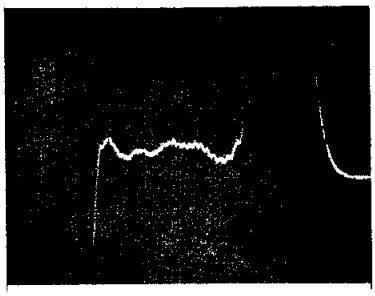

(b)

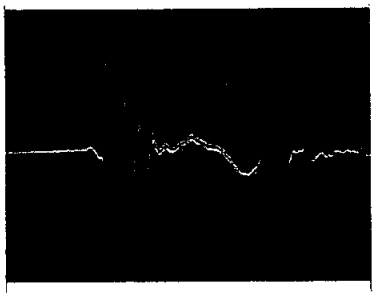

(c)

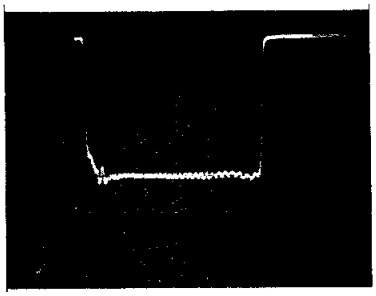

(d)

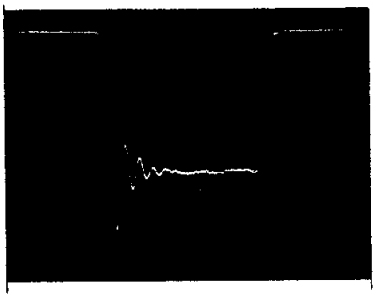

(e)

FIG. III-11 KLYSTRON 1-6

(a) Klystron beam voltage.
(b) Phase at output of klystron.
(c) Phase at output of accelerator section.
(d) RF envelope at output of klystron.
(e) RF envelope at output of accelerator section.

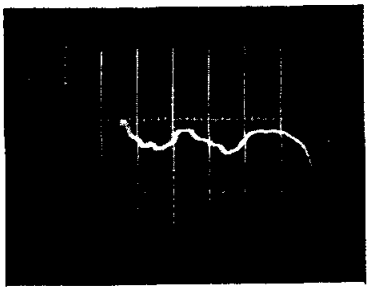

(a)

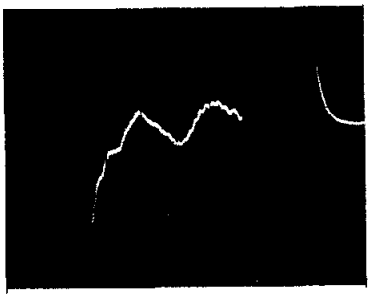

(b)

(c)

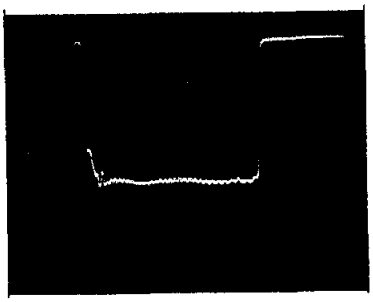

(d)

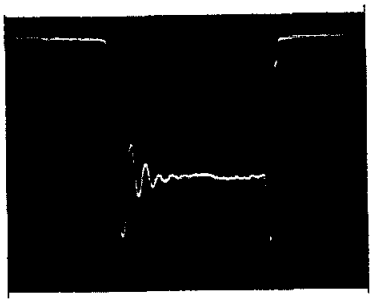

(e)

FIG. III-12 KLYSTRON 1-7

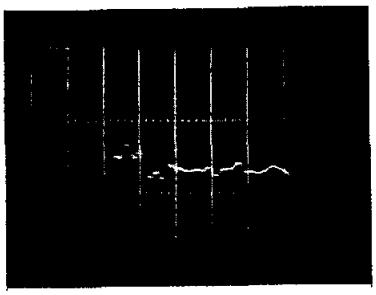

(a)

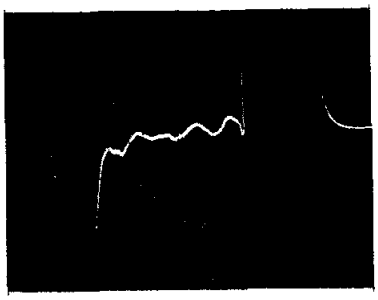

(b)

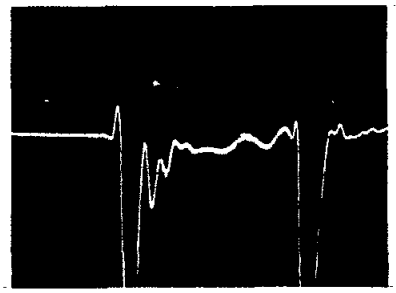

(c)

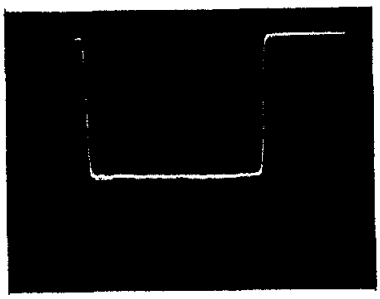

(d)

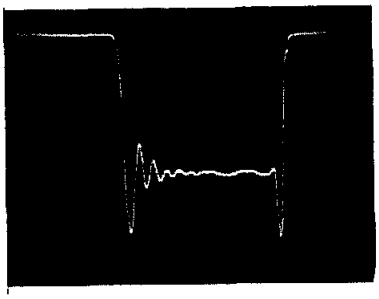

(e)

FIG. III-13 KLYSTRON 1-8

(a) Klystron beam voltage.
(b) Phase at output of klystron.
(c) Phase at output of accelerator section.
(d) RF envelope at output of klystron.
(e) RF envelope at output of accelerator section.

Table III-I gives klystron operating voltages, power outputs, and the computed phase shift as a function of beam voltage.

TABLE III-I

Klystron Data

Klystron	Power Output	Beam Voltage	$\Delta\varphi$ for $\frac{\Delta V}{V} = 1\%$
1-1A	18.2 MW	221 kV	4.5°
1-1B	19.1	226	4.5
1-1C	19.5	230	4.5
1-2	11.1	213	4.6
1-3	13.5	217	4.6
1-4	14.5	213	4.6
1-5	12.4	211	4.6
1-6	13.4	210	4.7
1-7	13.3	211	4.6
1-8	15.6	211	4.6

From observation of the photographs, the following conclusions may be drawn:

1. There is good correlation between the variations in beam voltage and phase of the klystron.
2. The phase at the output of the accelerator sections shows the phase shift from the klystron, with phase shifts due to the Leiss effect (pass-band filter nature of the accelerator section) superimposed.
3. The photographs of klystron rf envelopes are not of sufficient scale magnification to permit observation of amplitude variations corresponding to beam voltage variations.
4. The photographs of accelerator section output rf envelopes show the amplitude modulation due to the Leiss effect.

As an example of the validity of conclusion (1), we compute the phase shift in klystron 1-7 between the last downward peak and the last upward peak at the right of the beam voltage photograph:

$$\Delta\varphi = 0.7 \text{ cm} \times 4.6°/\% \times 1/2\%/\text{cm} = 1.6°$$

From the photograph of phase variation we obtain

$$\Delta\varphi = 1.2 \text{ cm} \times 1.75^{\circ}/\text{cm} = 2.1^{\circ}$$

Hence, within the accuracy of the voltage and phase measurements and their interpretation, there is reasonable agreement between the measured and computed values.

Although not shown in the photographs, the following observations were made:

1. The fine structure and ringing evident in klystrons 1-1A and 1-1B were apparently the result of RFI and ground loops associated with the modulators interfering with the phase measurement instrumentation.
2. Pulse-to-pulse jitter of amplitude and phase was negligible (a few tenths of a degree).
3. Changing repetition rate had no effect on short-term phase stability. The pulse-to-pulse jitter was less than one degree.

IV. REMARKS ON OPERATION OF PHASING SYSTEM

H. Hogg, A. Wilmunder, E. Farinholt

With the exceptions of Sections 1-A, -B and -C, the automatic phasing system was used continually and exclusively for optimizing klystron phasing during Sectors 1 and 2 tests. No attempt was made to phase 1-A, -B and -C automatically, although this will be done by a subprogrammer in the Sector 1 alcove when the machine is complete.

The initial system for remote-manual operation of all phase shifters (including 1-A, -B and -C) proved to be unsatisfactory due to the low starting torque characteristic of the two-phase servo motors. It was modified so that, in order to obtain positive slow phase adjustment, the two-phase motor was "stepped" around by the application of half-wave pulses at the rate of 3 per second. For more rapid phase rotation, the original amplitude-controlled 60-cycle system has been retained. In those cases where a more precise manual control and readout will be required frequently, I$\varphi\alpha$* and control phase-shifter units will be specifically modified to include a clutch-coupled dc motor drive with a coupled potentiometer readout, in addition to the standard two-phase motor.

The automatic phasing system did not work very well at first because the group delays in the accelerator sections and rf cabling caused the beam-induced and klystron pulses to lag behind the sub-drive line reference pulses by as much as 1.2 μsec. The pulse overlap was insufficient to permit a reliable phase comparison to be made. The problem was solved by using a cw reference signal, coupled off the varactor multiplier output. It was found that a cw reference signal as low as 0.5 mW per diode was sufficient to operate the phasing system reliably. Toward the end of the test period, a switch was added in Sector 2 which enabled the phase

*isolator/phase-shifter/attenuator package

tracking between the beam and the sub-drive line to be continuously monitored. This worked well, and is discussed further in Section V.

As with the beam position monitors, most of the troubles with the phasing system stem from the use of thermionic diode detectors. Their dynamic power range is limited at the lower end by the departure from linearity and at the upper end by cathode overloading, which causes the characteristic of each diode to change rapidly by a different amount, unbalancing the differential output. This rapid change in balance as the programmer switched from klystron to klystron was frequently observed. Often the resultant unbalance was sufficient to overload the input to the gated voltmeter, causing the klystron to be incorrectly phased. The only cure was to attenuate the input signal to the hybrid ring and diodes as much as possible. The limit here was the requirement that the signal induced by a 1-milliamp beam should be sufficient to operate the phasing system. A 1-milliamp beam gives approximately 50 milliwatts at the input to the rf detector panel. It was found that the rf power could be reduced to 1 milliwatt per diode before non-linearity became a problem.

Thus adjusted, the automatic system operated very satisfactorily. Degree scales were attached to the $I\varphi\alpha$ drums to check the re-setting accuracy of the automatic system. Repeated tests showed that most klystrons were reset to within 1 degree of their previous position, with the greatest error being 3 degrees. Tests in which klystrons were dephased manually by ± 5 degrees and ± 10 degrees also indicated that the optimum spectrum was produced by the automatic system. The time taken for automatic phasing was approximately 1 minute for each sector.

The machine was run continuously from 16.30 hours May 25 to 24.00 hours May 27. During this time the automatic phasing systems in Sectors 1 and 2 were each operated 29 times. On four occasions it was necessary to rebalance the diodes prior to phasing. The beam spectrum at the end of Sector 2 was recorded before and after each rephasing operation. Generally, rephasing improved the beam peak current energy by 10 to 30 MeV, depending on the drift which had occurred since the previous phasing operation.

The results are summarized (see next section) in Figs. V-1 and V-2, which record the phase-shifter positions in each Iφα unit after rephasing. The larger changes which occurred during the afternoon and evening of May 26 were due to changes in klystron operating conditions.

It is apparent that the problem of diode drift was not adequately solved. Long-term drift (over a period of days) would deteriorate the video balance beyond the 1/2-volt acceptance of the gated voltmeter. This problem was greatly reduced by adding a 10-dB attenuator in the video output line from the diode balancing network, and increasing the servo amplifier gain to compensate for it. Manual rebalancing was required on only one occasion after this modification, but further testing will be necessary before it can be determined whether this solution is adequate.

The rapid drift due to cathode overloading was still apparent when the machine repetition rate was increased to 360 pulses per second. The problem was accentuated by the variation in length and insertion loss of the phasing cables. The longest cable (from girder 1) has 4 dB more loss than the shortest (from girder 5). The difficulty has been removed by providing two alternative paths through the rf detector panel from the phasing cable to the hybrid ring. One contains a 20-dB attenuator and the other contains a phase-shifter to equalize the electrical lengths. Coaxial switches, operated by the existing programmer logic, send the low-power beam induced signal through the phase-shifter path and the high power klystron signal through the attenuator path. Further tests will be performed to check the phase stability of the two alternative paths.

V. LONG-TERM PHASE STABILITY OF THE DRIVE SYSTEM

H. Hogg, D. Farkas

On 27 May 1965, from 14.30 until 24.00 hours, Sectors 1 and 2 were automatically phased at approximately hourly intervals. The air temperatures in the middle of each Sector, about 5 feet above the ground, were recorded at the same time (see Figs. V-1 and V-2).

Over this period of time, the air temperature dropped approximately 18°F. Each phasing operation caused the first I$\varphi\alpha$ in each sector to increase its phase shift and the last I$\varphi\alpha$ in each sector to decrease its phase shift. The changes with time and temperature for all I$\varphi\alpha$'s can be seen in Figs. V-1 and V-2.

It has to be concluded that both sub-drive lines increased in electrical length as the temperature dropped. The indicated increases are 36 degrees in Sector 1 and 20 degrees in Sector 2. The reasons for the magnitudes and signs of these changes are not clear. The incompleteness of the support, anchoring water-cooling and insulation of the drive-line package makes it difficult to arrive at a satisfactory explanation.

In Fig. V-2, the curve labeled φ_c shows how the phase of the middle of the Sector 2 sub-drive line changed with respect to the beam. Since this measurement was made only at Sector 2, it is not possible to say whether the phase drift was due to the sub-booster or the injector. However, when such a measurement is made simultaneously in several sectors, it will be possible to draw conclusions about sub-booster and injector phase stability.

The stability of the master oscillators and the main boosters was very good. One of the main boosters suffered one major failure (loss of a rectifier stack). In addition, both main boosters still experience occasional trip-outs which are being investigated.

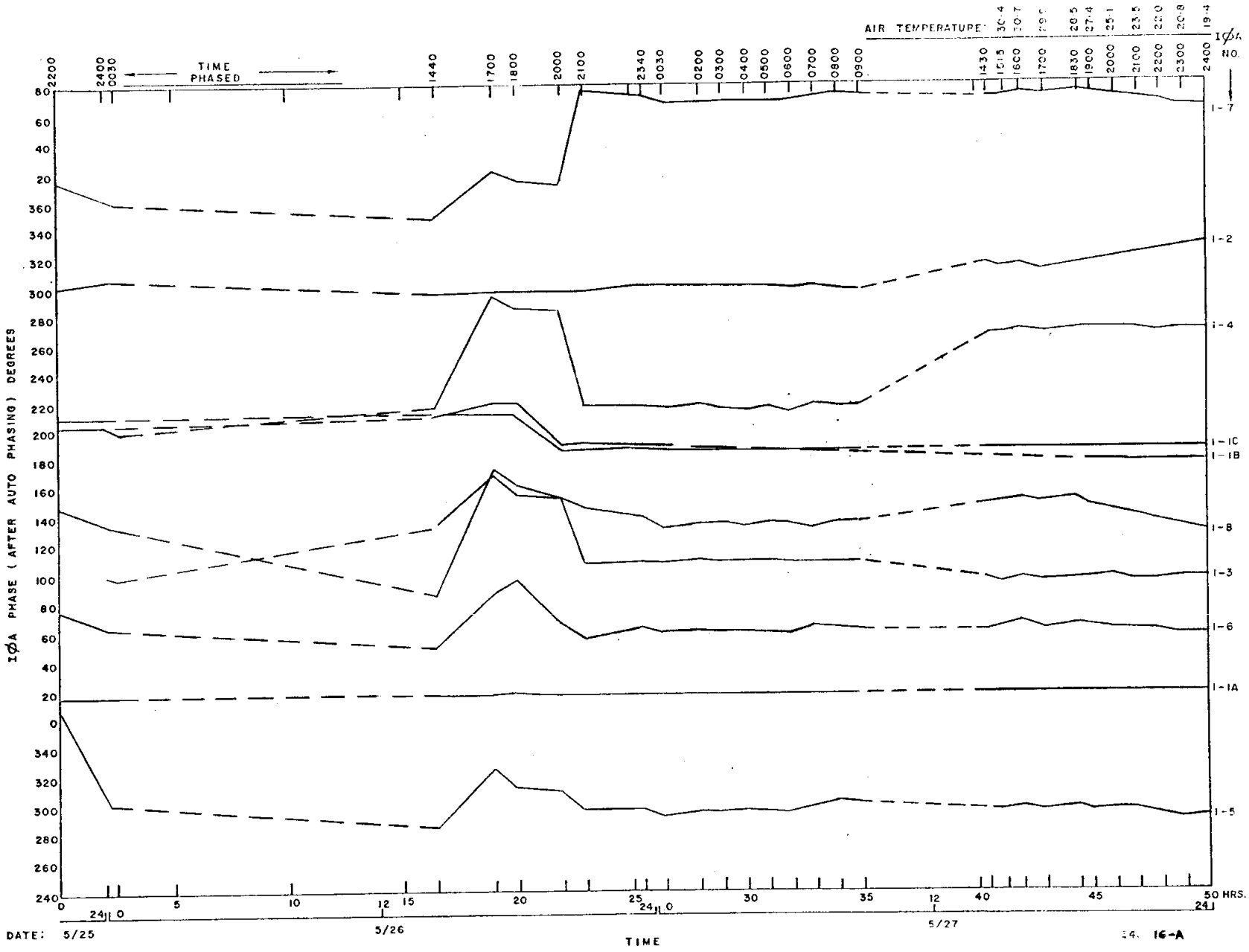

FIG. V-1 Sector 1 phasing tests, May 25-26-27, 1965.

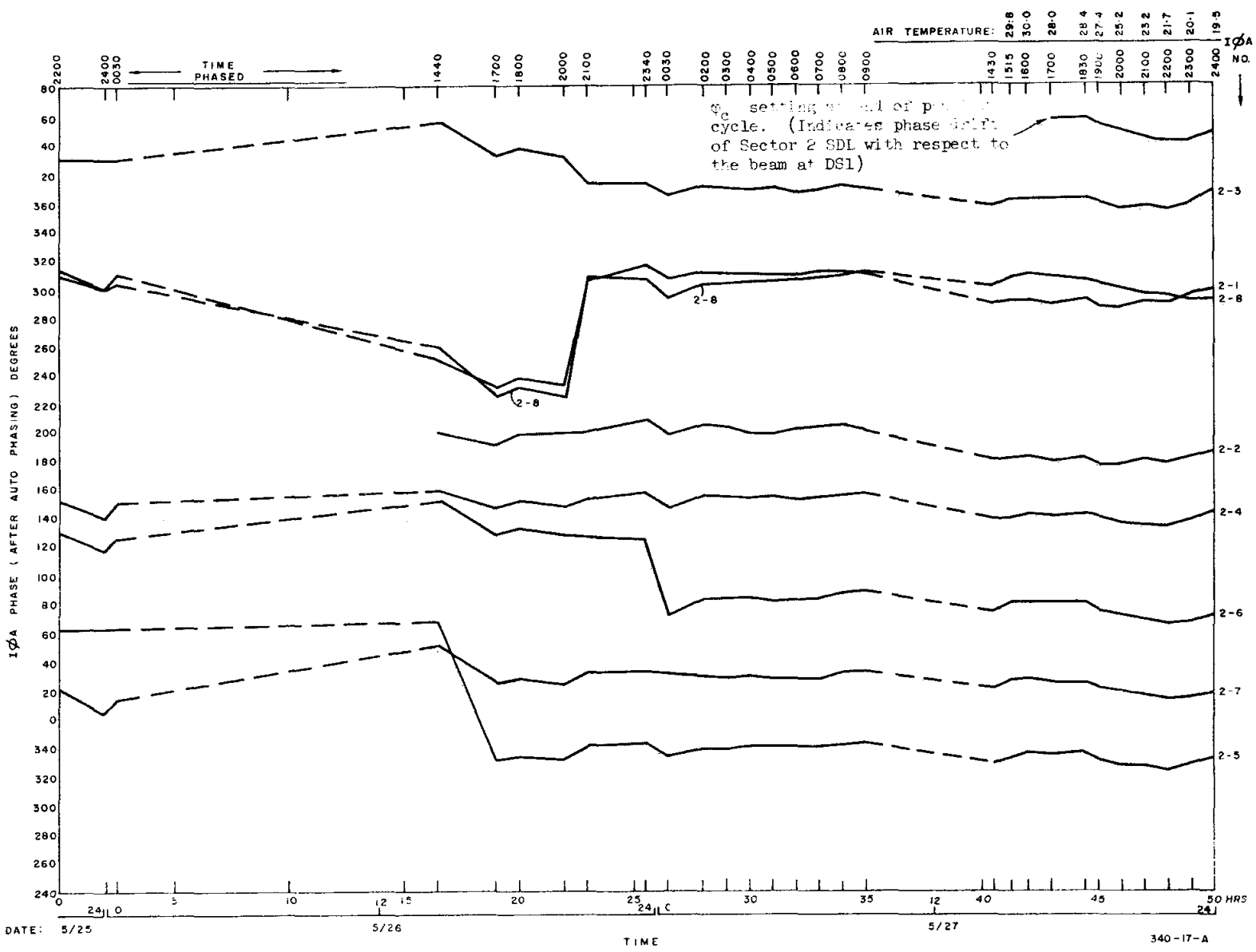

FIG. V-2 Sector 2 phasing tests. May 25-26-27, 1965.

VI. TYPICAL ENERGY SPECTRA

A. Wilmunder, E. Farinholt, G. Loew

The purpose of the tests consolidated under this section was to evaluate the effect of phasing, changes in repetition rate, frequency tuning, temperature adjustments, beam loading and trigger timing on the energy spectra obtained at the end of Sector 2. Before taking data at that point, a set of beam measurements was also made at BAS-1 at the 40-foot point. These are described in paragraph VI.A below.

A. TYPICAL ENERGY SPECTRA AT BAS-1

To set up the beam and tune the first three sections, 1-A, 1-B, and 1-C, a routine procedure was followed. First, the beam optics was optimized by adjusting the gun current, the two gun lenses and the prebuncher power and phase, with klystron 1-A in "ACCELERATE" and klystrons 1-B and 1-C in "STANDBY." After having obtained a well steered current pulse at the 30-foot toroid and beam position monitors, klystron 1-B was returned to "ACCELERATE" and its phase shifter was adjusted until the narrowest energy spectrum was observed on the scope. Since the electron bunches were not riding on crest in the first section, this adjustment of the phase of klystron 1-B did not give the maximum energy setting but rather achieved phase closure for the first two klystrons combined. Then klystron 1-C was put into "ACCELERATE" and its phase was adjusted for maximum energy contribution. With typical output powers of approximately 17 megawatts from these three klystrons, it was found that the corresponding high energy electrons amounted to about 34, 66 and 107 MeV. To study the effect of frequency variations on these first three sections, a variety of photographs of scanned spectra were taken in the vicinity of 107 MeV. These are shown in Fig. VI-1. The best spectrum corresponded to a frequency of 2856.00 Mc/sec. Frequency variations of $\pm$ 0.1 Mc/sec showed that although the spectrum shape deteriorated (partly because the various phase shifters were not readjusted), the net energy decrease amounted to less than the width corresponding to four scanning foils. These foils each have a 1/2% energy width; hence the maximum energy decrease was at the most 2% or approximately 2 MeV.

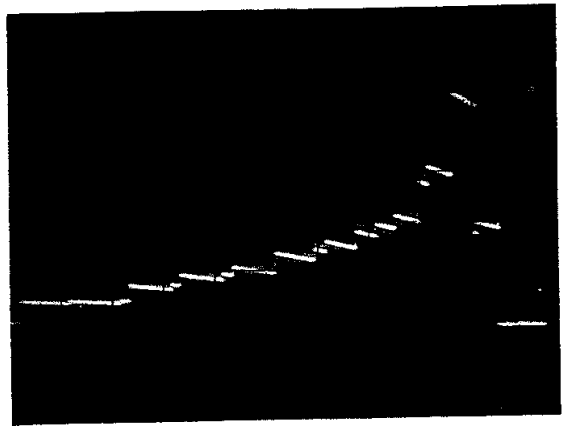

(a)

2856.00 Mc/sec

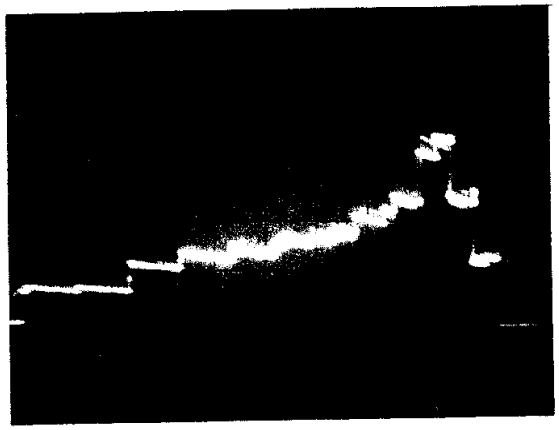

(b)

2856.05 Mc/sec

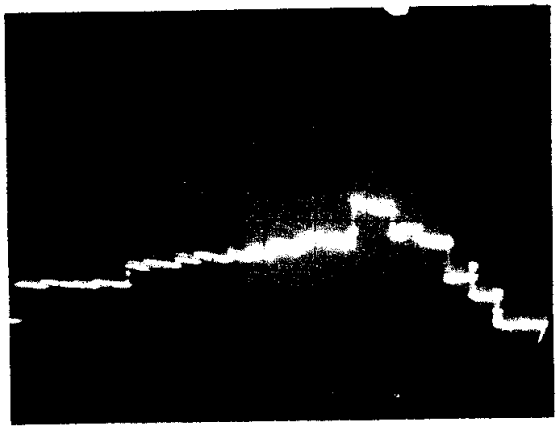

(c)

2856.10 Mc/sec

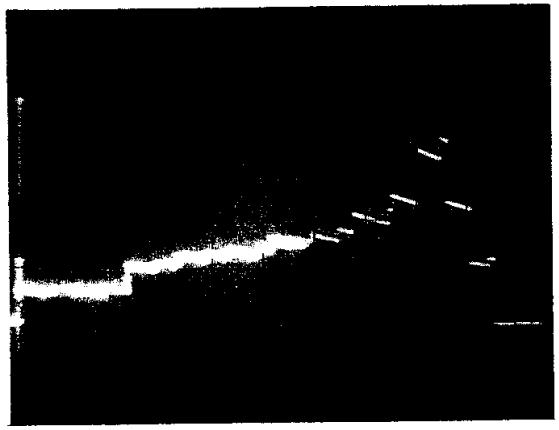

(d)

2855.95 Mc/sec

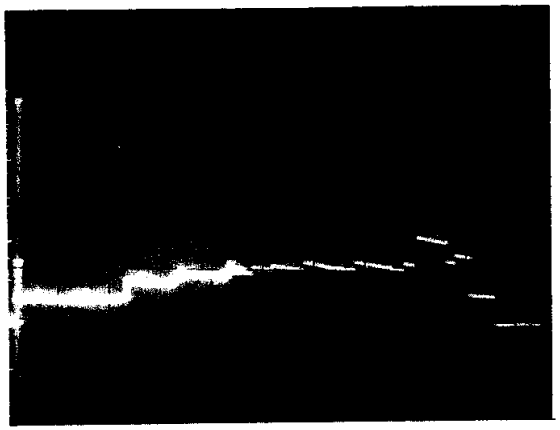

(e)

2855.90 Mc/sec

FIG. VI-1 Energy spectra at BAS-1 as a function of frequency.

Since in all subsequent measurements the rest of the machine was always rephased with respect to the 30-foot accelerator, it can be said that these energy changes were entirely negligible as compared to the variations observed and described in the subsequent subparagraphs.

B. EFFECT OF PHASING

The effect of phasing is illustrated in Fig. VI-2. In this case, spectrum 1 was obtained at the end of Sector 2 after the frequency had been adjusted from 2855.9 to 2856.0 Mc/sec without rephasing. Then, spectrum 2 was obtained after phasing and spectrum 3 after rephasing a second time. These curves illustrate the increase in energy obtained and the reproducibility of the phasing operation as well as the overall stability of the machine at that time. Considering that the magnet current sweep is operated by hand, a better overlap of the xy-recorder plot can hardly be expected.

C. EFFECT OF REPETITION RATE

This test was done to study the effect of changing the repetition rate at a fixed input water temperature of $T = 109.7 \pm 0.1^{\circ}F$ for both Sectors 1 and 2 and a fixed frequency of 2855.95 Mc/sec. In Fig. VI-3, spectrum 1 was taken at 360 pps, spectrum 2 was taken at 60 pps before rephasing, and spectrum 3 was taken after rephasing. It is seen that decreasing the repetition rate without changing the frequency, and hence without reachieving synchronism, implied a net energy loss of about 30 MeV or roughly 0.25% in energy. This result will be discussed further in the next paragraph.

D. EFFECT OF FREQUENCY CHANGES

The spectra shown in Fig. VI-4 were taken at a fixed repetition rate of 360 pps for the klystrons, a beam repetition rate of 60 pps, and various values of frequency. In all cases the temperature was $109.7^{\circ}F$. Spectrum No. 1 was taken at 2856.00 Mc/sec, spectrum No. 2 at 2855.95 Mc/sec, spectrum No. 3 at 2855.90 Mc/sec and spectrum No. 4 at 2855.925 Mc/sec. In all cases, the machine (except for the first three klystrons) was entirely rephased after each frequency adjustment. Within the accuracy of the measurements, it is seen that maximum energy was obtained for a frequency between 2855.95 and 2855.925 Mc/sec.

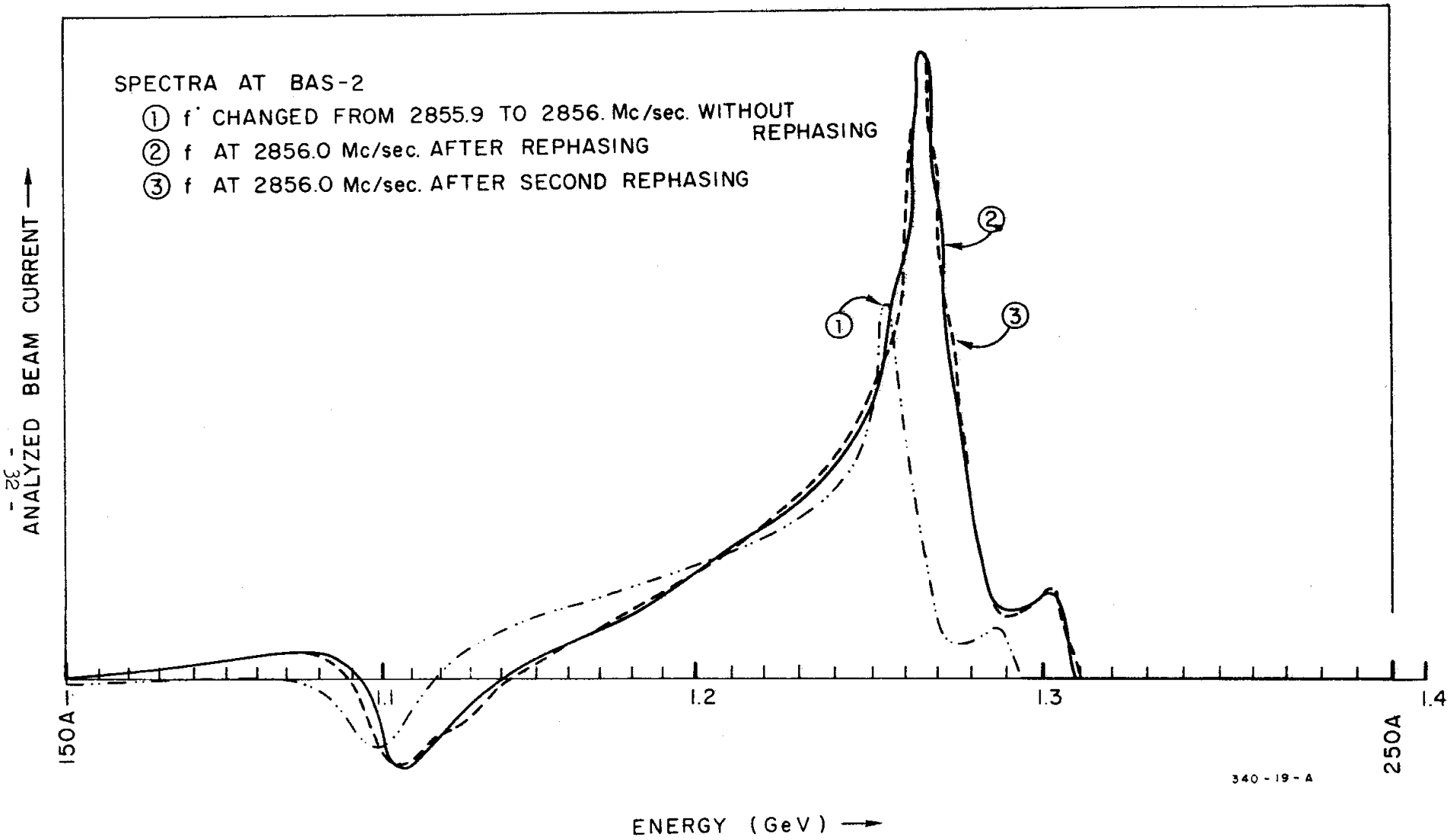

FIG. VI-2 Effect of phasing on energy spectrum.

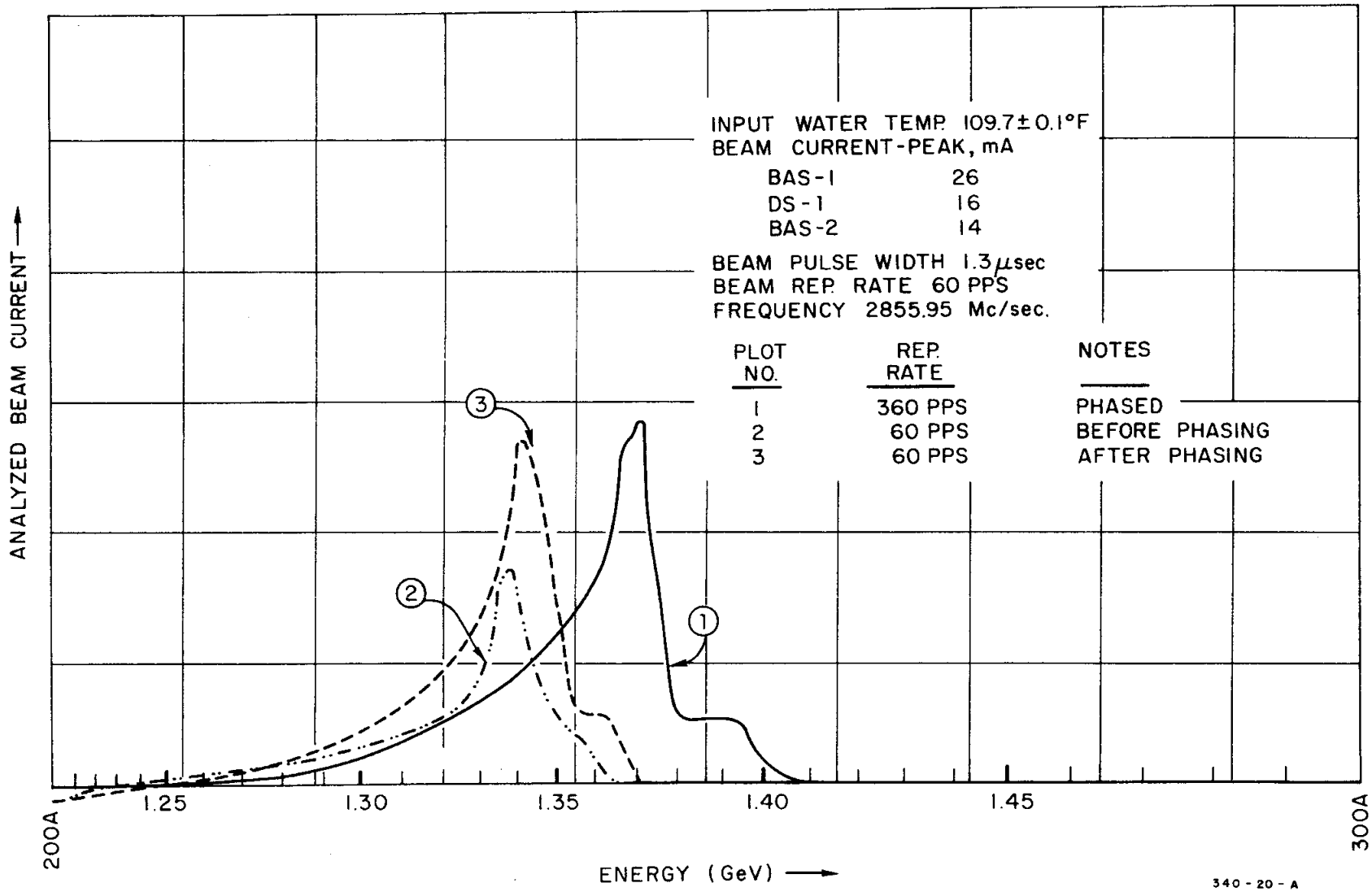

FIG. VI-3 Effect of changing repetition rate at fixed temperature and frequency.

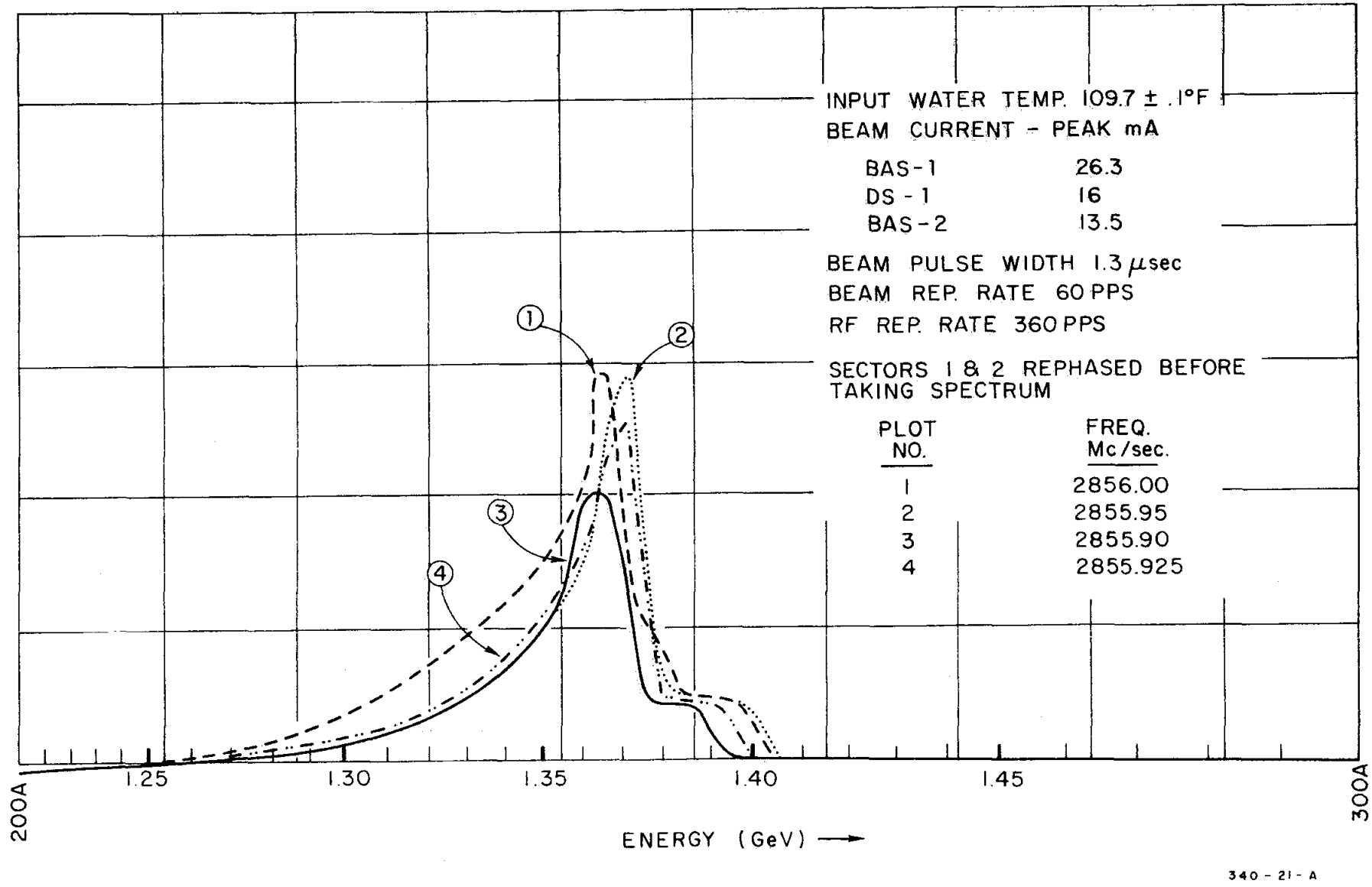

FIG. VI-4 Effect of changing frequency at fixed repetition rate (360 pps) and temperature.

These results did tend to indicate that the accelerator gives maximum energy for a slightly different frequency or temperature than actually designed for. The design parameters were

Frequency	f	= 2856.00 Mc/sec
Input water temperature	T	= 113°F
Repetition rate		= 0 pps

The input water temperature at any repetition rate is computed as $\Delta T = 0.748^{\circ}F/kW$ of average power into the accelerator section. Assuming an output power of about 18 MW per klystron and hence approximately 4 kW of average power into each accelerator section, one obtains $\Delta T \approx 3^{\circ}F$, hence an operating input water temperature of 110°F. At that temperature, maximum energy should be obtained for $f = 2856$ Mc/sec. However, as seen from Fig. VI-4, maximum energy was obtained for 0.05 to 0.075 Mc/sec lower. More work will have to be done on this subject when the machine is turned on again.

Figure VI-5 shows spectra obtained at a klystron repetition rate of 60 pps and a temperature of 109.7°F. Spectrum 1 was taken at 2855.95 Mc/sec, spectrum 2 at 2855.90 Mc/sec, spectrum 3 at 2856.00 Mc/sec, and spectrum 4 at 2856.05 Mc/sec. Maximum energy was obtained at 2856.00 Mc/sec. Since according to the above calculation $\Delta T \approx 1/2^{\circ}F$ at 60 pps, the input water temperature should have been 112.5°F for 2856.00 Mc/sec. Thus the optimum temperature was roughly 2.5°F lower and again a discrepancy was apparent. A 2.5°F change in temperature corresponds roughly to 0.070 Mc/sec.

E. EFFECT OF BEAM LOADING

Figures VI-6 and VI-7 show three-dimensional current pulse profiles as a function of time and energy. Each profile was obtained by taking a photograph of the current pulse picked up on the scanning foil at the end of Sector 2 for a given magnet setting. The current amplitude scales are arbitrary. Within the accuracy of these measurements, it is seen that the results seem to be in good agreement with the design parameters. For example, with a 5-MW input power per section and a beam current of 50 milliamps, the reduction in energy from no load to full load is

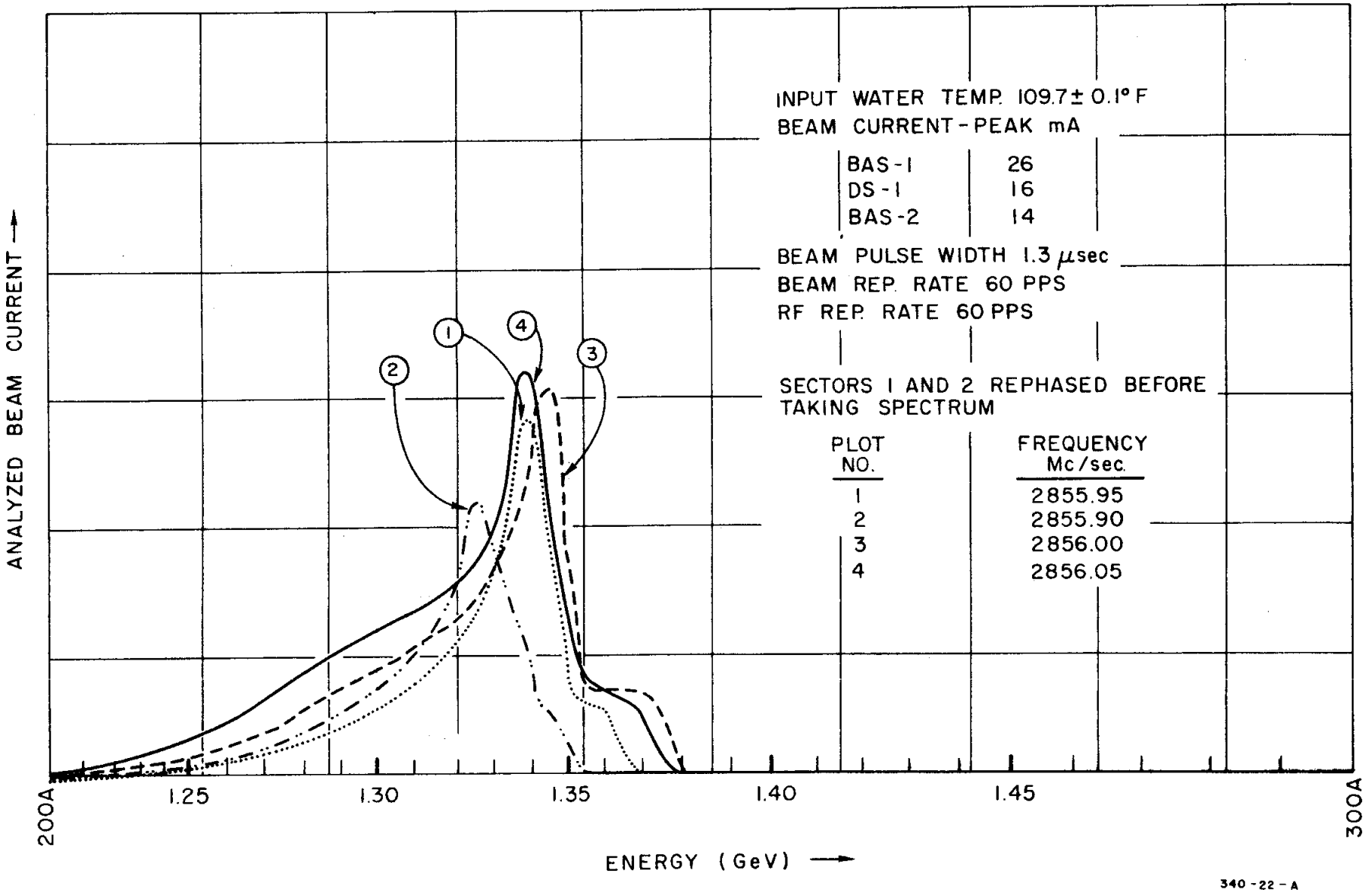

FIG. VI-5 Effect of changing frequency at fixed repetition rate (60 pps) and temperature.

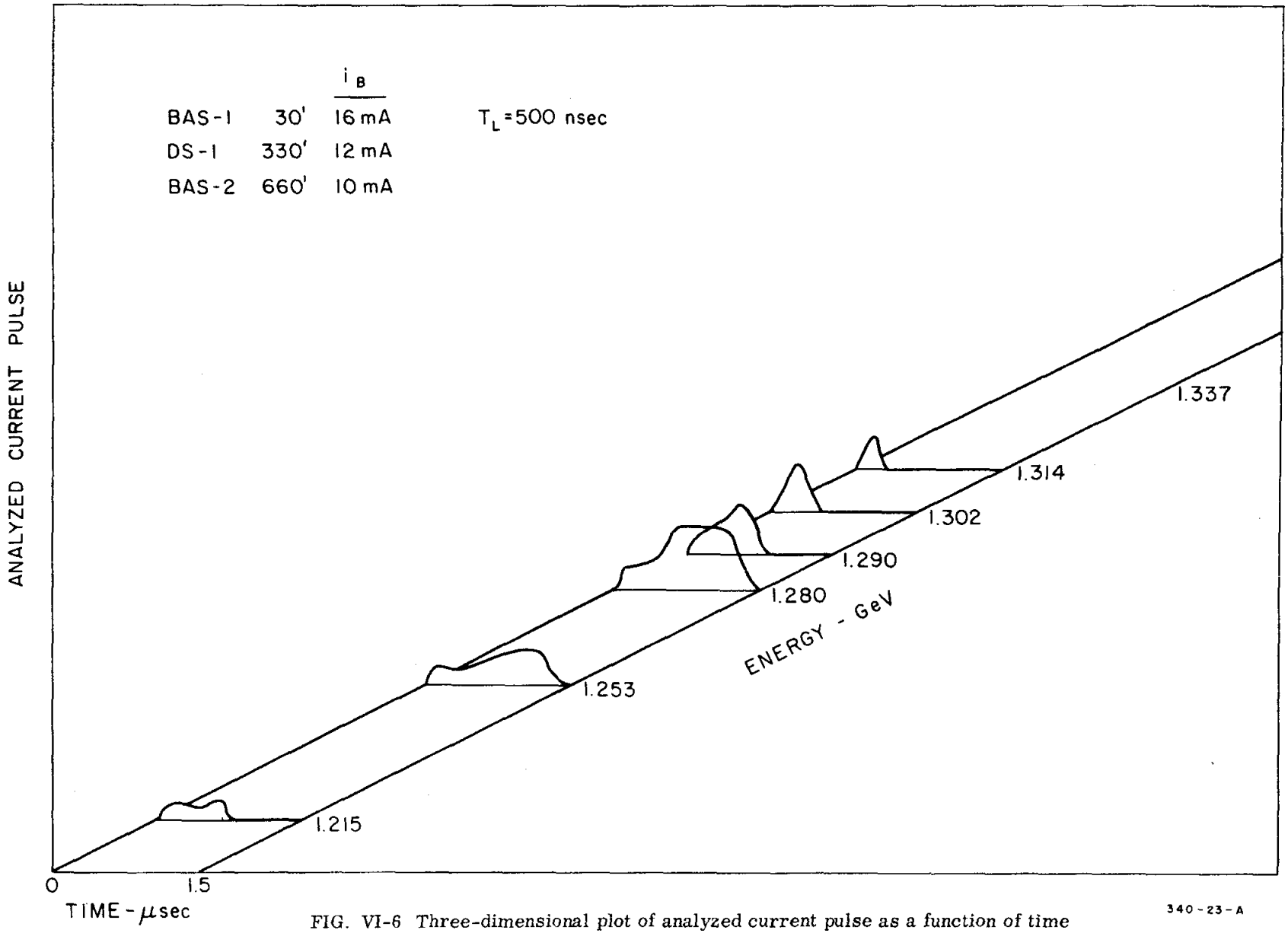

FIG. VI-6 *Three-dimensional plot of analyzed current pulse as a function of time and energy* ($i_{660'}$ = 10 mA).

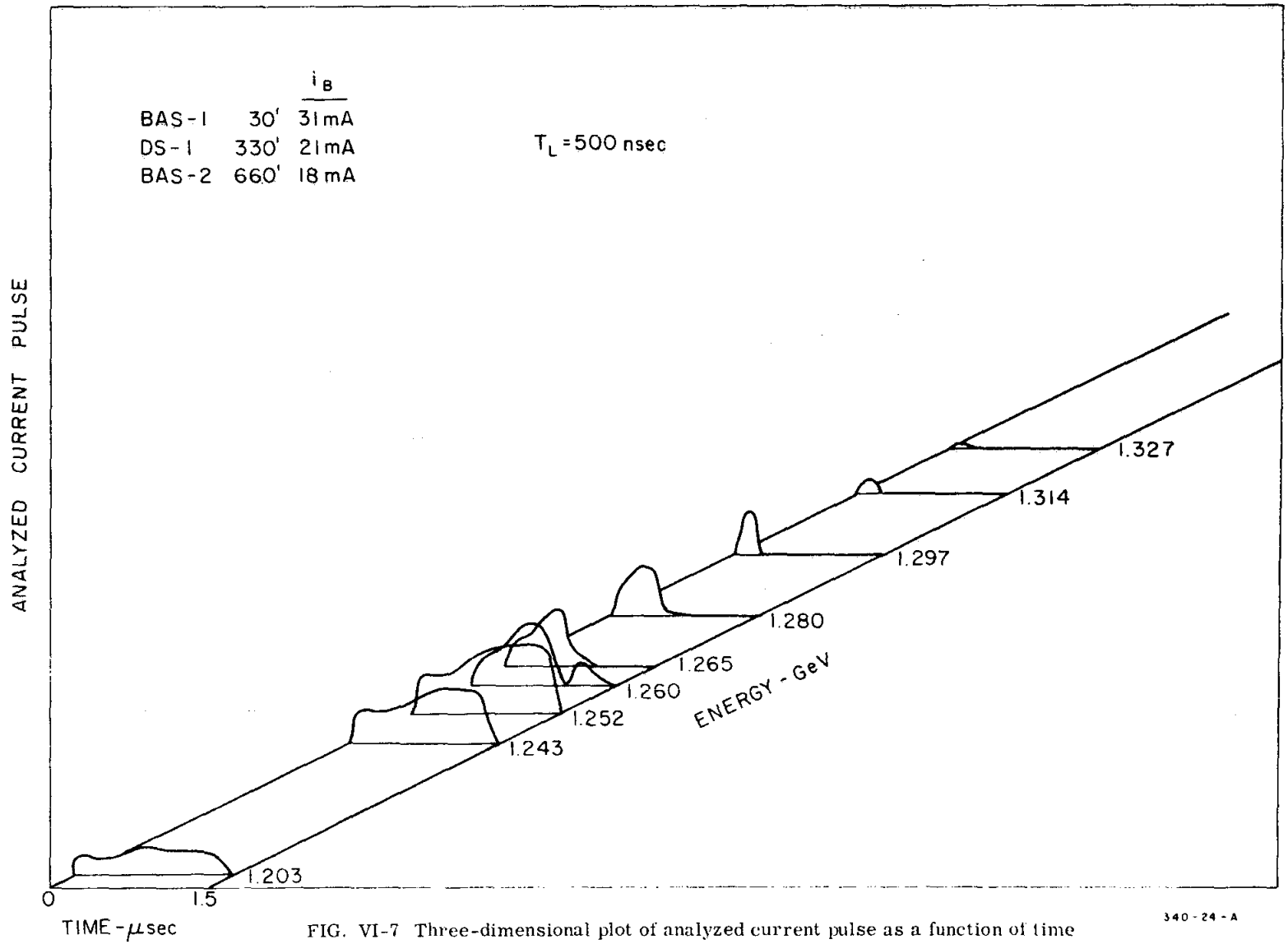

FIG. VI-7 Three-dimensional plot of analyzed current pulse as a function of time and energy ($i_{660'}$ = 18 mA).

supposed to be 8%. In Figs. VI-6 and VI-7, the maximum no-load energy is approximately 1.330 GeV. For a current of approximately 20 milliamps the full load energy is approximately 1.250 GeV or a reduction of 80 MeV. For a current of approximately 11 milliamps the full load energy is approximately 1.280 GeV or a reduction of 50 MeV.

F. EFFECT OF TRIGGER TIMING

All preceding spectra were taken with perfect trigger timing, i.e., with the beam pulse turned on no earlier than at least 1 filling time or 0.83 microseconds after rf turn-on. To decrease the effect of beam loading when the machine is completed, successive sectors or groups of sectors will be "stagger triggered." With only two sectors available, this operation is difficult unless one were to adjust the timing of each individual sector. Figure VI-8 shows the effect of delaying the trigger, T_L, for Sector 2 by known amounts from roughly 0 to 500 nanoseconds. It is seen, as expected, that the long high energy tail in the spectrum can be cut out. However, the electrons which disappeared from the high energy tail did not clearly seem to reappear at a lower energy as they should have. Perhaps this was due to the inaccuracies in the method of recording. This experiment will have to be repeated when the machine is completed.

G. METHODS USED TO OBTAIN SPECTRA AND PICTURES

Spectrum plots shown in this section were obtained from a secondary emission foil box. Two methods of display were used.

1. "Scanned Foil" Method

In this method, the analyzed beam strikes an array of 11 foils. The magnet current is held constant and an oscilloscope is sequentially connected to the foils at an approximate rate of 60 pps. The output of the detector consists of a series of steps, the amplitude of each step being proportional to the beam current intercepted by the corresponding foil (see Fig. VI-9).

The advantage of this method is that it gives dynamic presentation of the spectrum, permitting the experimenter to view immediately the results of machine adjustments. The disadvantage is its relative

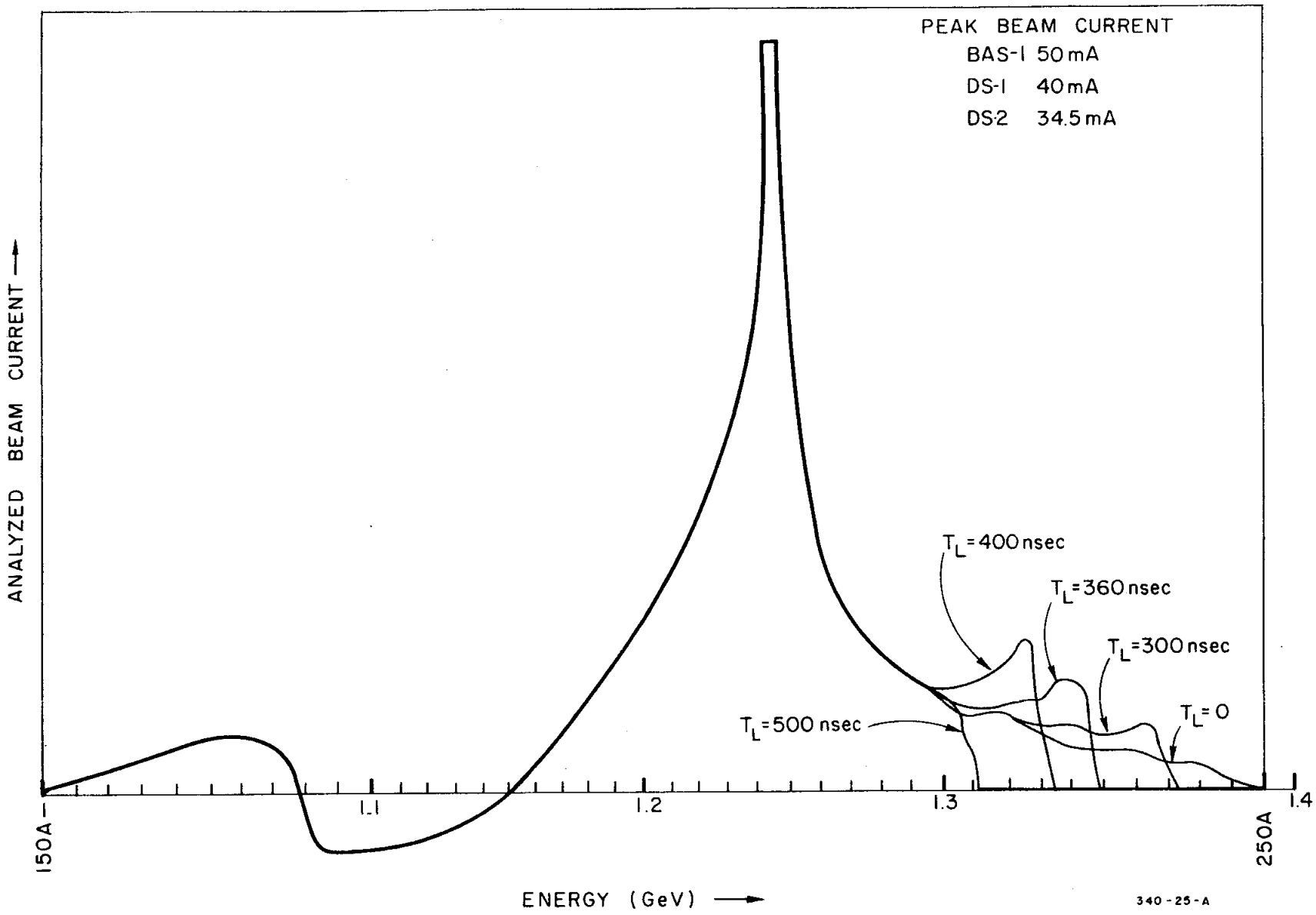

FIG. VI-8 Effect of trigger timing (delaying T_L on Sector 2).

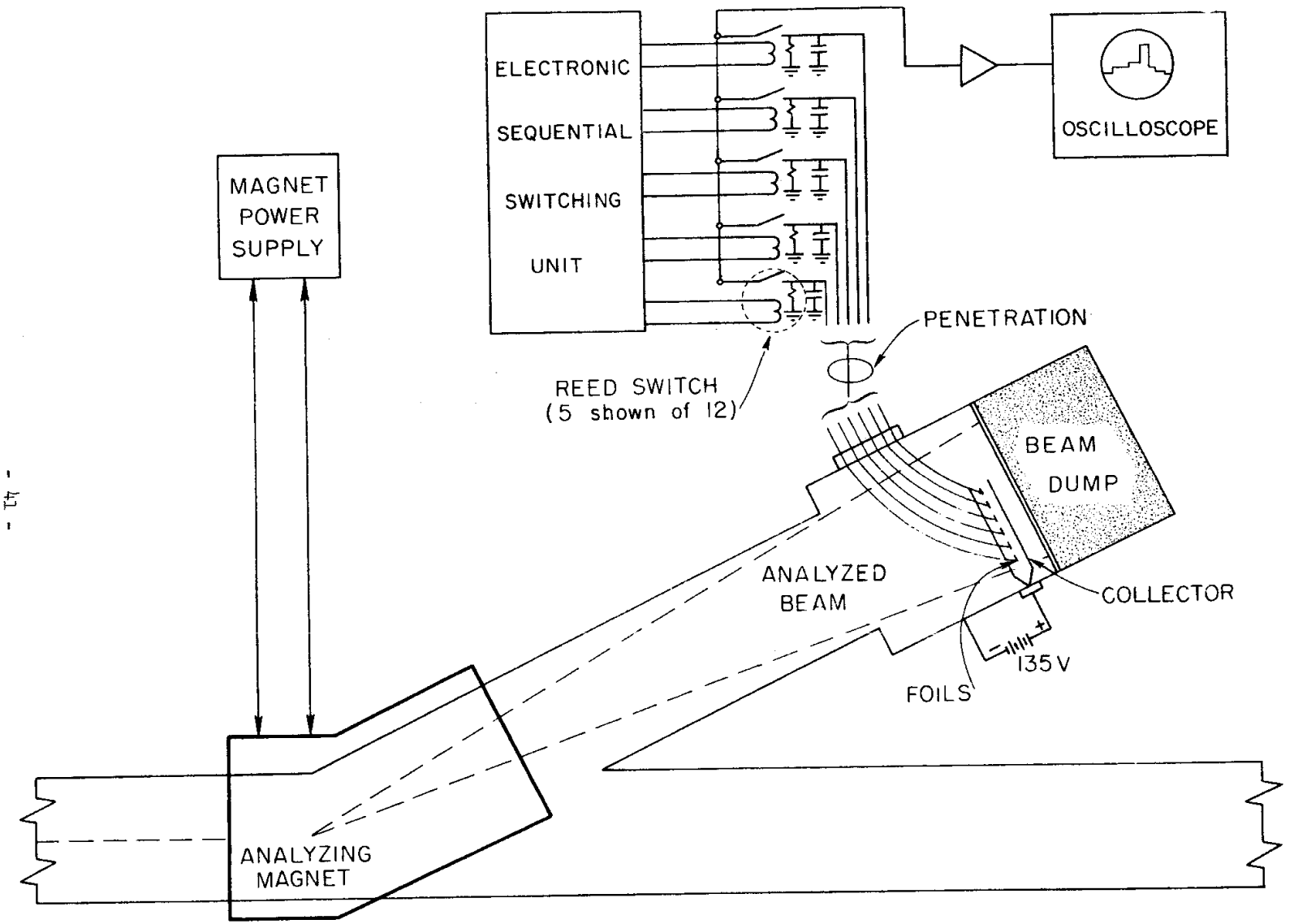

FIG. VI-9 Method of obtaining "scanned foil" spectrum display.

coarseness; the resolution is of course limited by the width of the foil. This method was used primarily at BAS-1 where such a presentation is essential for rapid adjustment of the many controls necessary to set up the injector and first three klystrons.

2. "Swept Magnet Current" Method

In this method a single foil located in the center of the foil box is connected to the detector and the analyzed beam is slowly swept through this foil by varying the current through the analyzer magnet. The detector in this case is a Moseley X-Y Recorder. The foil is connected through an amplifier to the Y axis and a voltage proportional to magnet current is connected to the X axis. Zero suppression on the X axis was set to allow the plot to start at either 150 or 200 amps and the gain was set for a scale of 10 amps per inch. This current scale was converted into a beam energy scale by using the magnet calibration chart.

This method was used primarily at BAS-II and is illustrated in Fig. VI-10.

3. Real Time Beam Current Measurement

In addition to the above two methods of display, photographs of beam current vs time within a pulse were obtained by placing a radiation resistant vacuum tube amplifier in the housing in close proximity to the beam analyzer to sufficiently amplify the signal obtained from the "scan foil," to overcome noise. The low impedance output from this amplifier drove a twinax transmission line which transmitted the signal through the penetration to a scope in the sector alcove. Resistive loading of the foil in the BAS and amplifier passband was sufficient to allow a bandwidth greater than 5 Mc. The system is shown schematically in Fig. VI-11.

4. Negative Branches Observed in Spectrum Plots

In many of the spectra taken with the x-y recorder, it was observed that within approximately 25% and on both sides of the energy at peak current, the spectrum exhibited a negative current swing. Although

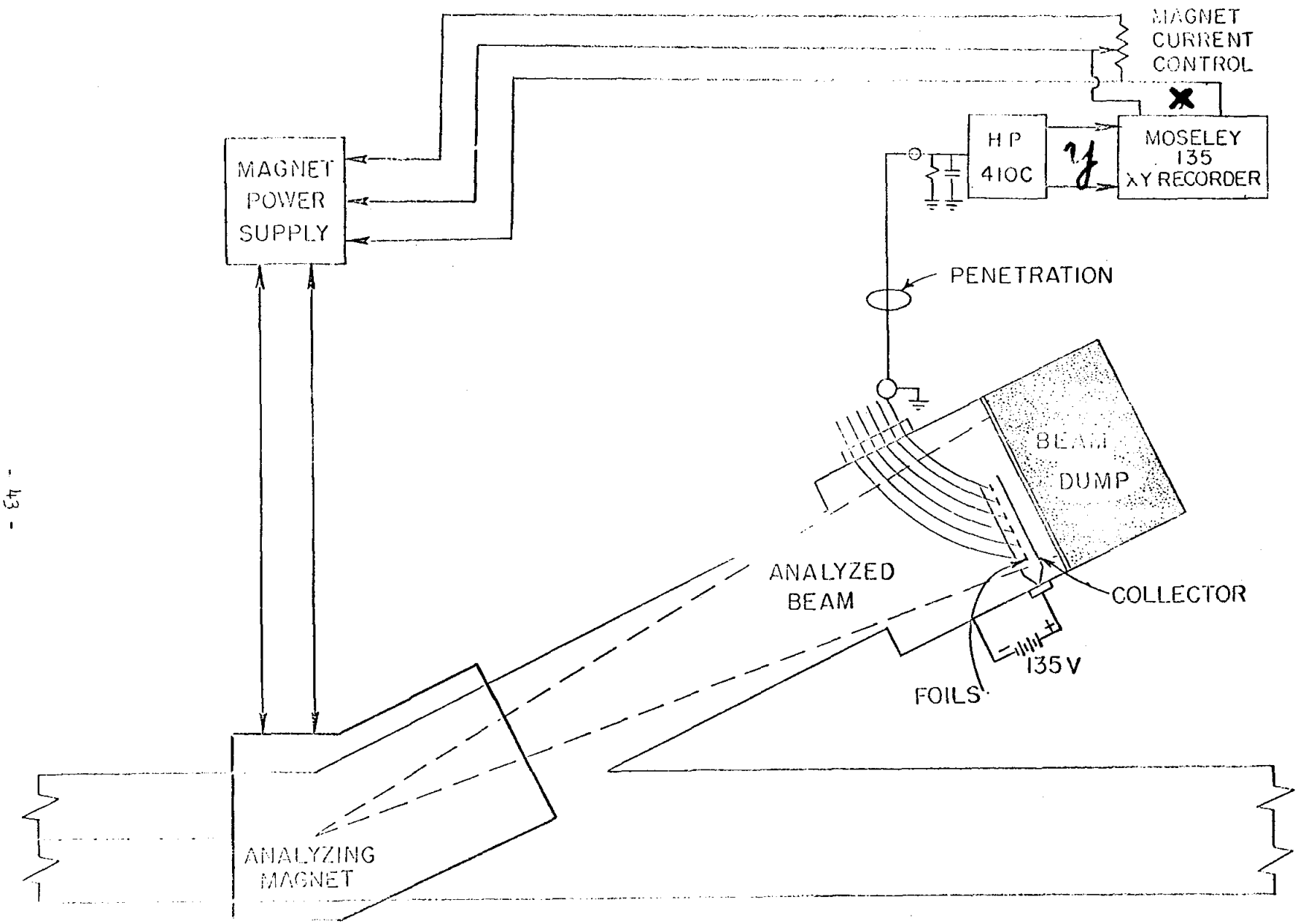

FIG. VI-10 Method of obtaining "swept magnet current" spectrum display.

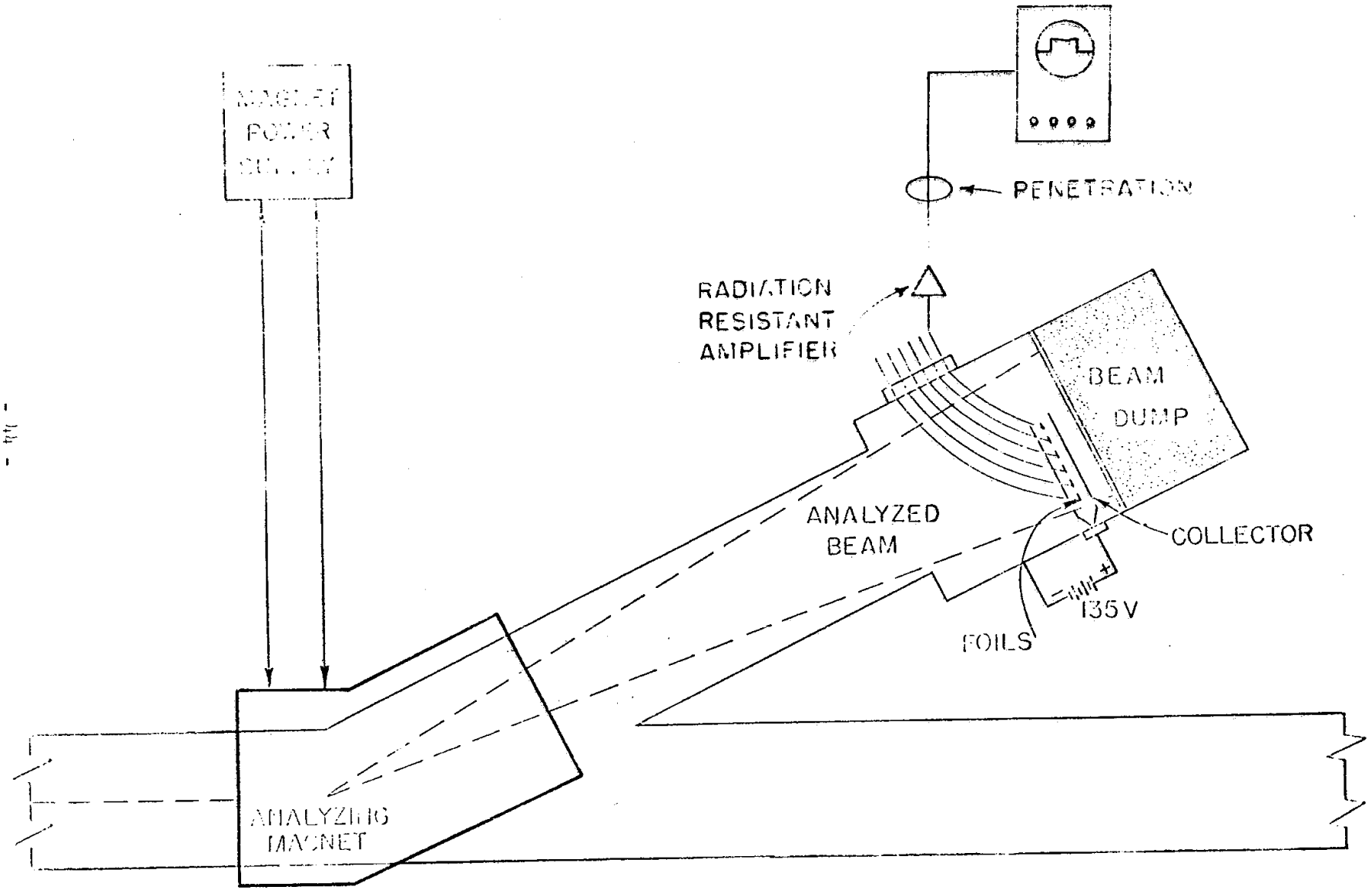

FIG. VI-11 Method of obtaining analyzed current pulse vs. time and energy.

many explanations were proposed for this phenomenon, no satisfactory solution was found. There is no doubt that these negative swings appear when the current maximum in the spectrum strikes the edges of the vacuum envelope, top or bottom. Some of the scattered or secondary electrons strike this scanning foil and perhaps also the cables leading to these foils. The end result is that the net current flowing from the collectors to the secondary emitter in the foil box seems to reverse. In order to avoid this phenomenon, it appears that it would be necessary to widen the vacuum envelope in front of the foil box or to build a heavy slit.

VII. KLYSTRON ENERGY CONTRIBUTION, RECYCLING, AND REPLACEMENT

A. ENERGY CONTRIBUTION FROM EACH KLYSTRON (R. Koontz)

On March 18, 1965, Sectors 1 and 2 were set up for a run with as high an energy as possible. All klystrons and modulators were operating. After automatically phasing the whole machine, the following peak beam currents were recorded:

$$i_{BAS-1} = 10 \text{ mA}$$
$$i_{DS-1} = 7.2 \text{ mA}$$
$$i_{DS-2} = 5 \text{ mA}$$

The repetition rate was 60 pps and the average peak klystron voltage was 240 kV.

An energy spectrum (see Fig. VII-1) taken at the end of Sector 2 showed an energy at maximum current of 1.45 GeV. Correcting for the fact that the first girder is fed by three klystrons rather than one, one obtains an average energy per sector of 680 MeV. Projecting this figure on to the machine, complete with 30 sectors, one should expect a final energy of about 20.4 GeV.

The beam energy contribution of each klystron in Sectors 1 and 2, except for klystrons 1-1A, 1-1B and 1-1C, was measured by taking the difference between two energy spectra, one with the klystron in "ACCELERATE," the other with the klystron in "STANDBY." The results are tabulated in Table VII-I. The values given for the parameter

$$K = \frac{E}{\sqrt{P}}$$

where E is beam energy and P is peak power, are based on klystron powers measured at the output of the klystron, in the gallery. Hence, they do not take into account waveguide losses. The average loss in the waveguide is assumed to be 0.54 ± 0.1 dB. The theoretical value of the parameter K, based on peak power input into an accelerator section,* is

*"Two-Mile Accelerator Project, Quarterly Status Report, 1 April to 30 June 1964," SLAC Report No. 32, Stanford Linear Accelerator Center, Stanford University, Stanford, California (1964), p. 85.

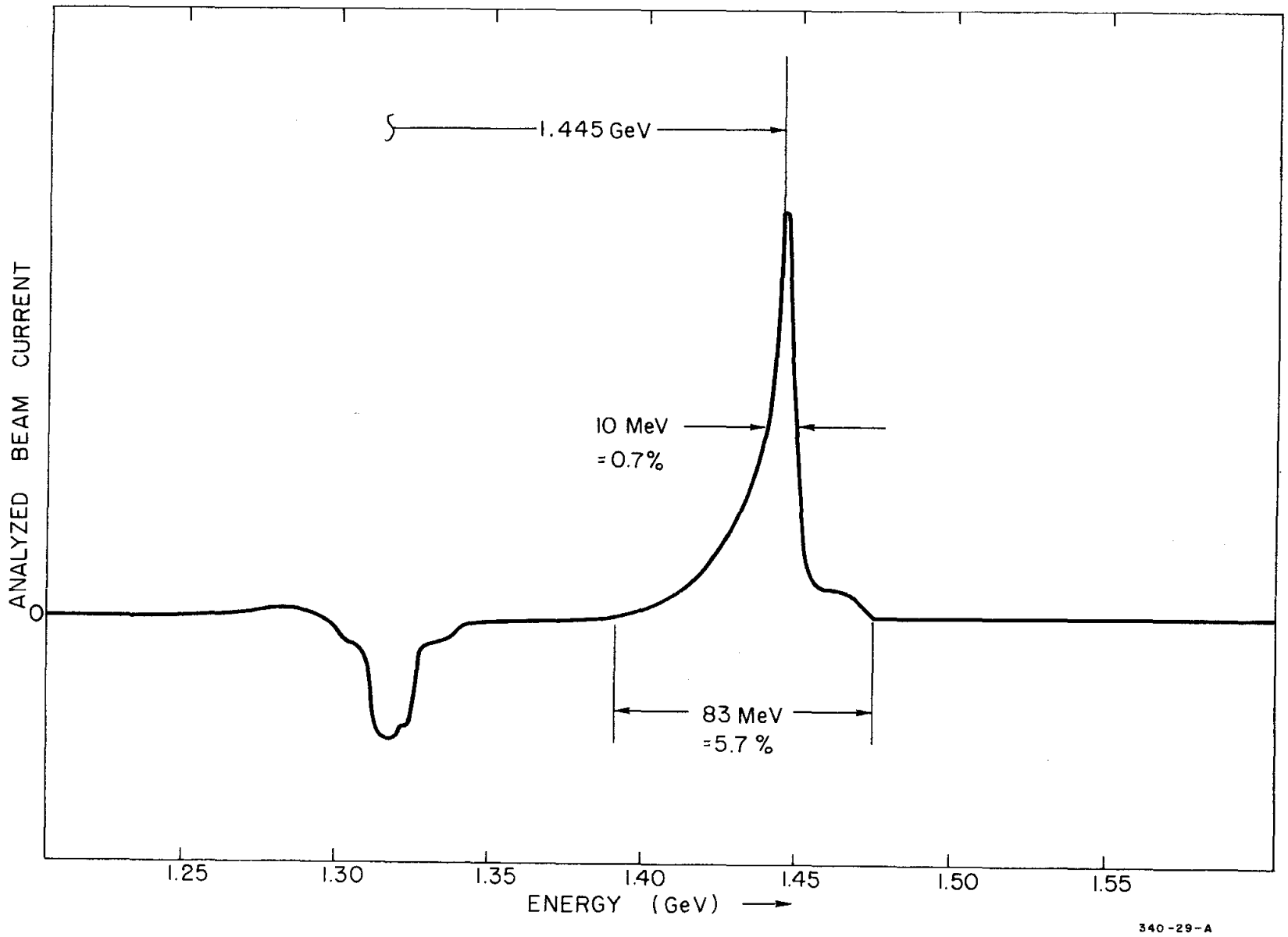

FIG. VII-1 Reproduction of high energy run spectrum, 22 March 1965.

is defined by

$$E = 4 \times 10.6 \sqrt{\frac{P}{4}} \ .$$

This yields a value of K = 21.2. Correcting this number by taking into account waveguide losses, one obtains a predicted value of K = 19.9. Measured values are plotted in Fig. VII-2 along with klystron output powers and beam energies. It can be seen that although klystron output powers varied from tube to tube, the experimental values of K remained closely grouped around the value of K = 21. Assuming that the klystron powers were not higher than measured (which is unlikely since the numbers are high already), this would indicate that the accelerator efficiency is about 5% higher than measured on the Mark IV Accelerator (assuming no error in spectrometer calibration). It also appears that on the average, certainly no gross errors have been made in tuning the rectangular waveguides and that the automatic phasing system was working satisfactorily and consistently.

Figure VII-3 shows beam transmission as a function of switching individual klystrons to "STANDBY." Effects in Sector 2 are relatively random, but Sector 1 shows a constant drop in transmission as klystrons are removed. This problem will be discussed further under the sections on beam transmission and coupler asymmetry.

B. EFFECT OF KLYSTRON RECYCLING (K. Mallory)

In connection with the klystron replacement scheme (described in the next paragraph), it was at one time proposed that it be possible to require all klystrons to accelerate the beam, even if sick, when the highest possible beam power was desired. This was in contrast to the normal scheme of switching a klystron to standby whenever its protection attenuator was being cycled. An investigation of the change of beam energy as a klystron recycled shows that the phase shift in the protection attenuators produces an energy drop of up to 40% for 30% of the attenuator removal time. A significant energy gain exists only during the last 30% of the time. Figure VII-4 gives data for three klystrons and the possible range of variation. It is clear that allowing klystrons to recycle on "accelerate" instead of "standby" can produce but a slight gain of average output energy. The effect on steering is also significant.

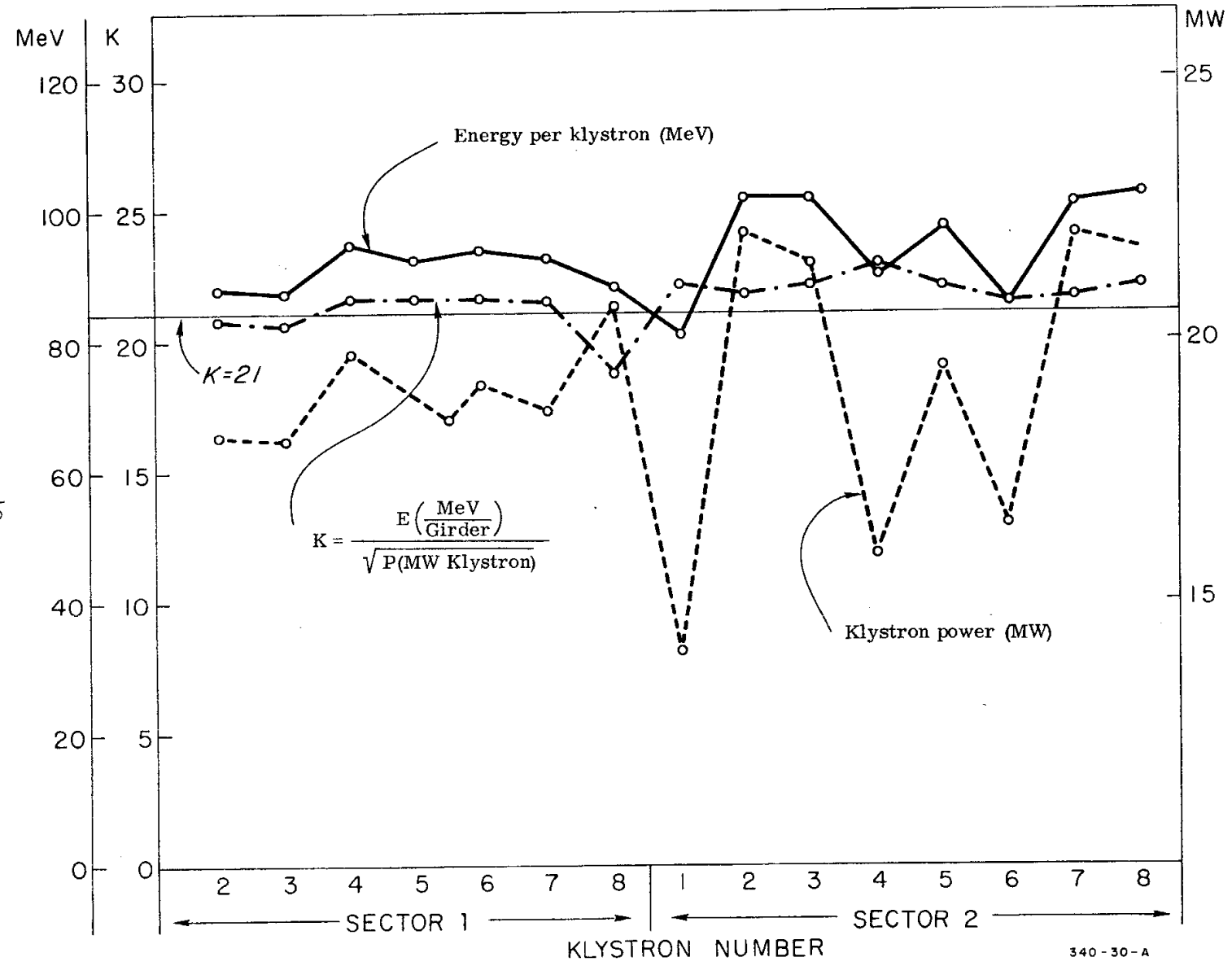

FIG. VII-2 Energy contribution per klystron.

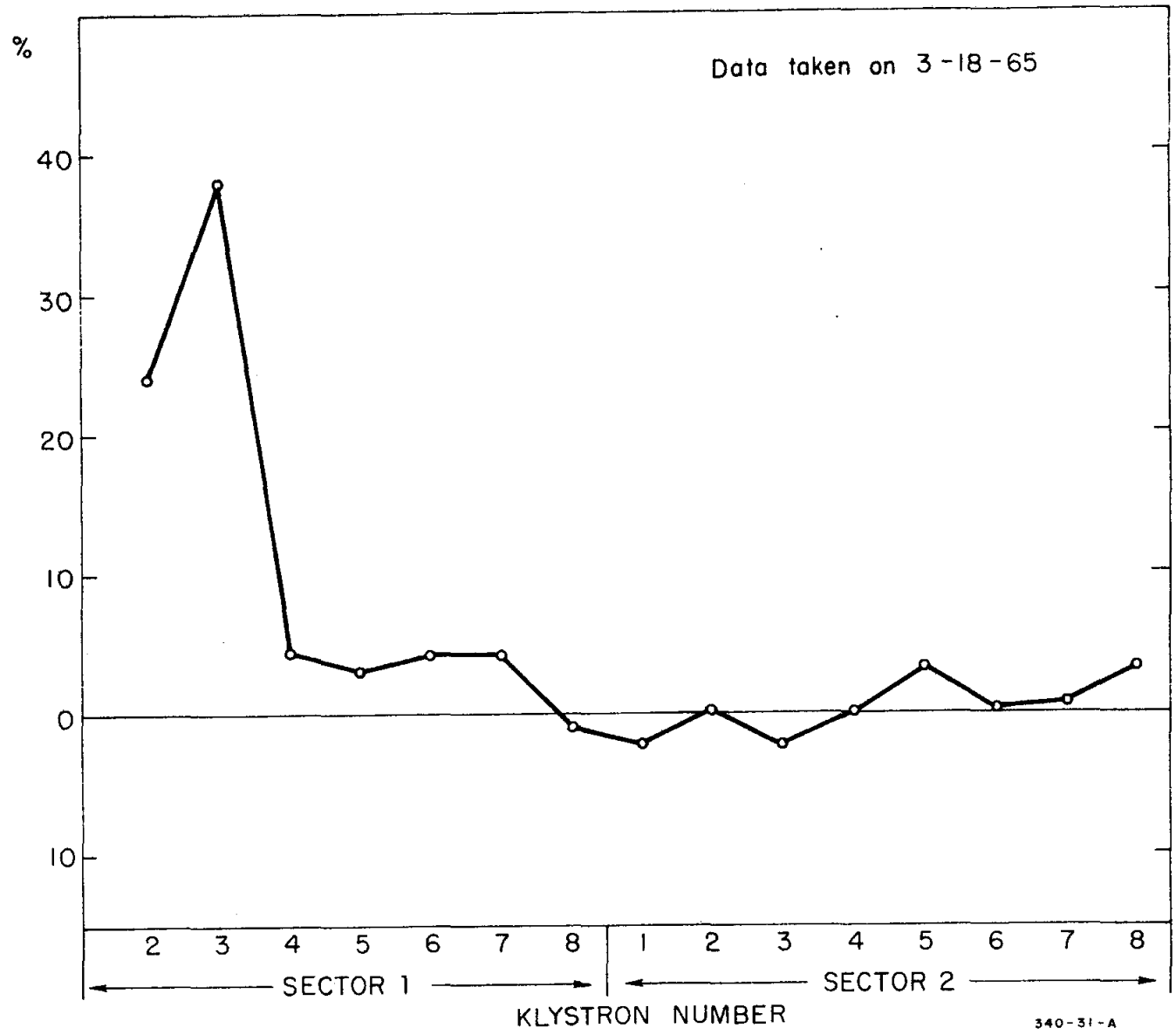

FIG. VII-3 Percent transmission drop per klystron.

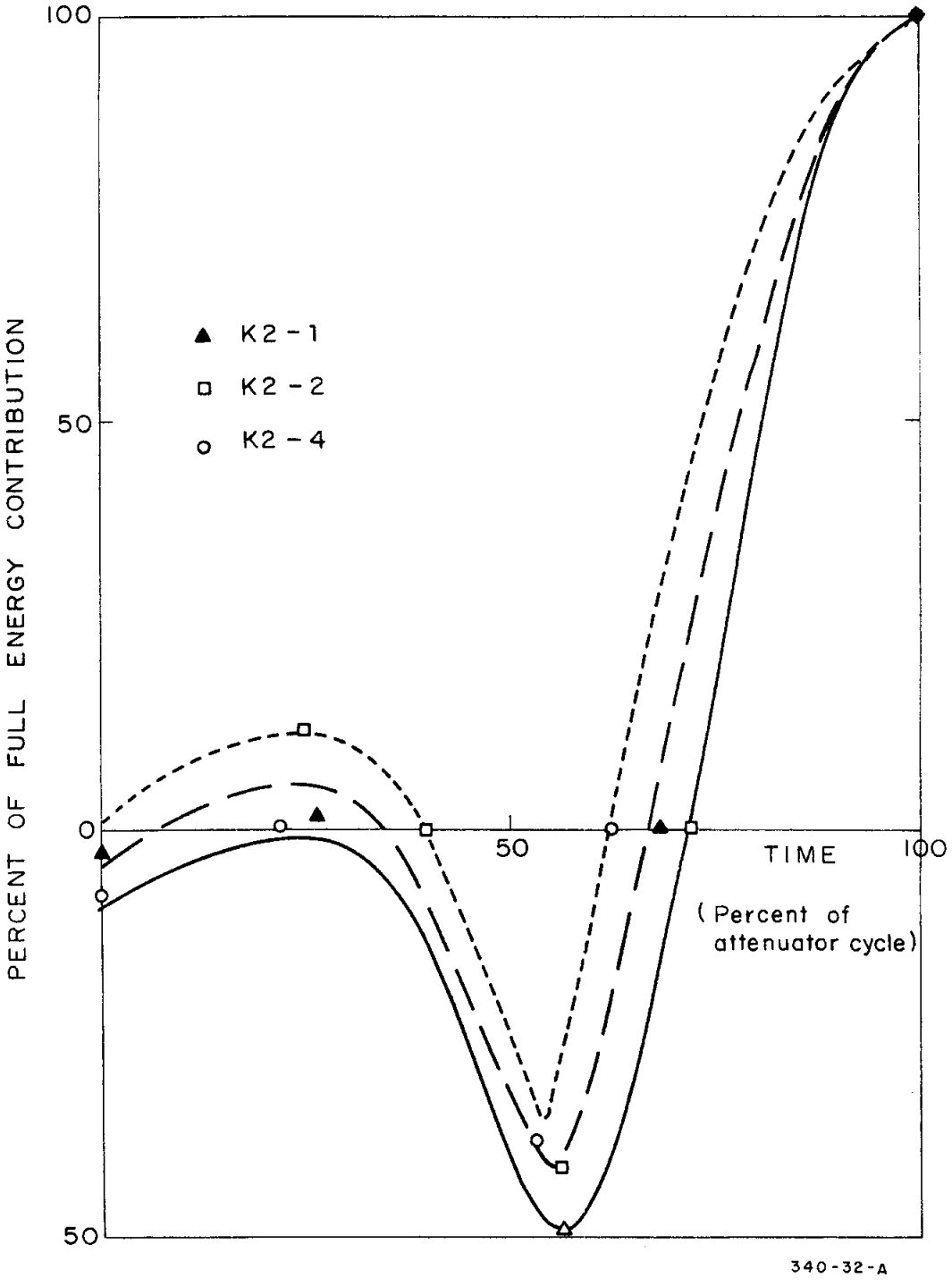

FIG. VII-4 Energy variation during removal time of protection attenuator.

TABLE VII-I

Klystron	Energy Contribution MeV	Klystron Power MW	$K = \frac{E}{\sqrt{P_{out} \text{ at klystron}}}$	Percent Current Transmission Drop per Klystron when Klystron set to standby
1-1A	134	21.6		
1-1B	134	21.1		
1-1C	134	20.0		
1-2	88.0	18.1	20.72	24.0
1-3	87.3	18.0	20.60	37.0
1-4	95.0	19.7	21.40	4.5
1-5	92.0	18.4	21.41	3.0
1-6	94.0	18.9	21.60	4.5
1-7	92.5	18.5	21.50	4.2
1-8	88.0	20.5	19.40	-1.2
2-1	81.5	14.0	21.80	-2.4
2-2	102	22.0	21.78	0.6
2-3	102	21.5	22.04	-2.1
2-4	89.5	15.7	22.60	0
2-5	97.0	19.4	22.03	3.3
2-6	86.3	16.4	21.35	0.6
2-7	101	22.1	21.45	1.2
2-8	102	21.6	21.95	3.6

C. KLYSTRON REPLACEMENT SYSTEM (W. C. Struven)

A prototype klystron replacement scheme was designed and installed in Sectors 1 and 2 for tests. Briefly, the system functioned as follows: Each klystron in a sector operates two relays, one in a series "standby" circuit and one in a series "accelerate" circuit (see Fig. VII-5). In addition, each standby relay operates a contact in a "sense" circuit. If a klystron recycles, for any reason, a pulse is applied to the "Sense" circuit which in turn switches the next available klystron from standby to accelerate. The standby and accelerate relays are controlled by the Trigger Mode relays on the MTMSCL chassis (Modulator Trigger Mode Switch Control Logic). The remote control receiver in a sector was used to preset klystrons to a particular accelerate-standby configuration.

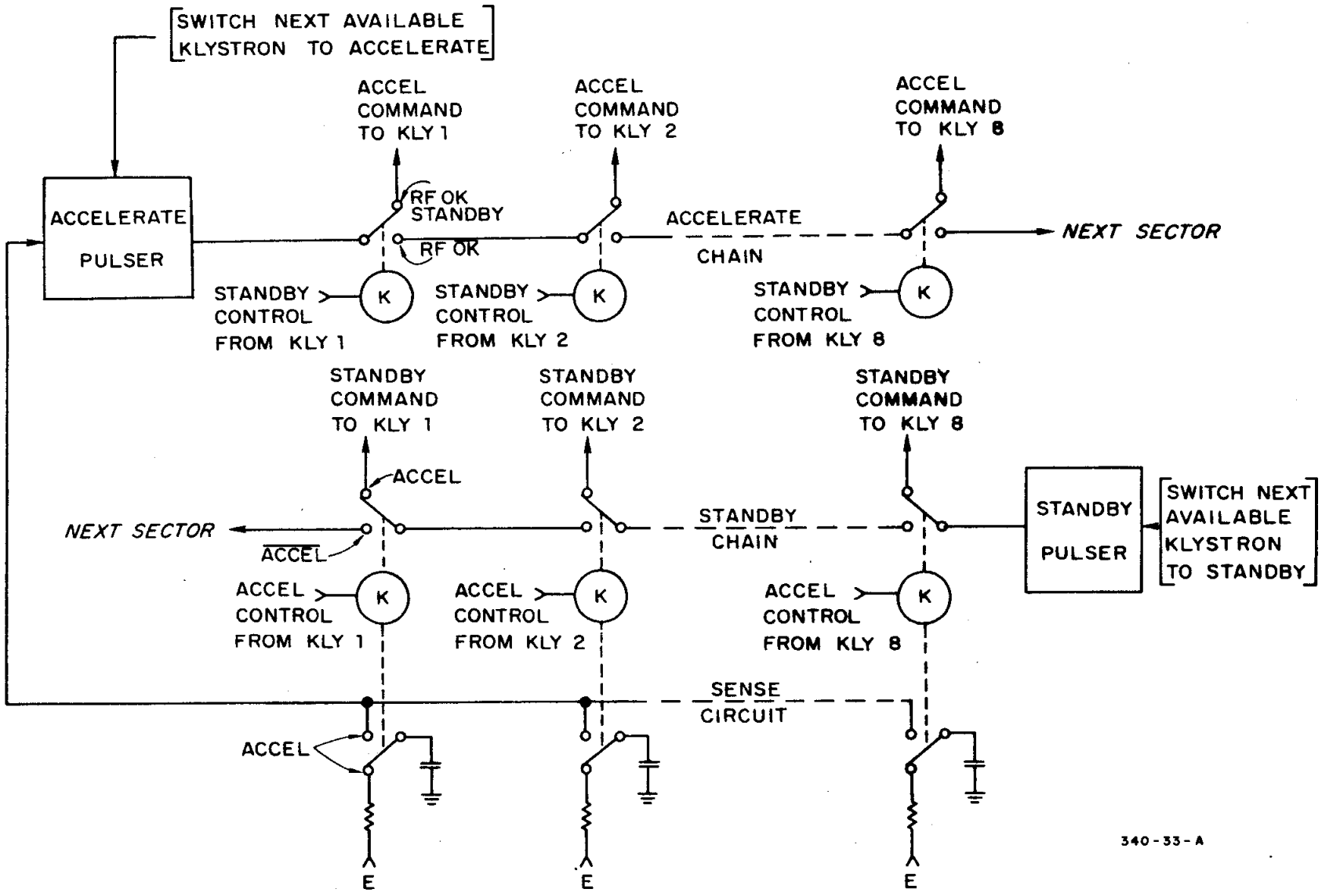

FIG. VII-5 Klystron replacement system.

Initial tests were performed by pulsing the next available inputs shown on Fig. VII-5. A pulse applied to "accelerate next available" input switched one klystron from standby to accelerate. A pulse applied to "standby next available" switched two klystrons to standby. The extra pulse (which switched a second klystron to standby) was generated by relay transients in the unit. Transient suppression diodes were added but the triggering circuit still proved to be too sensitive and a double standby effect was again noted.

A more thorough analysis of the sector prototype circuitry will be performed and further testing will resume when Sectors 1 and 2 have been rewired and put back in service. A further analysis may indicate that a logic redesign is in order.

VIII. REMARKS ON BEAM DYNAMICS, GUIDANCE, AND TRANSMISSION

A. MAGNETIC SHIELDING AND DEGAUSSING (W. B. Herrmannsfeldt)

After a series of magnetic field surveys, the following current settings were made in Sectors 1 and 2 on February 18, 1965.

	Vertical	Horizontal
Sector 1	8.45 amps	5.5 amps
Sector 2	10.8 amps	4.3 amps

After making these settings, the magnetic shielding was demagnetized using a current of about 60 amperes maximum at 60 cycles and reducing the current to zero in about 30 seconds.

The following table lists the approximate residual field at the intergirder bellows between each 40-foot girder. The data is listed for the downstream end of each girder.

TABLE VIII-I

Girder	Horizontal (gauss)	Vertical (gauss)
1-1	-0.07	-0.12
1-2	+0.08	-0.12
1-3	+0.06	+0.05
1-4	+0.07	+0.06
1-5	-0.14	+0.04
1-6	-0.06	+0.05
1-7	+0.01	-0.01
2-1	-0.03	+0.05
2-2	+0.08	-0.1
2-3	+0.01	0.0
2-4	-0.08	0.0
2-5	+0.05	+0.05
2-6	-0.02	+0.1
2-7	-0.02	-0.1
Nominal Uncorrected Field	0.2	0.4

B. STEERING, FOCUSING AND BEAM TRANSMISSION (R. Miller, G. Loew)

Of all the machine adjustments necessary to set up the beam from the gun to the end of Sector 2, steering and focusing required the most work and ingenuity.

The beam guidance equipment consisted of

Steering Dipoles: One special set at 2-foot point
One special set at 12-foot point
One standard set at BAS-1
Vertical: 216 $\frac{\text{gauss-cm}}{\text{amp}}$ Horizontal: 140 $\frac{\text{gauss-cm}}{\text{amp}}$
One special set at girder 1-4
Vertical: ~ 70 $\frac{\text{gauss-cm}}{\text{amp}}$ Horizontal: ~ 70 $\frac{\text{gauss-cm}}{\text{amp}}$
One special set at girder 1-6
Vertical: ~ 70 $\frac{\text{gauss-cm}}{\text{amp}}$ Horizontal: ~ 70 $\frac{\text{gauss-cm}}{\text{amp}}$
One standard set at DS-1

Lenses: Two at the gun

Quadrupole Triplets: One at BAS-1
One at DS-1

Toroids for Linear Q: One at the gun
One at BAS-1
One at DS-1
One at DS-2

Beam Intensity and Position Monitors: (log Q, x, y)
One set at BAS-1
One set at DS-1
One set at DS-2

Cerenkov Profile Monitors:
One at BAS-1
One at DS-1
One at DS-2

It was found that this equipment was not always sufficient to set up a well defined beam. Often, additional aids such as the long ion chamber (see Section VIII-F) and the induced beam signals available from the automatic phasing system were used, particularly in Sector 1 which

does not follow the baba-abab configuration. The special steering dipoles at girders 1-4 and 1-6 were installed specifically to provide coupler asymmetry compensation.

The main factors accounting for steering and focusing difficulties were:

1. Imperfect injector optics (to be improved)
2. Coupler asymmetry, particularly in Sector 1
3. Diode drift in position monitors (to be improved)
4. Lack of sensitivity of beam position monitors when beam is badly focused and fills entire hole
5. Coupling between steering and focusing
6. Saturation of profile monitor displays (difficult to improve with Cerenkov radiator and TV display)
7. Recycling of klystrons at the beginning of the machine and resulting beam displacement due to misalignment or coupler asymmetry (spare injector klystron will improve situation)
8. Possible stray and locally uncompensated magnetic fields (survey to be redone)
9. Insufficient diagnostic instrumentation between BAS-1 and DS-1 (to be added if new injector tests still justify it)
10. Insufficient reliability of beam guidance power supplies (adequate number of spares should be available)

These factors and perhaps others often made it difficult to find the same quality beam from one run to the next. Sometimes the various settings had to be changed substantially. A rubber stamped table of accelerator parameters was made to record these settings systematically. Samples of these tables are shown in Tables VIII-II, III, IV and V.

After some experience, a typical step-by-step procedure to focus and steer the beam down the machine was developed. It followed approximately the following pattern:

1. Set up and center beam at BAS-1
2. Measure energy
3. Degauss BAS-1 spectrometer carefully
4. Set horizontal steering dipole currents at 1-4 and 1-6 to approximately 4 amps (left) to compensate for the coupler asymmetry deflection (right).

26 MAY 1965

BUZZ JONES

0800 BUZZ JONES ON WATCH- VIA AT 117.0, VIB AT 11[illegible].36 - 360 PPS - GUN = 10 PPS-
0830 VIC WAITHMAN TURNED OFF 1-2 - PRESSURE TOO HIGH-
0845 CHANGING VAC GAGE POWER SUPPLY AT 1-1B (SLAC P.S. -METER JITTERS - WILL SEE IF JITTER IS ACTUALLY VAC OR IS IN P.S.). BEAM OFF.
0855 CHANGING THERMOCOUPLE PORTS IN ROTAMETERS AT EACH KLYSTRON, ONE AT A TIME.

RUNNING VAC. READINGS:

1-1A = 3.6x10⁻⁷		2-1 = 5.0x10⁻⁸	
1-1B = 5.0 "		2-2 = 3.0x10⁻⁷	VIC CARTY INSTALLING NEW THERMOMETER WELLS IN
1-1C = 7.0 "		2-3 = 1.0 "	EACH ROTAMETER-
1-2 = 9.3 "	OFF	2-4 = 4.0 "	
1-3 = 3.0 "		2-5 = 3.6 "	
1-4 = 1.6 "		2-6 = 4.8x10⁻⁸	
1-5 = 1.5 "		2-7 = 1.2x10⁻⁷	
1-6 = 1.2 "		2-8 = 2.0x10⁻⁷	
1-7 = 1.1 "			
1-8 = 8.0x10⁻⁸			

0857 BEAM ON FOR TED JENKINS- GUN = 60 PPS - BEAM NOT BENT-
0905 NEW SLAC VAC. GAUGE PWR. SUP. HAS NO JITTER (1-1B)

ACCELERATOR PARAMETERS

Operator: WAITHMAN Date: 26 MAY '65 Time: 0930

60	Pulse Rate	pps			DS1-1 Vert.	.24 Amps
117	VIA Reference	Volts			DS1-1 Horiz.	.94 Amps
11[illegible]3	VIB Reference	Volts			1-4 Vert.	1.1[illegible] Amps
					1-4 Horiz.	.5[illegible] Amps
30	Fil. Power	Watts		Steering	1-6 Vert.	5.8[illegible] Amps
	Cathode 2	6.0 [illegible]			1-6 Horiz.	1.5[illegible] Amps
	Cathode 1	31 [illegible]			[illegible] Vert.	.9[illegible] Amps
Gun	Grid 2	4.3 kv			DS1-9 Horiz.	1.8[illegible] Amps
	Grid 1	5 [illegible]				
	Beam 1 (peak)	11 [illegible]			D. 1-9 Vert.	10.8 Amps
	Beam 1 (pulse)	ma.		Degaussing	[illegible] Horiz.	[illegible] Amps
					[illegible] Vert.	8.[illegible] Amps
	Lens #1	1.8 [illegible]			DS1-9 Horiz.	5.5 Amps
	Lens #2	[illegible]				
	2 ft. Horiz.	.5[illegible] [illegible]			[illegible] 1-8	9 Amps
Gun Steering and Focussing	2 ft. Vert.	1.8[illegible] Amps		Quads	[illegible] 1-9	[illegible] Amps
	12 ft. Horiz.	.4[illegible] Amps				
	12 ft. Vert.	.8[illegible] Amps		300' Beam	I (peak)	95.3 ma
					[illegible]	Div
Prebuncher	Pulse 5396					
	Power .78	mw		600' Beam	I (peak)	12 ma
30' Beam	Energy	Mev				
	I (peak) 63	ma.				

1010 VIC CARTY FINISHED CHANGING WELLS, BUT NOT 1-8 #3 - VALVES WOULDN'T HOLD-
1015 MARK JENSEN HERE FOR GREG LOEW - WORKING WITH STEERING.
1045 BUZZ OFF- KEY TO VIC WAITHMAN-
11[illegible] TURNED 1-2 ON.
11[illegible] TALKED TO DROP TO 20 PPS FOR VICK McCALL (TOO MANY γ's FOR HIS NEUTRON MONITOR). BUT PULSER WON'T WORK AT 20 - WORKS OK AT 10, 30 & 60, SO WE'RE RUNNING AT 10 PPS NOW.

BUZZ JONES

1035 TRYING TO CONTACT BOB BRADFORD ON D'GING OF 1-6 & 2-1 -
1045 BRADFORD WILL SEND SOMEONE TO LOOK AT MODS. -
1125 BRADFORD SETTING D'GING ON SEVERAL MODS. -THEY WERE TOO LOW OR OFF -
1135 BRADFORD FINISHED — MOD. GROUP SHOULD BE NOTIFIED IF ANY MORE DROP OUT AS IT CAN BE DANGEROUS IF THEY ARE CRANKED UP AT RANDOM - 2nd QUAD SET IS OFF -
1140 REAGEN FINISHED - A. WILMUNDER & H. HOGG WILL CONTINUE BEAM TRANSMISSION WORK.

ACCELERATOR PARAMETERS

Operator: WILMUNDER Date: 5/27/65 1215

	Pulse Rate	60 pps		DS1-1 Vert. .84 Amps
	VIA Reference	117 Volts		DS1-1 Horiz. .94 Amps
	VIB Reference	114.3 Volts		1-4 Vert. .28 Amps
				1-4 Horiz. 1.24 Amps
	Fil. Power	30 Watts	Steering	1-6 Vert. 0 Amps
	Cathode 2	5.8 kv		1-6 Horiz. 3.44 Amps
	Cathode 1	21 kv		DS1-9 Vert. .84 Amps
Gun	Grid 2	2.75 kv		DS1-9 Horiz. 1.44 Amps
	Grid 1	4 kv		
	Beam 1 (peak)	8 ma		DS1-9 Vert. 8.5 Amps
	Beam 2 (peak)	ma		DS1-9 Horiz. 5.5 Amps
			Degaussing	DS2-9 Vert. 10.8 Amps
	Line 1	1.8 kv		DS2-9 Horiz. 4.3 Amps
	Line 2	3.5 kv		
	Grid 2 Pulse	0		DS1-8 8.5 Amps
Gun Steering and Focussing	Grid 2 Level	.14 Amps	Quads	DS1-9 OFF Amps
	Grid 1 Pulse	.152 Amps		
	12 kv Volts	1.28 Amps	300' Beam	I (peak) 39.4 ma
	Pulse	0469		Energy 1 Mev
Prebuncher	Power	1.16 mw	600' Beam	I (peak) 33.7 ma
	Energy	Mev		
30' Beam	I (peak)	33.4 ma		

1230 GUN REDUCED TO 10 PPS - ALLEN & HARRY GONE FOR LUNCH & TOOLS - WILL RETURN AT 1330 -
1300 GUN TO 60 PPS FOR TOM SHIPMANS RADIATION INSTRUMENT TEST -
1310 TOM DONE - GUN TO 10 PPS -
1350 VIA = 508V , VIB = 475V -
1355 WILMUNDER & HOGG WILL BEGIN AGAIN - GUN TO 60 PPS -
1400 MAIN BOOSTER H.V. KICKED OFF - RESET - REAGAN HERE TO TAKE PICS
1420 ALL D'GING CURRENTS ARE BETWEEN 15 AND 20 AMPS. - 2nd QUAD SET PUNCHED ON AGAIN -
1450 BACKWARD BEAM RADIATION MONITOR GIVING HIGHER READINGS MOMENTARILY DUE TO REAGEN'S STEERING & MIS STEERING AT INJECTOR -
1515 GEORGE GRESKE IS STRAIGHTENING OUT THE ORDER OF THE METAL TEMP. SENSING DEVICES ON SECTIONS 1-B & 1-C — ALSO THE INSTRUMENT SAYS THAT THE METAL IS COLDER THAN THE WATER WHILE EACH SECTION IS GETTING APP. 16.5 KW OF POWER FROM THE KLYSTRONS - HE'S LOOKING INTO THIS TOO -
1525 HARRY & ALLEN NOW HAVE "Ø OK" - "Ø NOT OK" LIGHT IN SECTOR II CONTOL PANEL HOOKED UP TO SHOW WHEN SECTOR II DRIVE Ø HAS DRIFTED WITH RESPECT TO SECTOR I CAVITY Ø BY ROTATING Ø REF. SHIFTER - BY HAND, ONE CAN TELL HOW MUCH & WHICH WAY -
1540 VIA = 509V, VIB = 478V -
1555 BOB BYERS HAS INSTALLED RECORDER ON VAC GAUGE AT 1-1B - 1-2 & 1-4 MIGHT STAND LESS ATTENU

TABLE VIII-IV

3 JUN 1965

ACCELERATOR PARAMETERS

Operator: Vernon A. Price (cops team) Date: June 3 65 Time: 1930

	Pulse Rate	360	pps		DS1-1 Vert.	-.8 Amps
	V1A Reference	11.97	Volts		DS1-1 Horiz.	-.2 Amps
	V1B Reference	11.90	Volts		1-4 Vert.	+0.3 Amps
					1-4 Horiz.	-0.1 Amps
	Fil. Power	30	Watts	Steering	1-6 Vert.	-0.3 Amps
	Cathode E	6	Kv		1-6 Horiz.	-5 Amps
	Cathode I	20	ma		DS1-9 Vert.	-.6 Amps
Gun	Grid E	4	Kv		DS1-9 Horiz.	-.2 Amps
	Grid I	5	ma			
	Beam I (avg.)	15	[illegible]		DS1-9 Vert.	Amps
	Beam I (peak)		[illegible]	Degaussing	DS1-9 Horiz.	Amps
					DS2-9 Vert.	Amps
	Lens #1	+2.0	[illegible]		DS2-9 Horiz.	Amps
	Lens #2	+3	[illegible]			
Gun Steering and Focussing	2 ft. Horiz.	-2.5	[illegible]	Coils	DS1-	10 μ Amps
	2 ft. Vert.	+1.2	[illegible]		DS1-9	0 Amps
	12 ft. Horiz.	-0.4	Amps			
	12 ft. Vert.	+0.8	Amps	300' Beam	I (peak)	33.4 ma
Prebuncher	Phase	08 - 80				
	Power	-1.46 m (-30.6)	mw	600' Beam	Energy	See plot Mev
					I (peak)	20 ma
80" Beam	Energy	104	Mev			
	I (peak)	39.4	ma			

150 mv / 3.8 mv/ma

PHASE SETTINGS

1A	16
1B	176
1C	180
1-2	280
3	52
4	247
—	
6	13
7	≈ 240
—	
2-1	—
2-2	203
—	
2-4	192
5	344
6	90
7	34
8	off

STATIONS 1-5, 1-8, 2-1, 2-3, 2-8 } all

15 JUN 1965

TABLE VIII-V

ACCELERATOR PARAMETERS

Operator: WAITHMAN Date: JUNE 15, '65 Time: 1330

VI

	Pulse Rate	60 pps	Steering	DS1-1 Vert.	1 [illegible]
	V1A Reference	116 Volts		DS1-1 Horiz.	0 Amps
	V1B Reference	90 Volts		1-4 Vert.	.2+ Amps
				1-4 Horiz.	5.5+ Amps
	Fil. Power	20 Watts		1-6 Vert.	1.8+ Amps
	Cathode E	61 Kv		1-6 Horiz.	6.1+ Amps
	Cathode I	32 ma		DS1-9 Vert.	0 Amps
Gun	Grid E	3.9 Kv		DS1-9 Horiz.	.8+ Amps
	Grid I	3 ma			
	Beam I (avg.)	7 ua		DS1-9 Vert.	8.5+ [illegible]
	Beam I (peak)	ma		DS1-9 Horiz.	5.3+ [illegible]
			Degaussing	DS2-9 Vert.	10+ [illegible]
	Lens #1	3.8+ Amps		DS2-9 Horiz.	4+ [illegible]
	Lens #2	3.7 Amps			
Gun Steering and Focussing	2 ft. Horiz.	1+ Amps	Quads	DS1-9	16 Amps
	2 ft. Vert.	3.2+ Amps		DS2-9	14 [illegible]
	12 ft. Horiz.	1.1+ Amps			
	12 ft. Vert.	1.7+ Amps	300' Beam	I (peak)	21.4 ma
	Phase	3.086		Energy	1.01 Bev
Prebuncher	Power	.95 mw	600' Beam	I (peak)	194 ma
30' Beam	Energy	Mev			
	I (peak)	31.5 ma			

.1V/cm

- 61 -

1350 V1A = 116V - V1B = 75V - RESATURATING & REPHASING -

1437 120 PPS - STEERING IN SECTOR I CHANGES BY ITSELF ONCE IN A WHILE.

1515 TOOK ENERGY FOR PAUL EDWARDS - .75 BEV - STEERING BEAM TO CENTER DOES NOT GIVE MAXIMUM CURRENT -

1572 180 PPS - CLIFF RASMUSSEN SAYS 660' THIN VALVE LEAKS -

1530 STILL GETTING DRASTIC CHANGES IN SECTOR I HORIZONTAL FOR "NO" REASON AT ALL - (BRADFORD'S DOING ADJUSTMENTS)

1545 PAUL EDWARDS, BOB BRADFORD & ROSS HAGEL FINISHED - HARRY HOGG WILL XPRT NOW -

1550 360 PPS - V1A = 116V, V1B = 114V - ROSS SATURATING TUBES - BOB CHECKING O'G' -

1555 BUZZ OFF - OPERATOR'S KEY TO VIC WAITHMAN - (Bie)

1620 Going back to 360 PPS, 114 V. ref., de Gaing does not return to same value as earlier readings - by considerably. Brad[illegible] is concerned problem is that the VVS output does not accurately follow the reference voltage - and I am inclined to agree. This is a serious problem, and some accurate measurements should be made, under load. - W. Chan told Thursday pm. to set up an experiment

1625 Operation is now under control of Donn Robbins - with H. Hogg also getting spectrum expts. in.

1635 Lowered dive to 1-4 to keep it on.

1700 V Price operator.

1705 Lowered V1B To 90 V. ref } at request of water department for their tests

1707 Lowered V1A To 90 V. Ref }

1800 V1A Back to 116 VOLTS

Alternately, it is also possible to start steering "left" at BAS-1, thereby requiring somewhat less steering at 1-4 and 1-6. Final steering to straighten out the beam can then be done at DS-1. (For checking purposes, the following rule of thumb seemed to apply: Doubling the steering currents in BAS-1 and DS-1 for normalization purposes and adding them to those in 1-4 and 1-6 gave approximately 9 amps.)

5. Try to get beam down to DS-1. If not successful, use long ion chamber (see Section VIII-F) and induced beam signals from Automatic Phasing System.
6. When successful, rephase Sector 1.
7. Observe intensity, position and profile at DS-1. Adjust steering and quadrupoles settings at BAS-1; if beam center moves at DS-1 when quadrupole current at BAS-1 is changed, resteer beam from 12-foot point to recenter beam in quadrupole. Presumably this step should not have been necessary if the Beam Position Monitor readings had not drifted. Adjust quadrupole at BAS-1 so that minimum beam diameter is obtained approximately at 120-foot point. An extra profile monitor or at least a beam intensity monitor at this point may be very useful.
8. When transmission is optimized at DS-1, go through same steps in Sector 2 until beam is obtained at DS-2.
9. Automatically rephase complete machine.
10. Get spectrum.
11. Record all settings. Sometimes, a reasonably round beam spot could not be obtained unless one went through this iterative procedure several times. Typical beam transmission data are given in Table VIII-VI.

C. BEAM POSITION AND INTENSITY MONITORS (E. Farinholt, H. Hogg, H. Woods, R. Larsen)

The purpose of the beam position monitor is to sense the position of the beam center in the horizontal and vertical planes. The experiments conducted during Sectors 1 and 2 tests are most readily discussed in three parts: (1) the cavities, (2) the rf detector, and (3) the electronics.

TABLE VIII-VI

TYPICAL BEAM TRANSMISSION DATA

(All numbers given in milliamps peak)

Date 1965	i_{Gun}	i_{BAS-1}	i_{DS-1}	i_{DS-2}
February 4	25	10	9	6
April 7	Not available	16	12	4
May 26	Not available	39	32	27
May 27	Not available	13.1	9.4	8.3
June 8	Not available	28	21	17
		50	29	24
June 17	Not available	16	12	10
		31	21	18

1. Cavities

Three sets of cavities were located in line with the accelerator at BAS-1 (30 feet), DS1 (330 feet) and DS2 (660 feet). A set consists of a phase reference cavity, a horizontal position cavity, and a vertical position cavity. Power output of the cavities was measured as a function of beam current and position. Sensitivities of the cavities were measured on the machine where possible.

a. Phase Reference Cavity - Sensitivities of the three phase reference cavities were compared to the toroids located about one foot downstream. The sensitivities measured were lower than expected. In the case of the 30- and 660-foot units this can be partly attributed to a change in resonant frequency of the cavities. Table VIII-VII shows the results of these tests. Sensitivities quoted are at the cavity output port.

The agreement between measured and theoretical values is within the accuracy of the technique used. Recently, equipment has been acquired that will improve the accuracy of future measurements. The cause of the change in resonant frequency has been discovered and corrected for future assemblies.

TABLE VIII-VII

Cavity Ser. No.	Location	Resonant Frequency In Lab	Resonant Frequency On Accel.	Off Resonance Decrease In Output
1	30'	2856.1	2857.8	6.2 dB
2	330'	2856.2	2856.2	0.1 dB
3	660'	2856.1	2857.3	3.2 dB

Cavity Ser. No.	Theoretical Sensitivity, On Resonance (mW/mA^2)	Measured Sensitivity Corrected For Off Resonance (mW/mA^2)	Difference dB
1	297	363	+ 0.9 dB
2	260	182	- 1.6 dB
3	252	153	- 2.2 dB

b. Position Monitor Cavities - The sensitivity of the horizontal position cavity at the 660-foot location was measured. The beam current was monitored by the adjacent toroid. The beam position was located by moving a servo-driven secondary emission monitor in air at the end of the accelerator. The sensitivity of the cavity was 44 $\mu W/mA^2mm^2$ at the cavity output port. This agrees with measurements on the injector test stand. The theoretical value is 65 $\mu W/mA^2mm^2$.

Because of an error in an earlier theoretical calculation, the expected output value, upon which the rest of the system design had been based, was 85 $\mu W/mA^2mm^2$. In order to improve upon the value actually obtained, it was decided to increase the loaded Q from 300 to 600 on all future units.

c. Mechanical Problems - The change in resonant frequency of the phase reference cavities mentioned earlier was most likely caused by compression of the cavity by a mounting bracket. This was experimentally verified in the laboratory and appropriate changes are in process.

The cavities installed for Sectors 1 and 2 tests, serial numbers 1, 2, and 3, will have to be replaced because of a stainless steel drift tube through a water jacket. This creates a possible electrolytic corrosion problem similar to that discovered on the waveguide loads.

2. RF Detector Panel

The microwave subsystem which divides and combines the signals from the cavities performed satisfactorily with two exceptions: (1) thermionic diode unbalance and nonlinearity and (2) high video output impedance. The first problem is discussed below and the second was solved by the addition of a small amplifier for isolation.

It was found both in the laboratory and on the machine that the thermionic diodes will not remain in balance nor are they sufficiently linear over the 50-dB range of beam currents to fully utilize the outputs of the cavities. The error in indicated center position due to unbalance is typically less than two millimeters.

The non-linearity of the diodes has two major adverse effects. The lesser problem is the error in the "ℓn Q" presentation. It is negligible at high beam currents and increases to -5% of full scale at 10 mA and -20% at 1 mA. However, the non-linearity causes a much larger error in the indicated X and Y outputs. Here the error is again small for large values of beam current but increases to +15% at 10 mA and to +200 to +300% at 1 mA. Work is continuing in the laboratory to reduce these errors.

3. Electronics

The video outputs from the detector panel are fed to the adjacent ℓn Q, X, and Y circuitry. In order to drive this circuitry in the optimum fashion, it was found advantageous to incorporate three complementary emitter followers, one per signal, at the detector panel output. This was only done with one unit, but this arrangement will subsequently be incorporated at all detector panel, ℓn Q, X and Y interfaces.

After the initial installation and turn-on of the three ℓn Q, X, and Y units, they were left switched on and allowed to run continuously unattended. No readjustment of any of the preset controls was found to be necessary over the six-month period of operation under discussion.

However, during the first month of operation the calibration was repeatedly checked using an external pulse generator. The low level offsets were found, as expected, to be somewhat temperature sensitive. However, no long term drifts were found, and the average value of the short term drifts was zero.

The baseband transmission system between the units and the control console in the Sector 2 alcove was found to work satisfactorily. The three time-shared traces from the 30-foot analyzer station and from the Sector 1 and Sector 2 drift sections were displayed one above the other on the same C.R.O. tube face. In addition, any one of the three traces could be selected and given extra gain.

This overall arrangement was found to be very useful for beam steering. Thus a decrease of the horizontal and/or vertical displacement was accompanied by an increase in the ℓ_n Q output. Note, however, that if a badly focused beam was being handled, zero net displacements could be indicated, together with small values of ℓ_n Q. That is, this system indicates essentially the average position of the centroid of the beam as a function of time, but gives no indication of the shape and size of the beam cross section.

Steering of the beam may be facilitated by having knowledge of the transverse beam position at additional points along the first sector. This may be obtained by providing additional position monitors, possibly of the wirewound type. These would not necessarily require normalization circuitry, but could be used to give zero output when the beam is on axis.

The three intensity toroids performed as designed. However, with a basic sensitivity of 3.8 mV/mA, only small output signals were obtained with the levels of peak beam current being used. Accordingly, the toroid outputs were amplified to give a sensitivity of 75 mV/mA, the output signal being fed by way of RG 22 B/U Twinax cable to the Sector 2 alcove. This allowed beam transmission measurements to be made with greater accuracy and ease than previously.

Only one so-called accurate "linear Q" circuit was installed, at the Sector 1 drift section. It was operated locally, and from the limited experience gained with it, appears to function satisfactorily.

D. BEAM PROFILE MONITORS (D. Reagan)

1. Cerenkov Radiator Profile Monitors

Three profile monitors were installed which used the Cerenkov light produced by the electron beam when it passed through 0.030-inch quartz

plates (see Fig. VIII-1). The plates were mounted at 45° with respect to the beam direction, so that the useful light would come out normal to the quartz surface. Television cameras detected the light, and receiver units were installed at the injector control point to observe the beam profile at BAS-1, and at Sector 2 alcove to observe profiles at DS1 and DS2.

The systems operated well, but had some shortcomings. Although the Cerenkov response is supposed to be quite linear, the system linearity was poor. A spot could be made to appear large or small, with a slight adjustment of the sensitivity control. Some misleading results arise from the peculiar "collimation" of the Cerenkov light. Figures VIII-2, -3, -4 illustrate an apparent beam break-up which occurred at the beam analyzing station. A later check showed that the splitting (Fig. VIII-4) disappeared when the camera was panned so that the lense properly intercepted the Cerenkov light cone. It was found that the effect of the Cerenkov cone could be eliminated, for practical purposes, by merely roughening (sandblasting) the downstream surface of the quartz radiator.

2. Scanning Profile Monitor

A scanning profile monitor was tested at DS1. In it a 0.050-inch × 0.050-inch cylindrical Mo target, hung on a 0.002-inch W(5% R_e) wire was mechanically scanned over the cross section of the electron beam. The electrons which passed through the target were scattered, and some hit the inner surface of the accelerator pipe, producing a cascade shower. The shower was detected with an external air filled ion chamber to give a measure of the relative number of electrons striking the target at that moment.

Figure VIII-5 shows the result of a single scan, which took about five seconds to make. The picture is that of a storage oscilloscope face. The vertical and horizontal scan motions were measured by linear motion potentiometers, electrically connected to the vertical and horizontal inputs of the oscilloscope. The ion chamber signal was also connected to the vertical sweep input.

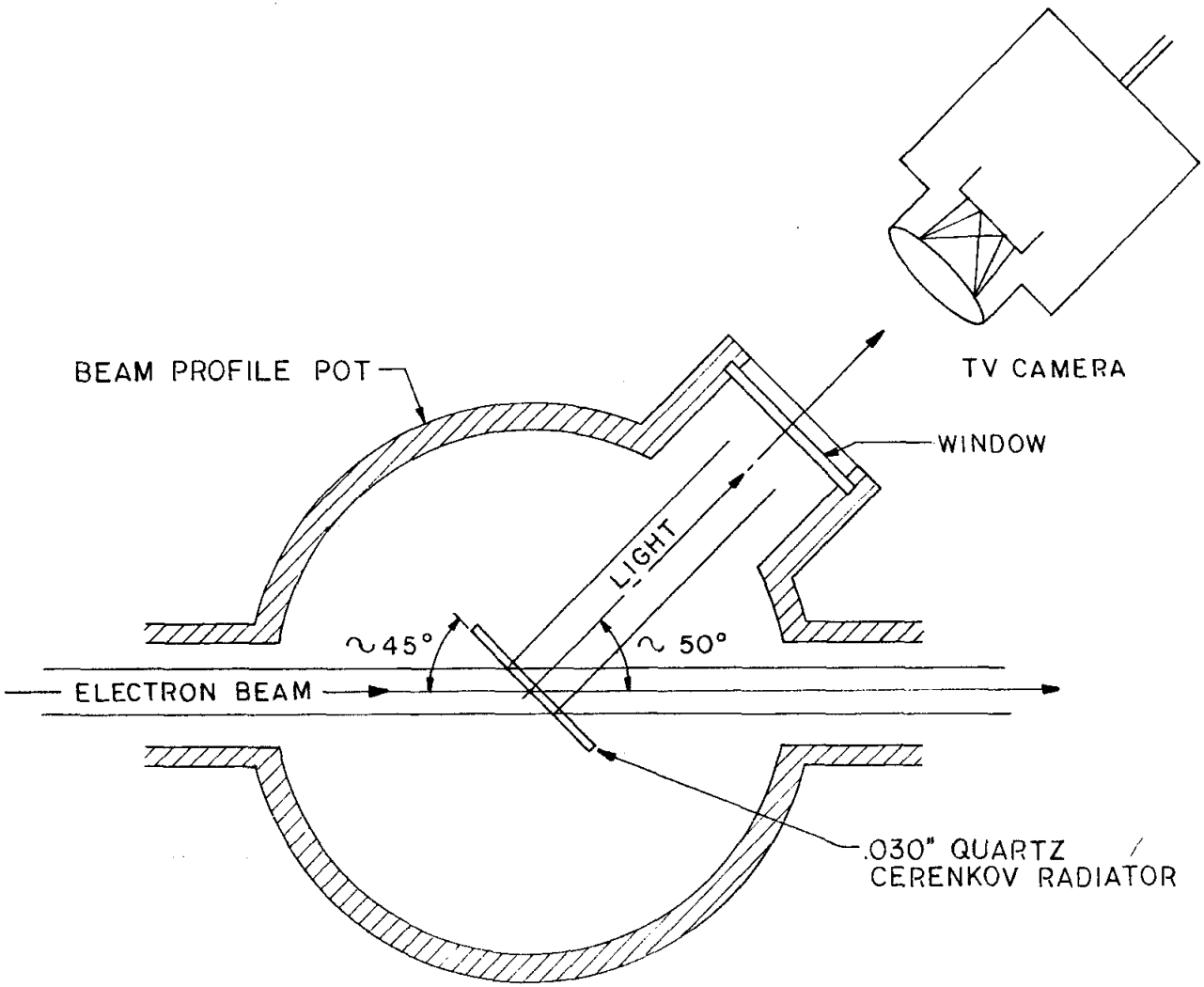

FIG. VIII-1-CERENKOV BEAM PROFILE MONITOR
(SCHEMATIC)

340-14-A

FIG. VIII-2 TV picture of spot with beam centered.

FIG. VIII-3 Spot with beam steered to left.

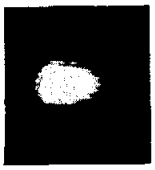

FIG. VIII-4 Spot with beam steered to right. The "splitting" was phoney, a result of misalignment of the TV camera with the Cerenkov light cone. After the camera was properly lined up, the spot looked like Fig. VIII-3, reversed.

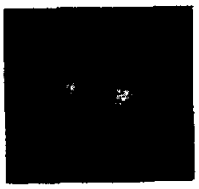

340-35.36 27-A

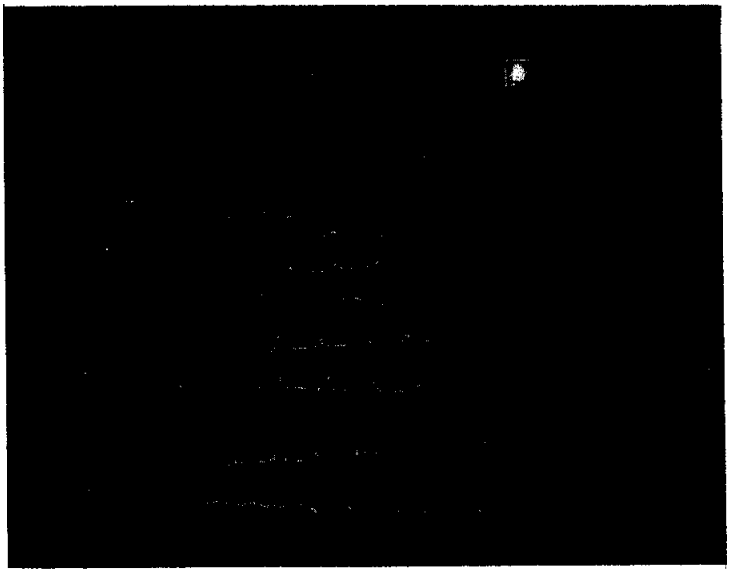

340-55-A

FIG. VIII-5 Storage oscilloscope record of a profile scan. The instantaneous base line position corresponds (with some geometrical distortion) to the scanning target position (beam's eye view).

E. FEASIBILITY OF MULTIPLE BEAMS (K. B. Mallory)

The feasibility of obtaining multiple beams from the accelerator was demonstrated in two types of experiments. It was found reasonable to operate the gun at 60 pps and the klystrons at 60 - 360 pps to obtain a 60-pps beam. It was also found possible to operate the gun and the klystrons at 60 pps but to switch the Sector 1 klystrons to the delayed standby pulses for 50 of 60 pulses, thus obtaining a 10-pps beam. This demonstrates that the accelerator can indeed be triggered to produce arbitrary beam patterns.

The second experiment was designed to test the assumption that all six phases of 60 pps making up a 360-pps beam are indeed identical. The test of ac steering effects was performed by first operating the klystrons of Sectors 1 and 2 at 360 pps and somewhat reduced plate voltage. The gun was then operated at 60 pps, and it was switched successively through the six possible beam phases. The phase switching could be accomplished instantaneously.

The beam profile monitor was watched to look for any possible shifts of beam shape or position coincident with the phase switch. No such effect could be detected, and it is estimated that a shift of about 1/2 millimeter would have been observable. Similarly, no change was observable on the beam position monitors. The beam energy spectrum was also recorded for each of the six phases. No differences could be detected, to the sensitivity of the spectrometer ($\pm$ 1/2%).

While this result is encouraging, the test is not sufficiently sensitive to show that ac steering effects will be negligible for the 30-sector machine.

F. USE OF LONG ION CHAMBERS (D. Reagan)

A 660-foot long ion chamber, made of coaxial cable filled with A(5% CO_2), has been installed in the accelerator housing in Sectors 1 and 2. When extended the full 10,000 feet of the accelerator, it will serve to detect radiation coming from the accelerator pipe. Its signal will, when necessary, initiate safety measures designed to prevent damage to the pipe due to excessive electron bombardment. Meanwhile, considerable effort has been devoted toward exploiting this tool as

an aid in steering and focusing the electron beam. The pulse is observed by means of an oscilloscope connected to the upstream end of the cable. In this way, electrons which strike the inner wall of the accelerator farther downstream will produce signals which will appear later in time on the oscilloscope trace.

In practice, electrons hit the inner wall of the pipe more or less continuously in time and distance, whenever the beam pulse is on, so that the received composite signal is an ambiguous, more or less smooth pulse, as shown in Fig. VIII-6. Several percent of the pulse amplitude are probably due to noise and cable ringing. Figure VIII-7 shows the expected pulse shape if equal amounts of beam power were lost per unit length for 660 feet, for a uniform 1.5-μsec square pulse. Figure VIII-8 shows the signal for the case where the beam power loss is uniform for most of the distance, and relatively large near the downstream end.

By adjusting steering and focusing controls it was possible to make changes, gross and subtle, in the pulse shape. The difficult problem was to understand what was happening. It seemed clear that better steering would make the early part of the pulse smaller. However, very bad early missteering would also achieve this result. One persistent feature of a well-steered pulse was called the "Miller knee." It was apparently due to scraping at the DS-1 beam scraper, although it appeared earlier in time than the big pulse from the DS-1 Cerenkov target did. The explanation seemed to be that radiation from the scraper occurred right at the scraper, while that from the Cerenkov target occured 50 feet or so downstream.

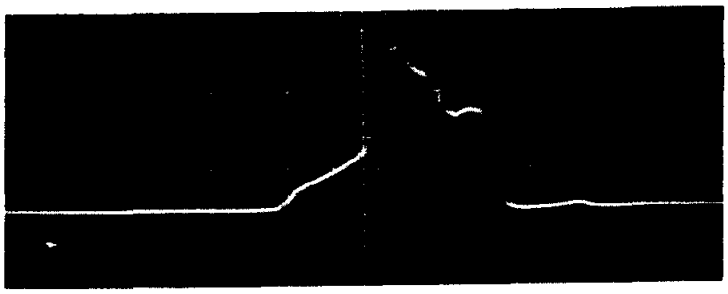

340-39-A

FIG. VIII-6 Long ion chamber pulse with beam steered through Sectors 1 and 2. Scales: 1μsec/cm and 0.1 volt/cm.

340-40-A

FIG. VIII-7 Pulse shape for uniform beam power loss.

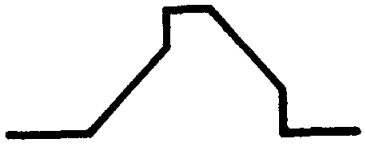

340-41-A

FIG. VIII-8 Pulse shape as above, but with large loss near end of 660-foot accelerator pipe.

IX. BEAM MEASUREMENTS OF COUPLER ASYMMETRY AND GIRDER ALIGNMENT

R. Miller

A. MEASUREMENTS

Several measurements have been performed which attempt to determine the transverse impulse given to the beam by each girder in Sectors 1 and 2. The experiments were conducted by successively turning each klystron off and on and observing the change in beam position by means of the beam position monitor at the following drift section. The electron beam displacement is related to the transverse impulse by the expression;

$$\frac{\Delta p_x}{\alpha} = \frac{\Delta x}{\lambda \ell_n \frac{\gamma_2}{\gamma_1}} \qquad (1)$$

where Δp_x = the transverse momentum impulse in units of mc.

$\alpha = \frac{eE\lambda}{mc^2}$ = energy gain per wavelength

Δx = Beam displacement

γ_1 = the electron energy in units of rest energy, at the point where the transverse impulse is applied.

γ_2 = electron energy at the point the displacement is measured.

The position monitors are capable of measuring beam position changes to about 0.002-inch but there could easily be a 0.30% error in measuring the sensitivity. The transverse impulse can be related to an equivalent girder misalignment (i.e., a girder misalignment which gives an equal transverse impulse) by observing that the transverse impulse given by a misaligned girder is

$$\frac{\Delta p_x}{\alpha} = \frac{1}{2}\,\theta\,\frac{\Delta p_z}{\alpha} \qquad (2)$$

where θ = angular misalignment of girder and

Δp_z = the longitudual momentum increase produced by the sectors.

The factor $\frac{1}{2}$ occurs because end-effects cancel half the transverse impulse produced in the interior of a misaligned section. Using $\Delta p_z = \alpha \frac{L}{\lambda}$ and the linear misalignment of a girder, $\Delta X = \theta L$, we obtain the following relationship between the equivalent girder misalignment ΔX and the beam displacement Δx

$$\Delta X = \frac{2\Delta x}{\ell n \frac{\gamma_2}{\gamma_1}} \qquad (3)$$

The factor $2/\ell n \frac{\gamma_2}{\gamma_1}$ varies from 1.3, for girder 1-3, to 32 for girder 2-8.

It should be pointed out that this derivation ignores the effect of the change in energy on beam deflections produced beyond the girder in question. It is believed that these are not too important since the machine was carefully degaussed and the measurements for Sector 1 were made using the beam position monitor of the end of Sector 1, and similarly for Sector 2. In Sector 1 the experiment was performed under two conditions: (1) with the steering coils on girder 1-4 and 1-6 turned off; (2) with these steering coils set to values calculated to compensate for the previously measured coupler asymmetry. The results did not differ significantly.

Furthermore, the measurements could not distinguish between a net transverse impulse produced by a girder and a transverse displacement of the beam produced by canceling transverse impulses, for example, one at the beginning and one at the end of the girder.

The results of the measurements are shown in Fig. IX-1, which presents the electron beam displacements at the end of the sector, and Fig. IX-2 in terms of equivalent girder misalignment in inches. The top graph presents the horizontal effects and the bottom the vertical. The klystron (or girder) numbers are displayed along the abscissa. The following comments can be made from this data.

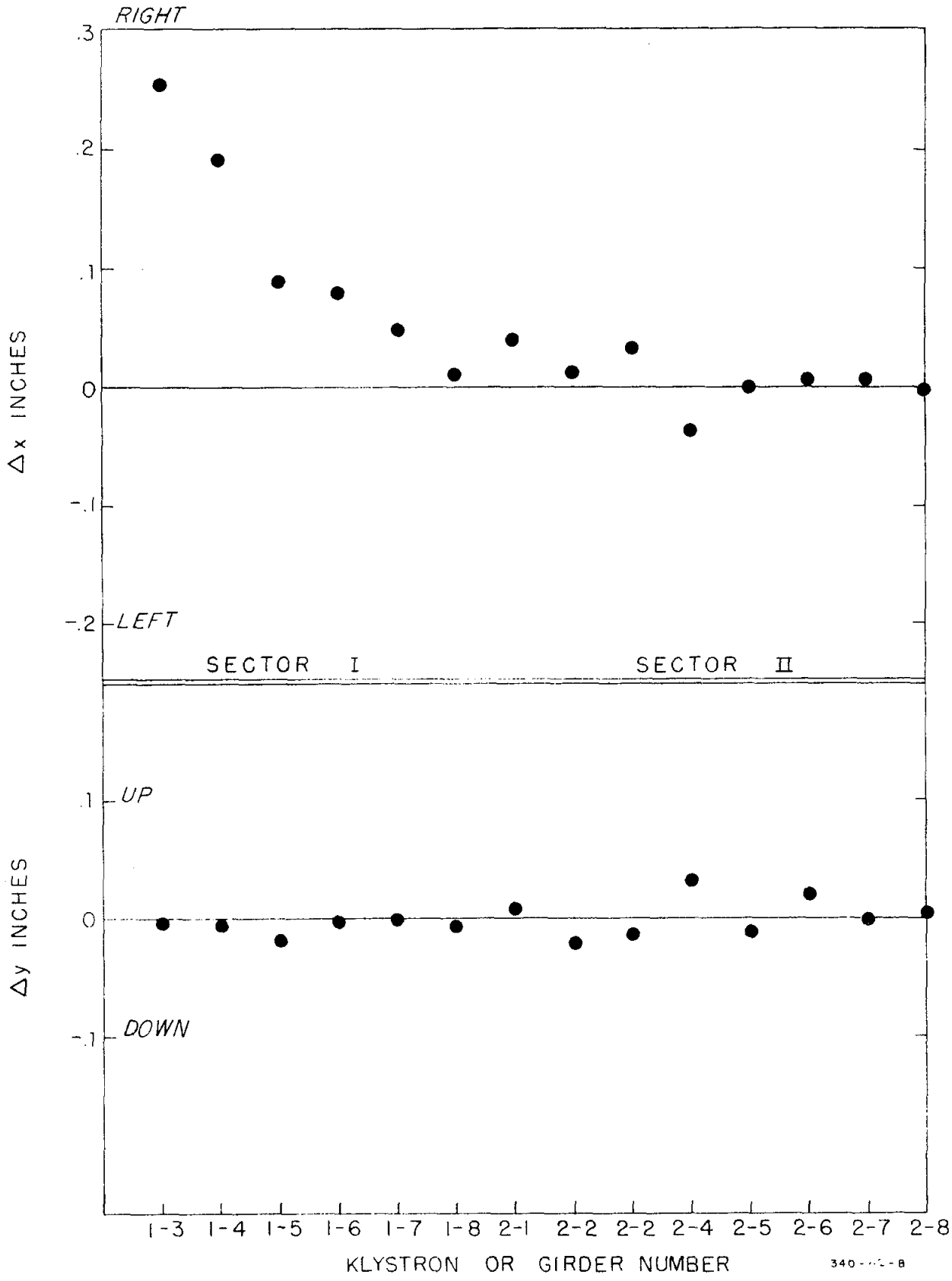

FIG. IX-1 Electron beam displacement.

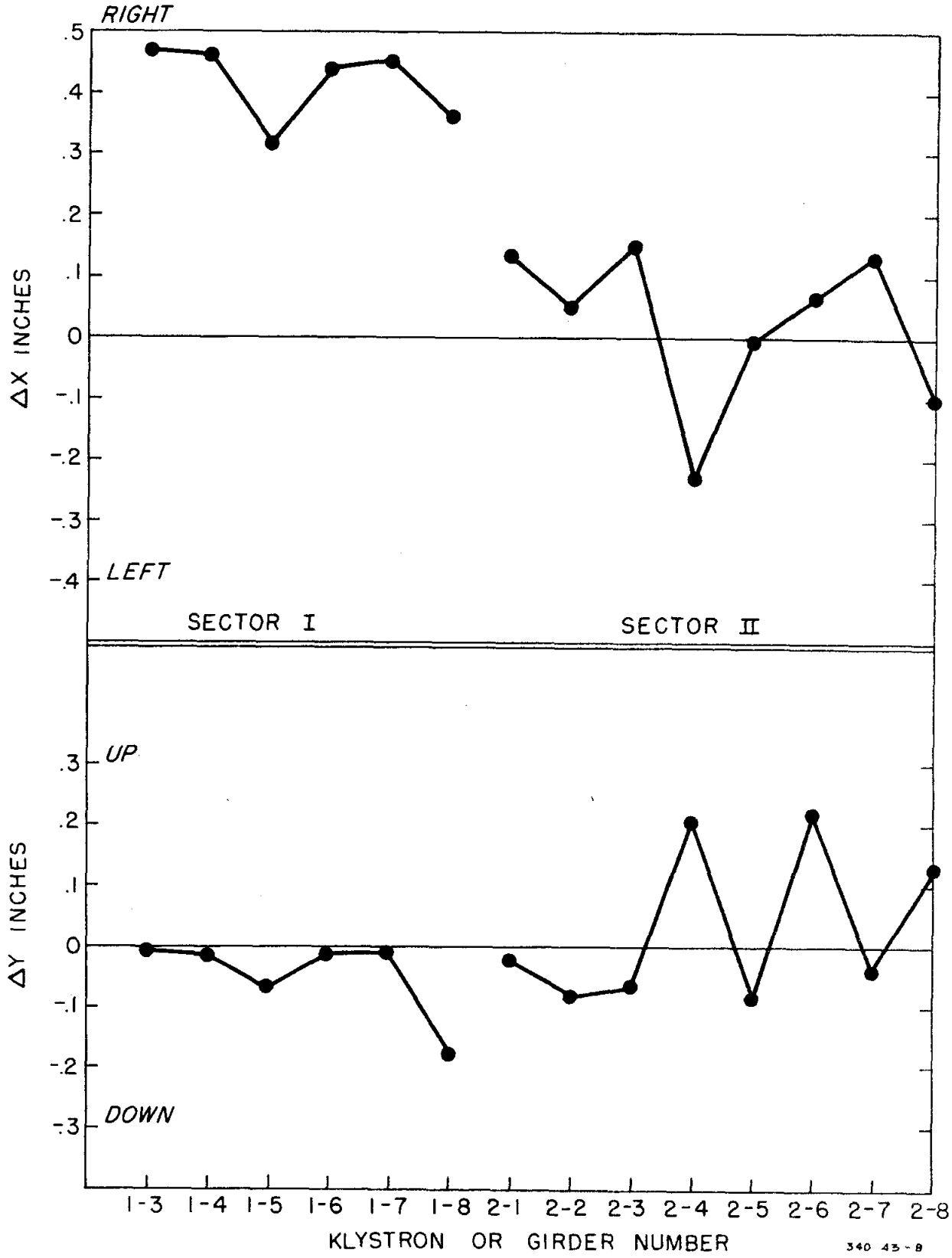

FIG. IX-2 Equivalent girder misalignment.

1. In Sector 1, the large systematic kick to the right, due to the uncompensated coupler asymmetry, is obvious.
2. In Sector 1, there are consistent small vertical impulses downwards.
3. In Sector 2, there are surprisingly large horizontal and vertical impulses which are random and/or perhaps alternating (up and to the left in even-numbered girders, and down and to the right in odd-numbered girders).
4. The equivalent misalignments in Sector 2 are much larger than the believed mechanical misalignments, which are of the order of 0.015"from girder to girder and 0.050"overall.

B. REALIGNMENT

In order to verify these measurements, Sector 2 was realigned in the horizontal plane to compensate for the measured effects. The correction applied to each jack was the algebraic sum of the equivalent misalignments of all previous girders. This was necessary because each girder is part of an unbroken chain of linked girders. Hence, moving one girder to correct for its misalignment causes the next girder to be moved by an equal and opposite amount. The beam impulse measurement was then repeated and the values of ΔX obtained by switching each klystron in and out are plotted in Fig. IX-3. This indicates that the beam measurements are accurate to within about 30%.

C. CONJECTURES

Although the transverse impulse effects in Sector 2 are not understood, the following possible causes are being investigated:

1. Higher order modes excited by the mitered bends near the input couplers.
2. Deflecting modes at harmonics of the fundamental frequency.
3. Mechanical distortion produced by the baba-abab configuration.

A microwave cold tests program has been started to investigate points 1 and 2. In addition, we are considering removing a klystron and feeding small amounts of harmonics into one of the girders when Sectors 1 and 2 beam tests resume. We also expect to consider investigating the effect of mechanical loading of the girders by the waveguides when beam tests resume.

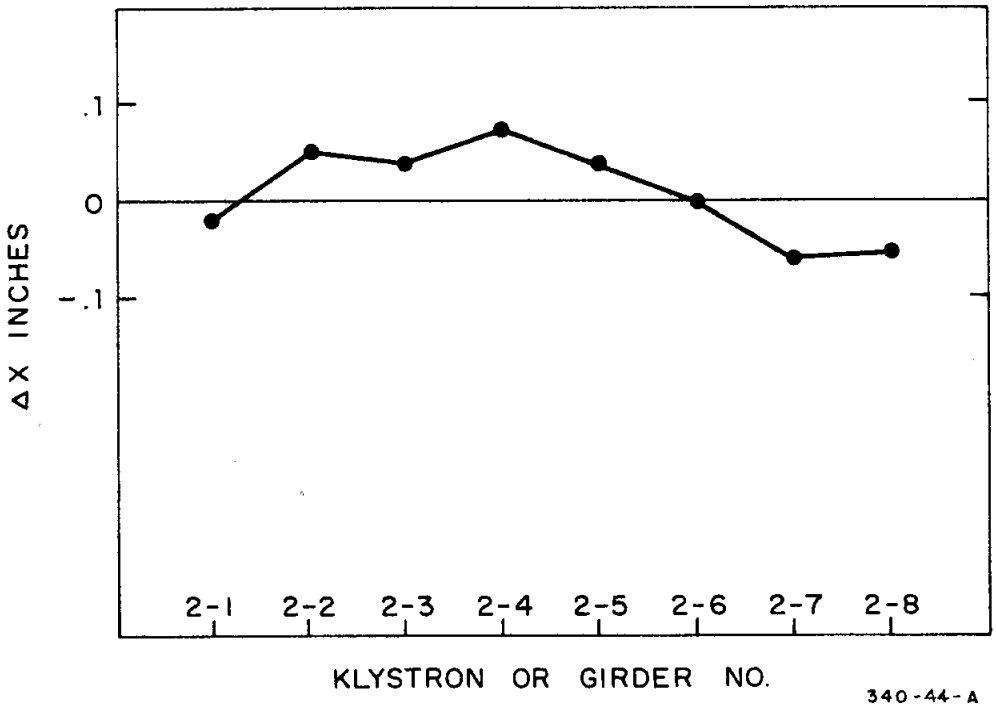

FIG. IX-3 Equivalent girder misalignment after compensation.

X. OVER-ALL SYSTEM OPERATION

V. Price, V. Waithman, J. Jasberg

The first electron beam in the accelerator was observed at 0215 January 6, 1965, at the 40-foot beam analyzer station. By 27 January 1965 a five-milliampere peak current beam with an energy of 620 MeV was measured at the end of Sector 2. Table X-I summarizes the day-to-day operation of the two-sector accelerator, giving the total high power rf-on time, the beam-on time, and the energy achieved during the run. The operating time was limited by the need to keep the radiation level to a negligible value at any place in the accelerator housing where workmen might enter. A temporary personnel protection system permitted interlock control of the accelerator housing during the rf-on operation time from Sector 0 through Sector 5.

In addition to the beam tests, the testing period provided an opportunity to evaluate the performance of the major systems such as power, vacuum, water and modulators. These tests are summarized as follows:

A. ELECTRICAL POWER REQUIREMENTS

The electrical power required to produce various beam energies at various repetition rates is illustrated in Table X-II. Given are the results of tests conducted on June 11, 14 and 15, 1965, and numbers obtained by extrapolation beyond the interim limits of klystron beam voltage. The power requirements for operation at 60 pulses per second are estimated with the de-Q'ing adjusted for the same functional limit of 2.5% to 3%, as is the practice for the 360 pulses per second level. Although the tests included 15 modulators served from variable voltage substation VV1-B, the data is presented herein on a per klystron basis by dividing the test results by 15. The power system loads in kVA per klystron and demands in kW per klystron are input values fed from the 12-kV lines. The auxiliary power requirements for Sectors 1, 2 and the Injector are given in Table X-III as total output of the 480-volt unit substations K-1A and K-1B.

TABLE X-I

January to June 1965 Beam Operation Summary

Date	RF-on Hrs	Beam-on Hrs	Energy	Notes
5-6 Jan	4	0.2		1st 40-foot beam
6 Jan	3.8	3	80 MeV	
7 Jan	4	2.5	101 MeV	
11 Jan	5	3.3		
12 Jan	4	0.4		
13 Jan	6	5.2		
14 Jan	4	3		
18 Jan	4.6	4.5		
19 Jan	4.5	4		
22 Jan	2	1.5		
25 Jan	4.5	-		
26-27 Jan			620 MeV	1st Beam through Sector 2
28 Jan	4.1	4.0		
2 Feb	4	-		
3 Feb	5.2	1		
4-5 Feb	5.5	4	1.22 GeV	
9 Feb	6	5.5	900 MeV	
10 Feb	2	1		
11 Feb	6.5	6.2	1 GeV	
15 Feb	5	2.5		
16 Feb	5	2.5	880 MeV	
17 Feb	6	4.5		
18 Feb	7	5.4		
24 Feb	4.7	4.5	1.1 GeV	
25 Feb	6	5.5	1.45 GeV	
1 Mar	4.5			
2 Mar	7.5	6	1 GeV	
3 Mar	3			
4 Mar	8.2	7.2	1.32 GeV	

TABLE X-I - Continued

Date	RF-on Hrs	Beam-on Hrs	Energy	Notes
10 Mar	10	7.5	1.16 GeV	
11 Mar	1.7			
12 Mar	6.3			
16 Mar	13	4	1.28 GeV	
17 Mar	10	5.5		
18 Mar	13	2	1.45 GeV	
23 Mar	11.5	3.5	1.42 GeV	
24 Mar	9	4	1.28 GeV	
25 Mar	12	5	1.32 GeV	
26 Mar	3.5			
30 Mar	13	3.5	1.45 GeV	
31 Mar	9	6.7	1.39	
1 Apr	5	4.5		
2 Apr	1.5			
6 Apr	10.5	4	1.45	
7 Apr	14	4.5		
8 Apr	13.5	4	1.38	
13 Apr	15	6	1.42	
14 Apr	12	4	1.18	
15 Apr	14	2.5	1.32	
16 Apr	7.4			
20 Apr	13	4.4	1.4	
21 Apr	12.5	3	1.38	
22 Apr	13	4	1.29	
23 Apr	7.3			
27 Apr	6	4	1.22	
28 Apr	15.5	6	1.36	
29 Apr	6.5	3	1.36	
4 May	0.5			
6 May	9.5			

TABLE X-I - Continued

Date	RF-on Hrs	Beam-on Hrs	Energy	Notes
7 May	4.3			
11 May	7	3.2		
12 May	15	3.3		
18 May	15	7.2		
19 May	10.2	8.9	1.3	
20 May	9	7.7	1.22	
25 May	24	7.4		
26 May	24	3.3	1.21	
27 May	24	20	1.43	
28 May	16			
3 Jun	13.5	2	810 MeV	
4 Jun	9.5	4.5	1.28 GeV	
7 Jun	8.5	6.7	1.35	
8 Jun	10	9.5	1.34 GeV	
9 Jun	9.5	8.3	1.34	
10 Jun	8.2	7	1.3	
11 Jun	9	8.8	1.25	
12 Jun	7	6.7		
14 Jun	9	5.5		
15 Jun	15.5	12.5	1.0	
16 Jun	7.5	4.5		
17 Jun	16	14.5	1.27	
Total	697.0	334.5		

TABLE X-II

VARIABLE VOLTAGE SUBSTATION INPUT FOR VARIOUS ACCELERATOR BEAM ENERGIES AND PULSE REPETITION RATES

VV1-B

	Meas.	Extrap.	Est.
Accelerator beam energy, MeV/klystron	81	92.5	
Pulse repetition rate, pulse/sec.	360	360	
De-Q'ing (%)	3.2	2.5	
Power system load, kVA/klystron	91.2	112	
Power system demand, kW/klystron	80.6	102	
Accelerator beam energy, MeV/klystron	81	92.5	92.5
Pulse repetition rate, pulse/sec.	60	60	60
De-Q'ing (%)	--	--	2.5
Power system load, kVA/klystron	20	24	22
Power system demand, kW/klystron	15.6	19.6	18
Accelerator beam energy, MeV/klystron	43		
Pulse repetition rate, pulse/sec.	360		
De-Q'ing (%)	5.9		
Power system load, kVA/klystron	45.1		
Power system demand, kW/klystron	35.7		
Accelerator beam energy, MeV/klystron	43		43
Pulse repetition rate, pulse/sec.	60		60
De-Q'ing (%)	12.7		6
Power system load, kVA/klystron	13.9		13.6
Power system demand, kW/klystron	7.0		6.6

All of the measured data in Table X-III are obtained with the same de-Q'ing control setting that gives a 2.5% to 3% limit at 360 pulses per second.

TABLE X-III

AUXILIARY POWER SECTORS 1, 2 AND INJECTION
480-VOLT UNIT SUBSTATION OUTPUT

K1-A and K1-B Total

	Power System Total Load kVA	Power System Total Demand kW
Total power including modulator auxiliary power	459	419
Total power excluding modulator auxiliary power	396	365

Modulator auxiliary power ≈ 3 kW/klystron

B. VACUUM SYSTEM

The vacuum system in general operated satisfactorily. One major leak opened up in BAS-2. Early in the period, there were several leaks in high voltage insulators on the ion pumps. However, these no longer occurred at the end of the period.

For the roughing systems, preliminary prototype pumps were used. The shortest pumpdown time was obtained by using a combination of two 15-cfm mechanical pumps and a two-stage molecular sieve cryopump. Each stage of the cryopump contained 150 lbs. of zeolite. The time to evacuate one sector from nitrogen at atmospheric pressure down to approximately 2×10^{-4} torr was 85 minutes.

Figure X-1 shows the plot of the pumpdown. In a subsequent pumpdown in May, using a 50-cfm mechanical pump, the time between the start of the roughing and the start of the ion pumps was reduced from 85 minutes to about 70 minutes. The cryopumping system functioned well, but certain modifications are needed to improve operation. One major problem is the higher than anticipated consumption of liquid nitrogen (300 to 350 liters were required for cooldown and pumpdown).

Several pumpdowns using the ion pumps were monitored in Sectors 1 and 2 during this period. On the average, the ion pumps start in 10 to 15 minutes when valved in from a manifold pressure of 5 microns or lower. Initially the pressure in the 8-inch manifold drops fairly rapidly and in about 10 minutes reaches mid 10^{-6} torr scale. The pressure

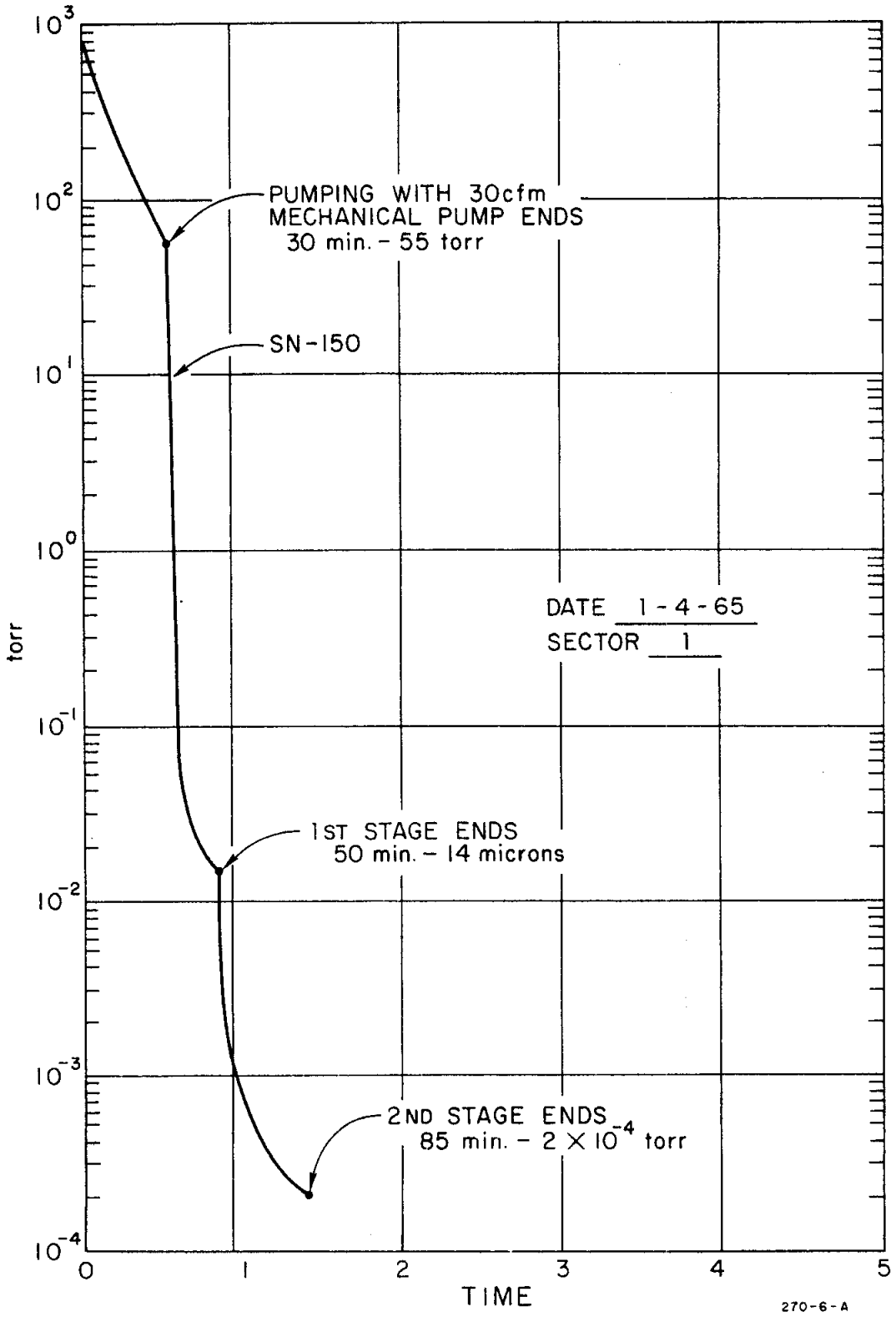

Fig. X-1 ROUGHING PUMPDOWN TIME
- MANIFOLD VOLUME - 9000 LITERS GN_2. WHOLE SYSTEM PRE-PUMPED WITH TWO 15cfm MECHANICAL PUMP ROUGHING CARTS. SN-150 PUMPS PRE-COOLED 75 MINUTES. ST ST'L + Cu.

in the 8-inch manifold and klystron window reaches low 10^{-7} torr scale in about 24 hours. These figures of course, represent an average and are based on pumpdown from nitrogen in a system without leaks and an ambient temperature of about 18°C. A typical curve of pressure vs time for pumpdown is shown on Fig. X-2.

C. WATER SYSTEM

The operation of the water systems for Sectors 1 and 2 has been quite satisfactory with the exception of a rather serious drift in temperature of the accelerator cooling water in both sectors. When discovered, Sector 1 input water temperature was about 108°F and that for Sector 2 was about 100°F while the controller in each case was set for, and indicated, 113°F. The trouble was due to a faulty component in the temperature control system and is being corrected.

D. MODULATORS

The overall operation of the modulators has been satisfactory. There were periods when all 18 modulators ran without trouble for days and with few "kickouts."

Some specific problems encountered are listed below:

1. Pulse capacitors: A few marginal capacitors failed early during the testing period. Toward the end, the failure rate decreased to practically zero.
2. Switch tubes: Only two switch tubes developed trouble during the period.
3. Erratic de-Q'ing: The trouble with de-Q'ing (caused by corona and arcing in the de-Q'ing divider) has been cured by re-design of the divider. The cause of de-Q'ing current drift, which has at times been ascribed to the de-Q'ing circuit, has not yet been determined; however, it is most likely external to the modulator.
4. Relay problems: There have been troubles with recycling and dropout of filament time delay.

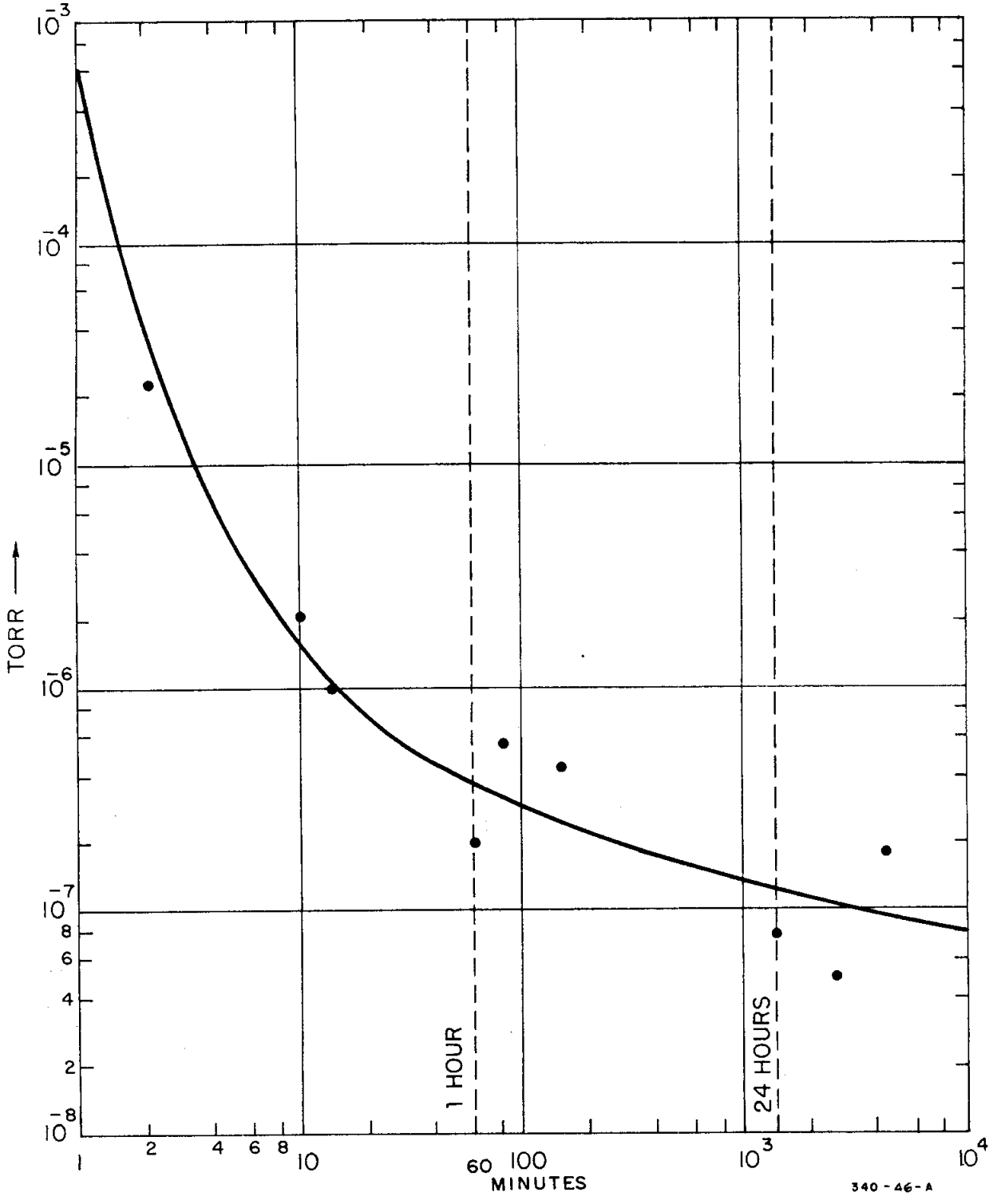

FIG. X-2 Typical pumpdown of one sector.

XI. FINAL REMARKS AND CONCLUSIONS

(G. Loew)

1. Aside from a slight frequency-temperature discrepancy between design and performance (yet to be resolved), the accelerator structure operated very well. In fact, the accelerator efficiency may be as much as 5% greater than expected (assuming no error in the spectrometer calibration). Except for Girder 1-8, the rectangular waveguide tuning appeared to be free from any major errors measurable through beam energy.

2. Coupler asymmetry problems, surprisingly in the y-direction, seem to have appeared, particularly in Sector 2. They may be due to rectangular waveguide bends or harmonics. Cold test checks are being made.

3. Additional work needs to be done to clear up the discrepancy between klystron output powers and voltages at different repetition rates. Improvements are also needed in getting the de-Q'ing to yield equal voltages for all klystrons.

4. Over-all klystron phase stability, within pulse and pulse-to-pulse, appears to be quite satisfactory.

5. After some modifications, the automatic phasing system and the beam position monitors operated nicely, but the diode drift problem, particularly the long-term drift, still remains to be solved.

6. Nothing final can yet be said about the long-term phase stability of the drive system because drive line anchors, insulation and other improvements had not been installed by July.

7. Some work remains to be done on the alignment of Sectors 1 and 2, both on an inter- and intra-girder basis.

8. The accelerator input water temperature seems to be very stable, most of the time. However, assurance must yet be obtained that the reference temperature will not drift unexpectedly as it did once.

9. If the final injector does not improve beam optics and transmission, improvements in beam guidance instrumentation may be needed in Sector 1. The remedies might include adding one or two intensity monitor toroids or beam position monitors in the middle of Sector 1.

10. BAS-2 is now considered so useful that a permanent spectrometer will be installed on girder 3-1.

11. Toward the end of the six months period, overall reliability of the machine was encouraging. However, klystrons at the beginning of the machine still recycled too often and caused the beam to move around more than desirable. It will also be important to watch the failure rate of the beam guidance power supplies. At the beginning of the machine, there is probably enough steering and focusing equipment so that during a supply failure and replacement, a reasonable beam can be recovered with a new combination of current settings. At DS-1 this may be difficult or impossible.